

EFFECT OF HEAT TREATMENT
ON THE ELECTRICAL PROPERTIES
OF BIJOYPUR WHITE CLAY

BY

FARUQUE-UZ-ZAMAN CHOWDHURY

SUBMITTED IN PARTIAL FULFILMENT
OF THE REQUIREMENTS FOR THE
DEGREE OF M. PHIL.



DEPARTMENT OF PHYSICS
BANGLADESH UNIVERSITY OF ENGINEERING AND
TECHNOLOGY, DHAKA

Nov. 1993



BANGLADESH UNIVERSITY OF ENGINEERING AND TECHNOLOGY
DEPARTMENT OF PHYSICS

CERTIFICATION OF THESIS WORK

A THESIS ON

EFFECT OF HEAT TREATMENT ON THE ELECTRICAL PROPERTIES OF BIJOYPUR
WHITE CLAY.

BY

MR. FARUQUE-UZ-ZAMAN CHOWDHURY

has been accepted as satisfactory in partial fulfilment for the degree of Master of Philosophy in Physics and certify that the student demonstrated a satisfactory knowledge of the field covered by this thesis in an oral examination held on 14th November, 1993.

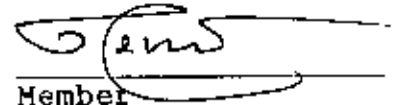
BOARD OF EXAMINERS

1. Dr. Abu Hashan Bhuiyan
Assistant Professor
Department of Physics
BUET, Dhaka-1000
BANGLADESH.



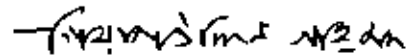
Supervisor &
Chairman

2. Dr. Tafazzal Hossain
Professor & Head
Department of Physics
BUET, Dhaka-1000
BANGLADESH.



Member

3. Dr. Gias Uddin Ahmad
Professor
Department of Physics
BUET, Dhaka-1000
BANGLADESH.



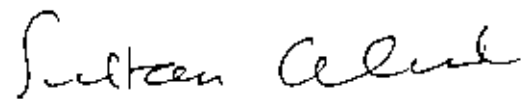
Member

4. Dr. M. Ali Asgar
Professor
Department of Physics
BUET, Dhaka-1000
BANGLADESH.



Member

5. Dr. Sultana Ahmed
Professor
Department of Physics
Dhaka University,
Dhaka-1000,
BANGLADESH



Member (External)

CERTIFICATE

This is to certify that the author is solely responsible for the work reported in this thesis and this work has not been submitted to any university or elsewhere for the award of a degree or diploma.

Faman

Candidate

(FARUQUE-UZ-ZAMAN CHOWDHURY)

Roll No: 8801 F

Session : 1986-87

Abu Hashan Bhuiyan

Supervisor

(DR. MD. ABU HASHAN BHUIYAN)

ACKNOWLEDGEMENT

The author expresses his sincere gratitude to Dr. Md. Abu Hashan Bhuiyan, Assistant Professor, Department of Physics, Bangladesh University of Engineering and Technology, Dhaka, for his guidance, valuable suggestions and continuous inspirations during this research work.

The author expresses his gratitude to Professor Tafazzal Hossain, Head, Department of Physics, BUET, Dhaka, and Professor Gias Uddin Ahmad and Professor M. Ali Asgar of the same Department for extending their generous help, encouragement and allowing him to work in the department. He is grateful to Mr. J. Podder, Assistant Professor, Department of Physics, BUET, for taking the microphotographs. He is also grateful to the other teachers of the Physics Department, BUET.

The author is indebted to the chairman, Department of Physics, University of Dhaka, for allowing him to work in the Solid State Physics Laboratory for dielectric measurements.

He is thankful to the authority of BCSIR, Dhaka, for taking DTA traces of Bijoypur White Clay and to the persons of workshop, BUET, Dhaka, for cooperation in doing different fabrications.

The author gratefully acknowledges the cooperation that has been shown by the general manager, Bangladesh Sanitary and Insulator Factory, Mirpur, Dhaka, regarding this work.

The author expresses his gratitude to the authority of Bangladesh Institute of Technology, Chittagong, to allow him to study in BUET, Dhaka. He is indebted to United Nations for offering a fellowship under the UNDP program.

Mr. Intaz Ali, draftsman, BIT, Chittagong, took great pains in drawing the diagrams and graphs and deserves sincere thanks. Thanks are also due to Mr. Shahadat Hossain who took the trouble of typing the thesis.

ABSTRACT

The Bijoypur white clay (BWC) is collected from mine in lump form. The collected materials are crushed to fine powder. This is kept in water for one week and then washed to remove silica and other insoluble ingredients. Two types of samples are prepared from the washed BWC. One is in the powder form for x-ray diffractometric (XRD) analysis, differential thermal analysis (DTA) and the other is in the pellet form at different pressures for electrical and microphotographic investigations. Both types of samples are heat treated at 773 and 1273 K for five hours.

The XRD analysis is done on as collected BWC, washed BWC, washed BWC heat treated at 773 K and washed BWC heat treated at 1273 K. The XRD analysis reveals that there are definite structural transformations due to heat treatment. Kaolinite transforms to metakaolinite and/or gamma-alumina structure. Surface microphotographic investigation reveals that porosity decreases with pressure.

The d.c. resistivity measurements are performed in the temperature range 300 to 673 K. The temperature dependence of the d.c. electrical resistivity shows electrolytic behaviour below 390 K and semiconducting above.

The activation energy values indicate that thermally activated hopping conduction mechanism may be operative in these materials.

The a.c. conductance and dielectric parameters are measured on washed BWC pellets, washed BWC pellets heat treated at 773 K and 1273 K prepared at pressures 2000, 3000 and 3500 psi. The measurements are carried out in the temperature range 243-398 K for the frequency range 1 kHz to 3 MHz. No loss peak is observed within the temperature and frequency ranges used in the present investigation. However, it is observed that slow relaxation processes are present in the material.

CONTENTS

CHAPTER - I INTRODUCTION

	Introduction	1
1.1	Geology of white clay (kaolinite mineral)	2
1.2	Importance of white clay	4
1.3	Bijoypur white clay (BWC)	8
1.3.1	Location, extent and topography	8
1.3.2	White clay (kaolin)	8
1.3.3	Deposition	9
1.3.4	Physical characteristics	10
1.3.5	Chemical characteristics	10
1.3.6	Reserves	11
1.3.7	Uses	11
1.4	Objectives of the present work	12
	References	14

CHAPTER - II LITERATURE REVIEW

2.1	X-ray diffraction (XRD)	15
2.1.1	Qualitative analysis	15
2.1.1.1	Procedure	15
2.2	Polarizing microscopy	17
2.2.1	Modes of observation in a polarizing microscope	18
2.2.1.1	Orthoscopic arrangement	19

2.2.1.2	Conoscopic arrangement	19
2.3	Differential thermal analysis (DTA)	20
2.4	D.c. conductivity	20
2.4.1	Electrical conduction mechanism in solids	22
2.5	Dielectrics and types of dielectrics	25
2.5.1	Dielectric dispersion	27
2.5.2	Phenomenology of dielectrics	30
2.5.2.1	Static fields	30
2.5.2.2	Time-dependent fields	33
2.5.3	Temperature as a variable	35
2.6	Literature review of previous works on kaolinite material	36
2.7	Review of previous works on Bijoypur white clay	42
	References	44
CHAPTER - III SAMPLE PREPARATION		
3.1	Collection of BWC	49
3.2	Method of BWC washing	49
3.2.1	Procedure	49
3.3	Drying and tablet preparation	50
CHAPTER - IV EXPERIMENTAL DETAILS		
4.1	X-ray diffractometer	52
4.1.1	X-ray investigation of the samples	52
4.1.1.1	Working procedure for taking XRD pattern	52

4.1.1.2	Formula for the calculation of interplaner spacing	52
4.2	Polarizing microscopy	52
4.2.1	Polarizing microscope	52
4.2.2	Procedure	53
4.3	DTA apparatus	54
4.3.1	Working procedure of DTA	55
4.4	D.c. electrical measurements	57
4.4.1	Keithley electrometer	57
4.4.2	Polisher	57
4.4.3	Die	57
4.4.4	Specimen chamber with an inbuilt heater	58
4.4.5	D.c. resistivity measurement	59
4.4.5.1	Experimental procedure	59
4.4.5.2	Precautions	60
4.4.5.3	Working formula	61
4.5	A.c. electrical measurements	62
4.5.1	Instruments used for a.c. conductance and dielectric measurement	63
4.5.2	A.c. conductance and dielectric measurement	67
4.5.2.1	Experimental procedure	67
4.5.2.2	Precautions	68
4.5.2.3	Working formula	68

CHAPTER - V RESULTS AND DISCUSSION

5.1	XRD analysis	70
5.2	DTA analysis	72
5.3	Polarizing microscopy	73
5.4	D.c. electrical measurements	74
5.4.1	Current-voltage (I-V) characteristics	74
5.4.2	D.c electrical resistivity	76
5.5	A.c. electrical measurements	79
5.5.1	A.c. conductivity	79
5.5.2	A.c. dielectric constant	80
5.5.3	Dielectric loss tangent	82
	References	84

CHAPTER - VI CONCLUSIONS

6.1	Conclusions	85
6.2	Suggestions for future work	86
	Appendices	88

CHAPTER - I

Introduction

Clay covers a huge range of natural substances differing greatly in appearance, texture and chemical and physical properties. Some, such as commercial kaolins, contain upto 90 per cent clay-substances, other such as certain brick clays, as little as 30 per cent. The justification for applying a single generic name to all of them is that they have certain important qualities in common. They are all plastic when wet; when merely dried they are all rigid, but will regain their plasticity when thoroughly rewetted; when fired they will become permanently nonplastic and mechanically stronger. The most abundant and accessible material on the earth's crust is clay. Early man was in constant touch with it. Having observed that, after heavy rain, clay left his footprints, he found he could shape it with his hands. He thus discovered that clay was plastic. Plasticity, the most important property of clay, made early man to realize the potentialities of this material which was the key to the foundation of ceramic products. Ceramic products touch upon our lives at widely differing points. Lavatory basins, synthetic diamonds and bricks, high-voltage insulators, resistors, radioactive waste absorbers, drain pipes and memory cells, spark plugs and blast-furnace lining - their variety makes the definition of ceramic difficult⁽¹⁾.

1.1 Geology of white clay (kaolinite mineral)

The source of clay forming minerals are aluminous rocks, especially those containing feldspar. The most important kaolin-forming rocks are the solidified acid magmas, such as granite and gneiss, which consist of orthoclase, quartz and mica, further the strongly acid residues of the granite-magma melt, pegmatite, which consist almost solely of orthoclase and quartz, and aplite an acid gangue of similar composition. Beside these archaean rocks, extrusive rocks may also function as kaolin formers - both eruptive and effusive types, e.g., liparite and quartz porphyry. Also basic archaean and eruptive rocks, such as andesite and porphyrite of Meissen and the gabbro of Neurode, can be transformed into kaolin and clay.

To discuss about white clay, firstly let us see what is clay. In order to answer this question we must first take a quick look at crystalline rocks such as granite and gneiss which form the greater part of the outer crust of the earth. The rocks are, in the main, heterogeneous mixtures of feldspar, quartz and mica, the most abundant component being feldspar. Feldspar is the name applied to a number of mineral aluminosilicates, the most common that of potassium ($K_2O.Al_2O_3.6H_2O.SiO_2$) and the next most common that of sodium ($Na_2O.Al_2O_3.6SiO_2$)⁽²⁾. There are two views about the origin of clays, one preferred by geologists, the other by chemists. In some deposits of china clays⁽³⁾, the mineralogical evidence shows that the potash feldspar first decomposes to secondary

kaolin formation from feldspar by leaching and for that of the formation of clays from solutions. The former would explain the formation of coarse-grained kaolin in primary deposits, the later that of fine-grained, colloidal, sedimentary clays. Both processes lead to the same thermodynamically stable end product.

1.2 Importance of white clay

The clays used in the ceramic industry may be simply divided into kaolins, which include China clay (white clay), and other clays. The kaolins are white and burn white. They have a grain size of about $0.5 - 2\mu$. Whereas the other clays are mostly colored and usually do not burn white. Before kaolins are used in ceramic manufacture the traces of parent rock remaining in kaolins must be removed by a costly washing process. Kaolin purified in this way often contains a very high percentage of clay substance (about 96-99 percent).

Even if we eliminate the accessory minerals in clays, it remains extremely difficult to devise a useful classification based on their ceramic properties; hitherto all attempts at a rigid classification have failed. Clays must be arranged in order on the basis of their chemical analysis or their softening point or their melting behaviour, but such classification do not suffice to explain their workability in the raw state, which is just as significant : workability or plasticity is in fact their most important ceramic property apart from refractoriness.

The clay is being diversively used in making ordinary bricks, lavatory basins, low and high tension electric post insulator, radioactive waste product absorber, spark plugs, blast-furnace lining etc. depending on nature of clay. At 20°C insulator porcelain has a volume resistivity of about 10^{16} Ohm-m, which is several thousand times as great as that of celluloid and between ten and a hundred times as great as that of rubber or of common glass containing soda. However insulating materials behave in the opposite way to conducting materials in that their resistivity decreases as their temperature rises, and in the case of porcelain a rise of temperature from 293 to 473 K reduces the volume resistivity 10,000 fold. The resistivity of any insulator must therefore sufficient to meet the demands made on it at the highest temperature to which it will be exposed in service. High volume resistivity is of little use if current can flow over the surface of an insulator from one side to the other. Surface resistivity must also be adequate. In fact, that of unglazed porcelain is good enough for all practical purposes, provided the atmosphere is dry; but in a very humid atmosphere unglazed porcelain with a fairly rough surface will collect a film of water and dirt, which may cut down its surface resistivity in dry conditions, and which increases it by about a hundred fold at very high humidities. For this reason ceramic insulators are glazed to provide a suitably smooth surface; water repellent silicon finishes have a similar

effect, though they are less permanent than a glaze.

Although excellent for insulation at lower frequencies, porcelain is far from being the ideal insulating material where high frequencies, or high temperatures, or both, are involved. With increasing temperature its conductivity rises steeply; at higher and higher frequencies it transforms more and more electrical energy into heat, with a corresponding loss of power. Yet ever since the beginnings of large-scale power production there has been a growing need for electrical insulation at high temperatures in all kinds of things, from domestic heaters to electric furnaces; and such modern means of communication as radio, television, and radar have created a vast demand for effective high frequency insulators. Prominent among the devices demanding new insulating materials was the spark plug. As internal combustion engine improved, the early porcelain spark plugs were no longer good enough, but then ceramists were beginning to develop alumina ceramics, which are now the most widely used of all new ceramic materials. In their latest form for spark plugs, alumina ceramics contain between 95% and almost pure alumina (Al_2O_3).

Ceramics are also widely used in the manufacture of electrical capacitors. Early condensers of the kind used in the radio receiving sets of the 1920s, consisted of metal plates separated by air. If high capacities were needed they had to be big and bulky because of the low dielectric constant of the air between the plates. (Dielectric constant, or

relative permittivity, is a measure of the amount of electrical stress that a given amount of material will store.) If air is replaced by some material with a much higher dielectric constant, then it is possible to make less bulky capacitors with greater capacity. Many different materials have been used, including porcelain, mica and paper. If the dielectric constant of air is taken as one, then that of porcelain is six to seven, and that of mica much the same.

Electrical ceramics have yet another important use, as supports for resistance elements. Where high resistances are used, perhaps in the form of a fine film of metal or carbon, and particularly where they are to operate at high temperatures, the support must have a very high resistivity, otherwise it will partially short-circuit the resistance element. Porcelain containing only alkali-free glass phases have been developed for such purposes.

In our country, Bijoypur white clay (BWC) is being utilized for the manufacture of various ceramic products and in processing rubber by many industrial units of Bangladesh. The mottled variety of white clay (kaolin) which is slightly sandy is used for making fire bricks.

The results of the experiments carried out by the Ceramic Institute, Dhaka (1960) indicate the suitability of this clay for its use in making good type of pottery and low tension insulators. If the quality of the white clay (kaolin) is improved it may be suitable for making quality products

ceramics, high tension insulators. If the present pyrometric cone equivalent (PCE) value of 28 of white clay (kaolin) is raised to around 33, it will be suitable for the manufacture of super duty bricks useful for blast furnace and many other such purposes. If the plasticity of the white clay (kaolin) is raised, its workability will be better, with the enhancement of brightness this clay may be used for paper industry also if other properties are favourable⁽⁶⁾.

1.3 Bijoypur white clay (BWC)

1.3.1 Location, extent and topography

Actually the clay is named after the location where it is found. The white clay deposits are exposed in a series of hillocks from Bhedikura in the west to Gopalpur in the east in a 10.5 km long narrow strip of about 610 m (fig 1.1). The area between Gopalpur and Bhedikura comprises a series of low rounded hillocks. These hillocks are separated by shallow, wide valleys. The maximum and minimum heights of the hillock are 43 m and 15 m respectively above mean sea level. The valleys are on the average 12 m above mean sea level.

1.3.2 White clay (kaolin)

White clay (kaolin) occurs in several layers with alternating sandy clay, sandstone and pebbly sandstone. White clay is grey to greyish-white mottled with pink, yellow and red color. This mottling is observed at and a few feet below the surface, after which the white clay is bluish-grey. In

most places the white clay is smooth and soapy to feel but at places it is gritty. It breaks irregularly and does not slake in water. The white clay is sticky and plastic when wet but becomes hard on drying. It is massive, jointed and fractured. At some places the white clay is sandy.

1.3.3 Deposition

Source, origin, structure, lithology, mode of occurrence and texture of the white clay indicate that it has been transported and deposited and its source is not far away. From the following considerations it seems that the source materials of white clay are in the Indian side and that it is of sedimentary origin⁽⁶⁾ :

(a) There is no material immediately below the white clay layers from which it can be formed. It is likely that the archaean gneiss and some other acidic rocks occurring in the shilling front of India may be their source materials.

(b) White clay layers are not much thick and they occur in lenses. White clay lenses are generally found within sandstone layers which are continuous for about 10.5 km. This suggests that white clay of the area was not deposited in-situ, rather it is sedimentary and transported.

(c) There are small pockets of sandstone in some of the white clay layers. It indicates that these layers were transported and deposited not far from the source area.

(d) Most of the white clay layers gain thickness with depth along the dip. This leads to infer that they were

transported and deposited in gentle slope of the basin.

(e) The presence of free iron and silica in the white clay deposit is indicative of its source being not far from its place of deposition.

1.3.4 Physical characteristics

Bijoypur white clay is light grey to grey and turns whitish on exposure to sun. Near the surface it is pinkish with yellow patches. It is mostly soapy to feel but at places gritty. It breaks irregularly into small fragments and flat pieces. The clay is sticky and soft when wet and medium hard on drying. It does not show any slaking behaviour in water. The specific gravity of the white clay is 2.55.

By infrared absorption spectroscopic study, M. Alim Biswas and co-workers⁽⁷⁾ of BCSIR, determined that Bijoypur white clay is kaolinite. Later by x-ray diffraction method the same conclusion was achieved.

The pyrometric cone equivalent (PCE) value of Bijoypur clay is 28 (1913 K), which indicates that when untreated it is not as good a refractory material as a good kaolin.

It is likely that PCE and plasticity of the clay may be enhanced, by washing and beneficiation free of fluxing ingredients like ferroginous materials, free silica and other materials.

1.3.5 Chemical characteristics

About 60% washed clay, 25% coarse sand 15% clay mixed with fine sand is found by washing Bijoypur clay obtained from

mine. And about 65.5% elutriated clay and 34.5% total of three categories is found by elutriation of the washed clay. The chemical analysis of Bijoypur clay is shown in Table 1.1^(*).

TABLE - 1.1

Different constituents present in BWC

Constituents	Bijoypur clay (raw)	Bijoypur clay (washed)	Bijoypur clay (elutriated)
SiO ₂ (%)	73.04	59.70	57.09
Al ₂ O ₃ (%)	19.10	29.44	30.04
Fe ₂ O ₃ (%)	1.40	0.34	0.32
CaO (%)	0.16	0.06	0.04
Na ₂ O (%)	0.30	0.22	0.21
K ₂ O (%)	0.18	0.15	0.11
TiO ₂ (%)	Trace	Trace	Trace
Ignition loss(%)	5.80	9.98	11.99

Several samples of Bijoypur white clay were studied by Kairols, Mamed Beg Ogli and M. A. Zaher^(*) by x-ray diffractometer, DTA and electron microscope. They found that the white clay having grain size less than 1×10^{-6} m is composed approximately of 90 per cent kaolinite, 10 per cent illite and trace of chlorite.

1.3.6 Reserves

The reserve of white clay of Bijoypur area is given in Table 1.2.

1.3.7 Uses

Bijoypur white clay is being utilized for the manufacture of good types of pottery and low tension insulators by different industrial units of Bangladesh. By increasing the

TABLE - 1.2

Reserve of WC in Bijoypur

Depth in meters	Reserve of white clay in tons
Upto 15	6,19,500
Upto 30	12,39,000
Upto 45	18,58,500
Upto 60	24,78,000

present PCE value to arround 33 it can be made suitable for the manufacture of high tension insulators, super duty bricks etc. Also by adding different proportion of graphite, pertex with white clay at different pressure and temperature it is possible to make electrical capacitors, resistors etc.

Some test revealed that mixing washed Bijoypur clay at definite proportion, it is possible to make whitewares (soft porcelain and earthen wares etc.) to Indian feldspar and quartz⁽³⁾.

1.4 Objectives of the present work

Since a good ceramic has potentials for application as semiconductors, insulators, high frequency dielectrics, in electronic circuits, etc., these need fundamental understanding of the electrical properties of locally available ceramic material, BWC which is a fundamental raw material. Thus, the objectives of the present study are :

a) to examine the x-ray diffractogram pattern of raw BWC,

- washed BWC and heat treated samples of BWC;
- b) to examine the changes which may occur during heating of washed and heat treated BWC by DTA technique;
 - c) to investigate the microstructure of the pellet of washed BWC and heat treated BWC by optical microscopy.
 - d) to investigate the d.c. electrical behaviours of washed BWC and heat treated BWC;
 - e) to study the frequency variation of the a.c. properties of the washed BWC with heat treated BWC.

References :

1. Herman Salmang, "Ceramics physical and chemical fundamentals," Butterworths & Co. Limited, London,(1961)
2. Maurice Chandler, "Ceramics in the modern world" Aldus books Limited, London,(1967)
3. Paul Rado, "An introduction to the technology of pottery," 2nd ed., Pergamon press, (1988)
4. Schwarz, R. and Trageser, G., Z. anorg. Chem, [215] 190 (1933)
5. Correns, C.W. and Von Engelhardt, W., Chem. d. Erde [12] 20 (1938)
6. Kairols Mamed Beg Ogli and M.A. Zaher, "White clay (kaolin) deposits of Bijoypur area, Netrakona district, Bangladesh, " Records of Geological Survey of Bangladesh, Vol.4, Part 3, (1985)
7. M. A. Biswas and A. K. Basak, Pak. J. Sci. and Ind. Research (Dhaka), [4] 118 (1961)
8. M. Qudrat-I-Khuda, M. Alim Biswas and A. K. Basak, "Beneficiation of Bijoypur (Mymensingh) clay," Pak. J.Sci. and Ind. Research (Dhaka), [1] 43 (1964)
9. M. Alim Biswas and Shamim Jahangir Ahmed, "Plastic, dry and fired properties of Bijoypur (Mymensingh) clay of white bodies," Pak. J. Sci. and ind. Research (Dhaka) [1] 81 (1964)

CHAPTER - II

2.1 X-ray diffraction (XRD)

X-ray diffraction is a tool for the investigation of the fine structure of matter. This technique had its beginning with Von Laue's discovery in 1912 that crystals diffract x-rays, revealing the structure of the crystal. At first, x-ray diffraction was used only for the determination of crystal structure. Later on, however, other uses were developed and today the method is applied not only to structure determination, but to such diverse problems as chemical analysis and stress measurement, to the study of phase equilibria and the measurement of particle size, to the determination of the orientation of the crystal or the ensemble of orientations in a polycrystalline aggregate.

2.1.1 Qualitative analysis

The powder pattern of a substance is characteristic of that substance and that forms a sort of fingerprint by which the substance may be identified. If there is a collection of diffraction patterns for a great many substances, one could identify an unknown by preparing its diffraction pattern and then locating the file of known patterns one which matched the pattern of the unknown exactly. The collection of known patterns has to be fairly large, if it is to be at all useful, and then pattern-by-pattern comparison in order to find a matching one becomes out of the question.

2.1.1.1 Procedure

After the pattern of the unknown is prepared, the plane

spacing d corresponding to each line on the pattern is calculated, or obtained from tables which give d as a function of 2θ for various characteristic wavelengths. Alternatively a scale may be constructed which gives d directly as a function of line position when laid on the film or diffractometer chart; the accuracy obtainable by such a scale, although not very high, is generally sufficient for identification purposes. If the diffraction pattern has been obtained on film, the relative intensities are usually estimated by eye, on a scale running from 100 for the strongest line down to 10 or 5 for the weakest. On a diffractometer recording the intensity is taken as the maximum intensity measured above background.

After the experimental values of d and I/I_1 are tabulated, the unknown can be identified by the following procedure⁽⁴⁾:

1. To locate the proper d_1 group in the numerical search manual.
2. To read down the second column of d values to find the closest match to d_2 . (In comparing experimental and tabulated d values it is always allowed for the possibility that either set of values may be in error by $\pm 0.01\text{\AA}$.)
3. Later the closest match has been found for d_1 , d_2 and d_3 , to compare their relative intensities with the tabulated values.
4. When good agreement has been found for the lines listed in

the search manual, locate the proper data card in the file, and compare the d and I/I_1 values of all the observed lines with those tabulated. When full agreement is obtained, identification is complete.

2.2 Polarizing microscopy

The polarized-light microscopy provides a powerful tool to study the optical properties of transparent, translucent and opaque materials by using the polarized light. Polarized light technique, in recent years, has wide application in research and industrial technology.

The polarizing microscope is essentially an ordinary compound microscope, with the difference that it has a revolving, graduated circular stage, a polarizing device below the stage, called the polarizer (upper polar) and a similar device above the objective, called the analyser (lower polar).

Each polar transmits light wave vibrating in one direction only and for most purposes the polars are oriented so that their planes of vibration are mutually perpendicular or parallel.

The incident light passes through the polaroid disc, the polarizer, and is thus constrained to vibrate in one plane only. The polarizer can be rotated in its own plane and a second polaroid disc, the analyzer, is mounted in the body tube of the instrument. The analyser can be rotated or withdrawn from the field of view to enable a sample to be viewed in unpolarized light. When both the polarizer and

analyser are in the "crossed position", and they will not permit light to reach the eye piece so long as the medium between them is entirely isotropic. This is because light emerging from the polarizer is completely extinguished by the analyser according to the principle of Malus in optics.

There is a compensator or tint plate, inserted in the body tube of the instrument. The tint plate made of gypsum plate (also called first-order red plate) is placed at an angle of 45° to the vibration planes of the polarizer and the analyser when they are in the crossed position.

The condensing lens system is situated between the rotating stage and the polarizer. Its primary function, as in the compound microscope, is to bring the incident light to a focus in the plane of the specimen.

The eye piece lens system, fitted to the microscope body is of the binocular type, having a X10 magnification. This together with the different objectives produces an overall magnification ranging from X25 - X1000.

The illumination of the microscope is provided with ^a6V, 15W low-voltage halogen bulb. The bulb is contained in a well ventilated housing with a circular opening for the emission of light.

2.2.1 Modes of observation in a polarizing microscope

Two modes of observations are available in a polarizing microscope: orthoscopic and conosopic.

2.2.1.1 Orthoscopic arrangement

A microscopic arrangement is said to be orthoscopic when a beam of parallel light rays are made to fall on the specimen crystal normally and all of them travel along the same crystallographic direction within the crystal. In this type of observation there are three combinations of polarizer and analyser that enable three different sets of observations and measurements to be made.

In accordance with their behaviour between crossed polars, all non-opaque substances can be divided into two groups, namely, isotropic and anisotropic substances. The former remains dark, like the rest of the field of the microscope whatever be their orientations. On the other hand, anisotropic substances will appear coloured on rotation in most orientations and only in certain definite positions will become dark.

2.2.1.2 Conoscopic arrangement

The conoscopic arrangement requires, in addition to the polarizer and analyser, the insertion of an Amici-Bertrand lens and a substage condensing lens. The former converts the microscope into a low-power telescope focussed at infinity. The latter causes the object on the stage to be illuminated by a cone of light rather than by a bundle of near-parallel rays as it is with orthoscopic case. Important additional informations may be obtained by passing a strongly convergent beam of light through the crystal when it is

possible, by various means, to examine the optical characters in many directions at once at the same time. This is done by viewing between crossed polars, not the image of the crystal, but another optical image formed in the principal focus of the objective by the strongly convergent beams of light. This image is called the interference figure. Each point in the field corresponds to a given direction through the crystal. In effect, the Bertrand lens and the eye piece constitute a system used to examine the pattern in the back focal plane in the objective.

2.3 Differential thermal analysis (DTA)

DTA technique is an important tool to study the structural and phase changes occurring both in solid and in liquid materials during heat treatment. These changes may be due to dehydration, transition from one crystalline structure to another, destruction of crystalline structure, oxidation, decomposition etc. The principle of DTA consists in measuring the heat changes associated with the physical or chemical changes take place when any substance is gradually heated. This technique was first employed by Le Chatelier⁽²⁾.

2.4 D. c. conductivity

Electrical conduction is the transport of charge carriers through a medium under the influence of an electric field. The rate at which an element of charge dQ is transported over an area A in a time dt is given by the current, $i = dQ/dt = nqV_dA$, where n is the number density of charge carriers, q is the

charge per carrier, and V_D is the drift velocity of the charge carriers. If we assume that the drift velocity under an applied field is proportional to the applied field, i.e., $V_D = \mu E$ and $i = nq\mu EA$, where μ ($m^2 V^{-1} sec^{-1}$) is the drift mobility and E ($V m^{-1}$) is the applied field. The conductivity ($Ohm^{-1} m^{-1}$) is defined by $\sigma = id/VA$, where d is the sample thickness in m , A is area in m^2 and V the applied voltage. Assuming the electric field E to be uniform across the medium, i.e., $E = V/d$,

$$\sigma = nq\mu \dots\dots\dots(2.1)$$

If there is more than one type of charge carrier the conductivity is

$$\sigma = \sum_i q_i n_i \mu_i \dots\dots\dots(2.2)$$

In any particular system the number and mobility of the charge carriers will depend upon the material and the experimental parameters of voltage, temperature and ambient atmosphere. If the material is crystalline or oriented, the conductivity will depend on the direction with respect to some molecular axis in which the measurement is made. These dependencies can be expressed by writing:

$$n = n(T, V);$$

$$\mu = \mu(T, V, Z); \text{ and } \sigma = \sigma(T, V, Z)$$

where T represents temperature, V the applied potential, and Z the direction in which the measurement is being made.

Phenomenologically, the conductivity is obtained by measuring the current flowing through a piece of the material

and using the sample dimensions to calculate σ from the equation :

$$\sigma = \frac{d}{AV} i \dots\dots\dots(2.3)$$

where $d(m)$ is the sample thickness, A its area (m^2), and V the potential across the material in volts.

The usual type of electrical measurement has involved measuring the current as a function of potential, temperature and in some cases ambient atmosphere. The conductivity and its changes with voltage, ambient atmosphere and temperature are then related to the physical processes thought to be occurring in the material. Frequently, it is found that the conductivity varies exponentially with temperature T according to the equation

$$\sigma = \sigma_0 \exp(-E_r/kT) \dots\dots\dots(2.4)$$

where k is the Boltzmann constant and E_r the activation energy.

The resistivity is the reciprocal of conductivity. Therefore,

$$\rho = \frac{1}{\sigma} = \rho_0 \exp(E_r/kT).$$

The activation energy E_r can readily be evaluated from the slope of the linear $\ln \rho$ vs. $1/T$ plot, which describes the nature and types of carrier involved in the conduction process.

2.4.1 Electrical conduction mechanism in solids

Electrical conduction in insulating solids may occur through the movement of either electrons or ions. There may be

contribution to the conductivity from several different types of carriers, notably electrons and holes in electronic conduction and cation and anion pairs in ion conduction. In most of the insulating materials, it is very difficult to observe any electronic conductivity and whatever conductivity there is, it usually depends on the movement of adventitious ions. Therefore (a) ionic conductivity and (b) electronic conductivity are all important in their own way in insulating solids. Again, the electronic conductivity may be of (i) band conduction and (ii) hopping (tunnelling) conduction within localized levels in the forbidden gap.

(a) Ionic conduction

In bulk material ionic conduction occurs due to the drift of defect under the influence of an applied electric field. The degrees of ionic impurities which may be totally ignored in the context of other properties may have a significant effect on conductivity. A theoretical expression may be derived, for the current density, flowing through a sample, on the basis of a simple model and is given by

$$j \propto \text{Sinh}(eaE/2kT) \dots\dots\dots(2.5)$$

where E is the electric field and "a" is the distance between neighbouring potential wells.

(b) Electronic conduction

(i) Band conduction

Electronic conduction in insulating solids may differ in several important ways from the more familiar kind in metals

and inorganic semiconductors. That is not to say that they are separate subjects and indeed, the well-known band theory of atomic lattice has provided the essential basis of concepts for the discussion of conduction in solids, as in polymers.

In crystalline solid like silicon, where many atoms strongly interact, splittings of energy levels occur. Sets of energy levels form two continuous energy bands, called the valence band and the conduction band.

(ii) Hopping conduction

Disorder in a lattice affects both the energetic and spatial distribution of electronic states. For a random distribution of atoms the density of electronic energy states tails into what is normally the forbidden zone and the electrons in these tails are localized. When the electrons are excited to higher energy, conduction via localized electron implies discrete jumps across an energy barrier from one site to the next as shown in fig 2.1. An electron may either "hop" over or "tunnel" through the top of the barrier; the relative importance of these two mechanisms depending on the shape of the barrier and the availability of the thermal energy. For variable range hopping the electrical conductivity is given by

$$\sigma = \sigma_0 \exp \left\{ -\left(T_0/T \right)^{\frac{1}{d+1}} \right\} \dots\dots\dots(2.6)$$

where "d" is the dimensionality of transport (e.g. d=3 for three-dimensional motion etc).

σ = conductivity, σ_0 = initial value of conductivity,
 T = absolute temperature and

T_0 = activation energy in terms of temperature.

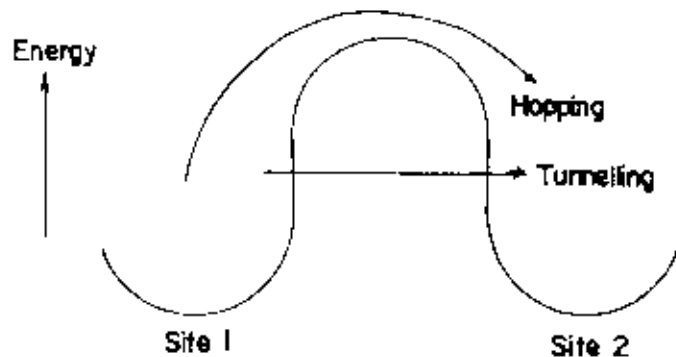


Fig 2.1 Diagram of electron-transfer mechanisms between adjacent sites separated by a potential-energy barrier.

2.5 Dielectrics and types of dielectrics

Dielectrics are materials which are electrical "insulators", i.e., have direct current resistivities greater than about 10^{10} Ohm-m. Insulators have the very useful ability to store electrical charge, a common device used for this purpose is a capacitor. In dielectric, electric charge do not move freely through the material. Although there are no perfect insulators, the insulating ability of fused quartz is about 10^{23} times as great as that of copper, so that for many practical purposes some materials behave as if they were perfect insulators.

The dielectric molecules are in general divided mainly into two classes (i) polar and (ii) non-polar. The polar molecules have permanent electric dipole moments while in the non-polar molecules, there exists no permanent dipoles.

In polar molecules the electric dipole moments tend to align themselves with an external electric field. Because the molecules are in constant thermal agitation, the degree of alignment will not be complete but will increase as the electric field is increased or as the temperature is decreased.

In non-polar molecules, they acquire them by induction when placed in an electric field. The external electric field tends to separate the negative and the positive charges in the atoms or molecules. This induced electric dipole moment is present only when the electric field is present.

Microscopically, when a dielectric material is placed in an electric field it takes a finite amount of time for the polarization to build up. This time may be as short as 10^{-14} second upto several days, depending on the material. The dielectric constant attained when the field has been applied for a sufficient length of time for the polarization to reach its limiting value is called the static dielectric constant ϵ_s . On the otherhand, if the polarization is measured immediately, after the field is applied, allowing no time for dipole orientation to take place, then the observed dielectric constant denoted by ϵ_0 will be low and due to deformational

effect alone. Somewhere, in between these extremes of time scale, there must be a dispersion from a high to a low dielectric constant.

In addition to charge storage all real dielectric materials use part of the energy stored in them to produce heat. The intrinsic property, which measures power loss is the "dissipation factor". Dissipation factor is defined as the ratio of energy lost to energy stored. Synonyms are $\tan \delta$ and $1/Q$. Related quantities are: loss index $\epsilon'' = \epsilon' \tan \delta$ and power factor = $\sin \delta$. Values of $\tan \delta$ range from less than 10^{-4} for low loss materials upto 1 for very lossy materials. The power dissipated per unit volume, P is

$$P = \sigma E^2 \dots\dots\dots(2.7)$$

where σ is the a.c. conductivity.

2.5.1 Dielectric dispersion

(a) Molar polarization in a dielectric


The molar polarization P_M of a material is found to depend on the frequency of the applied alternating electric field (fig 2.2).


In general, the polarizability can be written as the sum of four terms, i.e.,

$$\alpha_m = \alpha_e + \alpha_a + \alpha_d + \alpha_i$$

where e = electronic contribution

a = atomic contribution

d =  dipolar contribution

i =  interfacial contribution

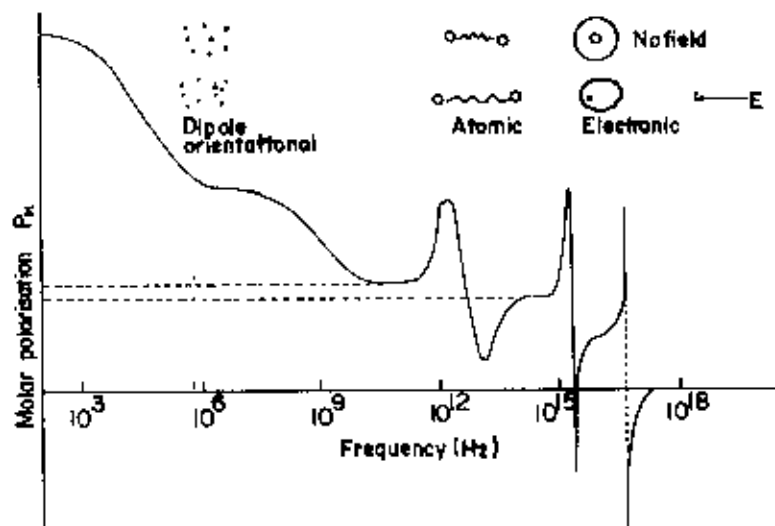


Fig 2.2 Dispersion of molar polarization in a dielectric (schematic)

The interfacial contribution is the slowest process having a frequency range from 10^{-4} to 10^4 Hz. The dipole orientation takes place in the frequency 10^1 to 10^{10} Hz, atomic polarization generally occurs near 10^{12} Hz while electronic contribution is effective at a frequency near 10^{15} Hz.

The dielectric techniques vary widely with the process one is interested to observe (fig 2.3).

(b) Lossy dielectrics

Most materials of which dielectric dispersion has to be measured dissipate energy in the form of heat in the

specimen. The specimen is then equivalent to parallel combination of resistance (R_p) and capacitance (C_p) as shown in fig 2.4.

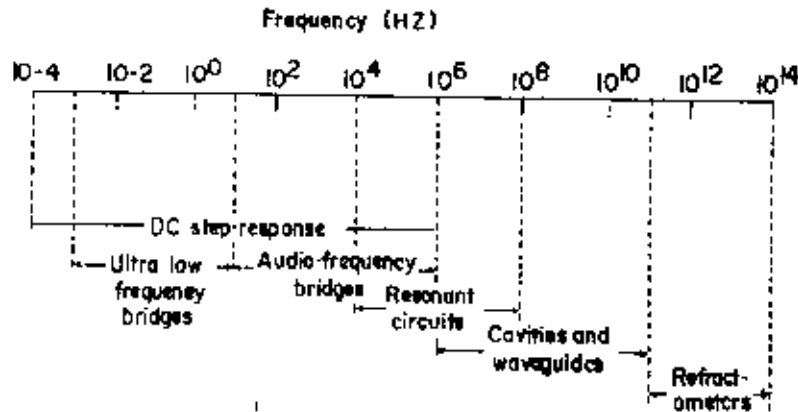


Fig 2.3 Chart of dielectric measurement methods.

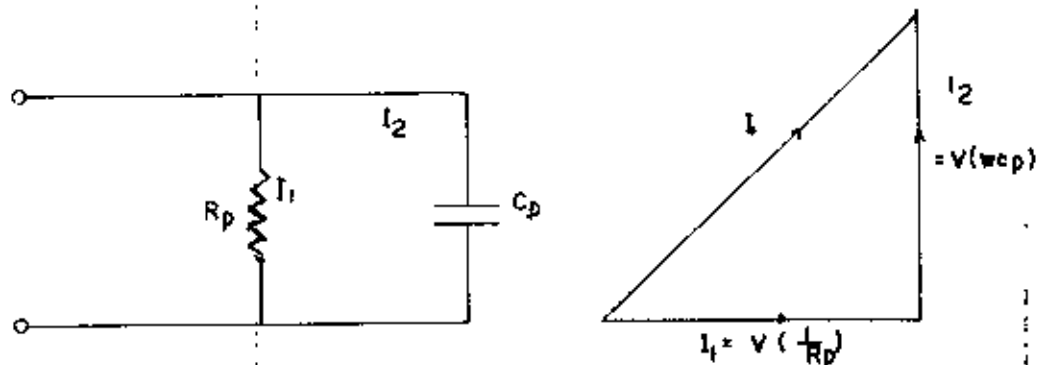


Fig 2.4 RC equivalent circuit for a dipolar material.

If an a.c. voltage (V) of frequency ω is applied across (R_p) and (C_p), a current

$$I = V(1/R_p + j\omega C_p) \dots\dots\dots(2.8)$$

flows. The admittance is

$$Y(\omega) = 1/R_p + j\omega C_p = G(\omega) + jB(\omega) \dots\dots\dots(2.9)$$

$$\text{and } \tan \delta = G/B = 1/\omega R_p C_p \dots\dots\dots(2.10)$$

Let a capacitor which in the absence of dielectric filling,

has a capacitance (C_0) be of negligible losses. When a lossless dielectric is added, the capacitance simply increases to ϵC_0 , where the dielectric constant is a real number.

When the dielectric is lossy it is convenient to redefine the dielectric constant as a complex number.

$$\epsilon^* = \epsilon' - j\epsilon'' \quad \dots\dots\dots(2.11)$$

The reason for using this definition is that when the expression for admittance Y of a pure capacitor is used,

$$Y = j\omega C = j\omega(\epsilon C_0) = j\omega(\epsilon' - j\epsilon'')C_0 = \omega\epsilon''C_0 + j\omega\epsilon'C_0 = G + jB$$

We get the form of eq. 2.9. The conductance

$$G_P = 1/R_P = G(\omega) = \omega\epsilon''C_0$$

$$\epsilon'' = 1/(\omega C_0 R_P) = G_P/\omega C_0 \quad \dots\dots\dots(2.12)$$

Similarly, $B(\omega) = \omega C_P = \omega\epsilon' C_0$

$$\epsilon' = C_P/C_0 \quad \dots\dots\dots(2.13)$$

Dividing eq. (2.12) by eq. (2.13), we get $\epsilon''/\epsilon' = G_P/\omega C_P$

$$= 1/(\omega C_P R_P) = \tan \delta \quad \dots\dots\dots(2.14)$$

2.5.2 Phenomenology of dielectrics

The macroscopic phenomenological theory of dielectrics^(3,4) is discussed here.

2.5.2.1 Static fields

The electric field E in electrostatics may be defined as the force per unit charge acting on an indefinitely small test charge placed in the field. A closely related quantity is the displacement field D . Which may be defined through Gauss law (in integral form) as

$$\oint_S \vec{D} \cdot d\vec{s} = q \quad \dots\dots\dots(2.15)$$

where q is the charge within a volume enclosed by the surface s . If eq. (2.15) is applied to a single point charge in vacuum by integrating over a sphere of radius R , and if we keep in mind Coulomb's law, then in vacuum evidently E and D are related as

$$D = \frac{q}{4\pi R^2} = K_0 E \quad \dots\dots\dots(2.16)$$

where K_0 is a constant and is called the permittivity of free space. Its value is

$$K_0 = 8.854 \times 10^{-12} \text{ Farad/meter.}$$

In the case of two infinite plates in vacuum containing surface charges q of density σ , we have

$$\sigma = q/A$$

where A is the area of the plates.

From the symmetry, \vec{D} must be directed normal to the plates.

Then integration of eq. (2.15) gives $D \oint ds = \sigma A$

$$\text{or, } D = \sigma \quad \dots\dots\dots(2.17)$$

and from eq. (2.16)

$$K_0 E = \sigma \quad (\text{free space}) \quad \dots\dots\dots(2.18)$$

If a dielectric material is inserted between the plates, which contain surface charges σ , the effect of the electric field is to induce polarization in the material in such a way that the material remains neutral but induced charges σ' appear on the plates in addition to the original ones (σ) (fig 2.5).

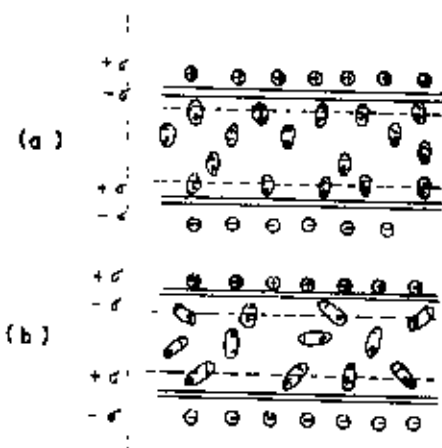


Fig 2.5 Induced surface charges (σ') appearing from polarization of a dielectric in an electric field (arising from placed surface charges σ): (a) Induced electronic or atomic polarization, (b) Polarization by spatial orientation of permanent dipole.

Thus the electric field between the plates is now

$$E = (\sigma - \sigma') / K_0 \dots\dots\dots(2.19)$$

However it is the essence of the definition of the displacement field D that q in eq. (2.15) means only "real" charges, deliberately placed as sources of external electric fields and q by definition does not include charges included in continuous dielectric media by external fields. Therefore, D retains its value in eq. (2.17). Thus comparing E and D

$$K_0 E = (\sigma - \sigma'), \quad D = \sigma$$

The induced surface charge density σ' is often called the polarization and given the symbol P , so that

$$D = K_0 E + P \dots\dots\dots(2.20)$$

Since $(A \sigma')d/v = P$ (where v is the volume), the polarization is the induced dipole moment per unit volume and is uniform through the dielectric. For the usual field strengths, P is proportional to E and

$$P = XK_0E \quad \dots\dots\dots(2.21)$$

where X is called the susceptibility and therefore

$$D = (1+X)K_0E \quad \dots\dots\dots(2.22)$$

we now define the dielectric constant as

$$D = \epsilon (K_0E) \quad \dots\dots\dots(2.23)$$

or, $\epsilon = 1 + X$

Note that for free space $X=0$ and $\epsilon = 1$. Since the capacitance C is defined as

$$C = q/v = (\sigma A)/v$$

and $v = Ed = d\sigma / K_0\epsilon$, where V is the voltage across the plates, then

$$\epsilon = (Cd)/(K_0A) \quad \dots\dots\dots(2.24)$$

or, $\epsilon = C/C_0 \quad \dots\dots\dots(2.25)$

where C_0 is the capacitance of the condenser with the dielectric removed.

2.5.2.2 Time-dependent fields⁽³⁾

For the case of a time-dependent field, the quantities D , E , and P in eq. (2.20) will be time dependent. Due to resistance to motion of charges there will be a delay in P in responding to a change in E . Considering this fact, Debye gave his famous molecular theory of dielectrics and arrived at the following equations⁽⁶⁾.

The real and imaginary parts of complex dielectric constant written as

$$\epsilon^* = \epsilon' - i\epsilon'' \quad \dots\dots\dots(2.11)$$

where

$$\epsilon' = \epsilon_0 + (\epsilon_R - \epsilon_0)/(1 + \omega^2\tau^2) \quad \dots\dots\dots(2.26)$$

$$\epsilon'' = (\epsilon_R - \epsilon_0)\omega\tau/(1 + \omega^2\tau^2) \quad \dots\dots\dots(2.27)$$

The above equations are known as the Debye equations.

For a single relaxation process the variation of ϵ' and ϵ'' with frequency as in equations (2.26) and (2.27) is given in fig 2.6.

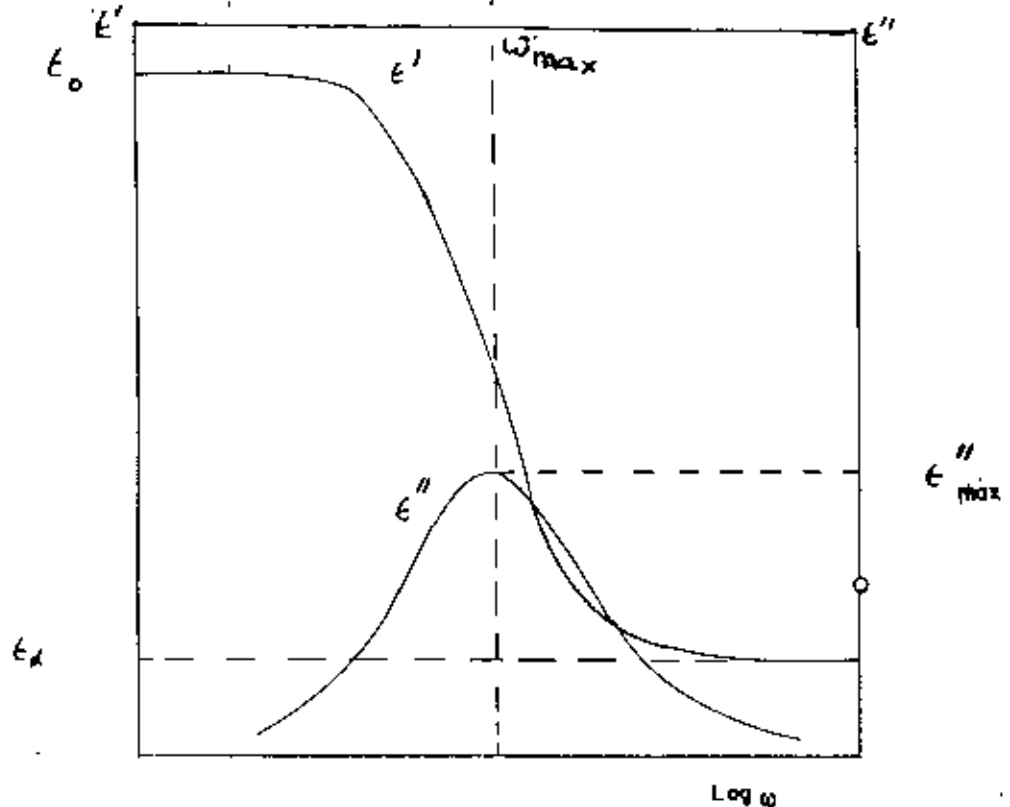


Fig 2.6 Debye dielectric dispersion curves

The dissipation factor is then given by

$$\tan\delta = \epsilon''/\epsilon' = (\epsilon_R - \epsilon_0)/(\epsilon_R + \epsilon_0)\omega\tau \quad \dots\dots\dots(2.28)$$

From eq. (2.27), it can be easily proved that the maximum loss

(ϵ''_{max}) will occur at ($\omega\tau = 1$) so that $\omega_{max} = 1/\tau$.

Locating the loss peak by an experiment will then give the relaxation time τ . Two parameters (in addition to ϵ_U) are required to characterize the dipolar relaxation, a relaxation strength (defined as ($\epsilon_R - \epsilon_U$)) and a relaxation time τ . While dipolar relaxation in many simple liquids following the early observations of Fuoss⁽⁶⁾ and Baker and Yager⁽⁷⁾.

2.5.3 Temperature as a variable

In general, the relaxation times are temperature dependent. A complete study of the dielectric properties might be represented by contour maps ϵ' or ϵ'' vs. frequency and temperature. More often in practice however, isothermal scans vs. log frequency are plotted as families on a single figure. The frequency at which ϵ'' is a maximum is determined (f_{max}) and treated as analogous to a rate constant. Thus a convenient summary of the effect of temperature on the relaxation process is a log f_{max} vs. $1/T$ or relaxation map^(8,9,10). When characterization is the principal goal, the loss plotted vs. temperature is necessary. If a family of such curves at few frequencies is generated, a log f_{max} vs. $1/T$ can be made and the activation energy can be determined. Plots of log f_{max} vs. $1/T$ from isothermal and isochronal scans need not be the same. When the relaxation strength ($\epsilon_R - \epsilon_U$) is strongly

temperature dependent or when the width of the loss process (cole-cole β parameter⁽¹¹⁾ or Fuoss-Kirkwood u parameters⁽¹²⁾) is strongly temperature dependent, the two types of scans can lead to significantly different relaxation maps and activation energies for the same materials^(13,14).

2.6 Literature review of previous works on kaolinite materials

Kaolin is an ionic solid which undergoes the following phase transformations on heat treatment: Kaolin \rightarrow metakaolin \rightarrow spinel type phase \rightarrow mullite. X-ray diffractogram reveals the existence of a spinel type phase when kaolin is heated at 1253 K. A controversy arises as to whether the spinel phase is γ -Al₂O₃ or Si-Al spinel. S. Mazumder and B. Mukherjee⁽¹⁵⁾ have shown by calculating the lattice energies of the structures confirms that the spinel phase is γ -Al₂O₃ and not Si-Al spinel, as the lattice energy of this phase is lower⁽¹⁶⁾. When metakaolin is heated at 1253 K, a considerable amount of silica is discarded, leaving behind a weakly crystalline, spinel type phase. The discarded silica also crystallizes into cristoballite around that temperature.

K.J.D. Mackenzie, I.W.M. Brown, R.H. Meinhold, and M.E. Bowden⁽¹⁷⁾ have examined the previously proposed metakaolin in light of the published experimental data and new information obtained by solid-state high-resolution ²⁹Si and ²⁷Al NMR. They proposed a new model for metakaolinite because the metakaolinite model suggested by Brindley and Nakahira⁽¹⁸⁾ suffers from some defects.

I.W.M. Brown, K.J.D. Mackenzie, M.E. Bowden, and R.H. Meinhold after proposing the model for metakaolinite, they made investigation on high temperature transformations of metakaolinite.

At about 1253 K, a weak diffuse x-ray pattern becomes distinguishable in many kaolinite samples, corresponding to a cubic phase and/or very poorly crystalline mullite. The nature of the cubic phase has attracted much discussion, despite the fact that its role in the reaction sequence (i.e., whether it is an intermediate or a byproduct has not been clearly established). Earlier workers identified the cubic phase as γ -Al₂O₃, bnt, arguing from considerations of structural continuity, Brindley and Nakahira⁽¹⁹⁾ suggested that this phase is a silicon-containing spinel of composition Si₈Al_{10.67}□_{5.33}O₃₂ rather than γ -alumina (Si₈Al_{13.5}□_{2.5}O₃₂). More recently this formulation of the spinel, with full Si occupancy of the tetrahedral sites, has been criticized from a number of viewpoints. The infrared measurements⁽¹⁷⁾, radial electron density (RED) measurements⁽²⁰⁾ and lattice energy calculations⁽¹⁵⁾ suggest that the γ -Al₂O₃ is the phase which will form. Both the NMR results and x-ray cell parameter measurements suggest⁽²¹⁾ that the initial mullite formed concomitantly with spinel is very silica poor, but on heating to higher temperatures, become progressively more silicons, eventually tending toward 3Al₂O₃.2SiO₂. Brindley and Nakahira sum up the overall picture of the reaction series. They

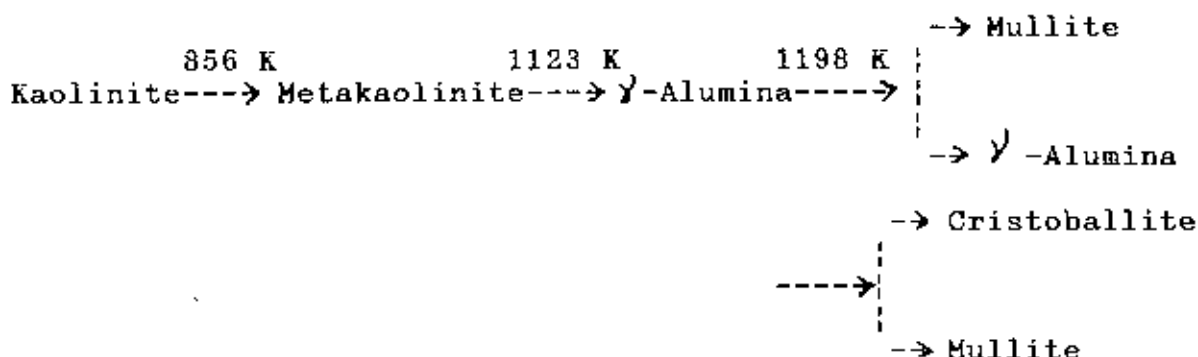
interpreted^(18,19,22) the thermal effects accompanying the reactions as follows :

- | | |
|-------------|---|
| 773 K | Dehydrations of kaolinite and formation of metakaolin, $2Al_2O_3 \cdot 4SiO_2$. |
| 1198 K | Metakaolin layers condense to form spinel type phase of approximate composition $2Al_2O_3 \cdot 3SiO_2$ with discard of silica; a "sharp" transformation. |
| 1323-1373 K | Spinel type structure transforms to a mullite phase, precise composition not certain, with further discard of silica, appearing visibly as cristoballite. |
| 1473-1673 K | Continued development of cristoballite and mullite, the later with lattice parameter consistent with the composition $3Al_2O_3 \cdot 2SiO_2$. |

In view of the continuity of these reactions, it is conceivable that some mullite may appear at a temperature lower than 1323 K.

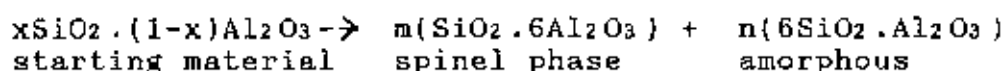
P.S. Nicholson and R.M. Fulrath⁽²³⁾ measured 9 kcal/mol for the 1253 K exothermic reaction enthalpy corresponds to the calculated heat of crystallization of silica at this temperature. They suggested, from the above observation, that most of heat release at 1253 K on firing kaolinite accompanies the reaction SiO_2 (amorphous) $\rightarrow SiO_2$ (β -quartz).

In an investigation the reaction is :



Many works have concerned the characterization of spinel phase formed by way of the kaolin mullite reaction sequence. However, there is uncertainty regarding its composition, and four opinions have been proposed :

1) Brindley and Nakahira⁽¹⁸⁾ propose the composition $3\text{SiO}_2 \cdot 2\text{Al}_2\text{O}_3$ for spinel phase. 2) The composition $2\text{SiO}_2 \cdot 3\text{Al}_2\text{O}_3$ is proposed by Chakraborty and Ghosh.⁽²⁴⁾ 3) Another opinion which states that it is $\gamma\text{-Al}_2\text{O}_3$. 4) Another chemical composition of spinel phase formed in the fired kaolin group minerals, reported by K. Okada and N. Otsuka⁽²⁵⁾, to be near $\text{SiO}_2 \cdot 6\text{Al}_2\text{O}_3$. They proposed the following decomposition reaction into spinel phase and amorphous compound :



They achieved the conclusion through x-ray quantitative analysis, infrared absorption spectra and analytical TEM methods.

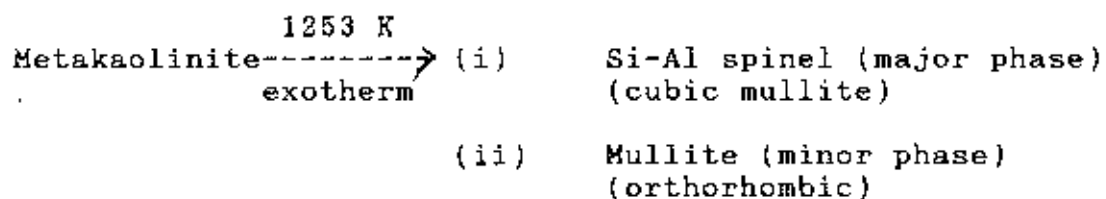
The crystallization behavior of Al_2O_3 in the presence of SiO_2 was investigated by A. K. Chakravorty and D. K.

Ghosh⁽²⁴⁾.

Recently Hoffman et al⁽²⁷⁾ reported that the 1233 K exotherm of single-phase gel is due to mullite formation only. But K. Okada⁽²⁸⁾ observed the spinel phase whose reflection were at about $2\theta=37^\circ$, 46° and 67° in $\text{CuK}\alpha$ as well as amorphous SiO_2 .

Comment on the Hoffman et al's work made by A. K. Chakravorty and D. K. Ghosh⁽²⁹⁾. The single-phase xerogel showed the 1233 K exotherm in differential thermal analysis (DTA) and weakly crystalline mullite in the diffractogram of gel heated to 1288 K. From this they (Chakravorty et al) concluded that the 1233 K exotherm of single-phase gel is due to mullite formation only. However, DTA of diphasic gel neither exhibited the 1253 K exotherm nor showed any crystalline XRD pattern in the case of gel heated to 1288 K. In reply⁽³⁰⁾ S. Komarneni et al said that their main objective was to show the difference between single and diphasic gels in their reactions and they did not comment extensively on the nature of the 1233 K exotherm.

A. K. Chakravorty and D. K. Ghosh reexamined⁽²⁴⁾ the 1253 K exothermic reaction for kaolinite and it has been established as follows :



- (iii) Aluminosilicate phase
(amorphous)
- (iv) Silica (amorphous)

In the another work⁽³¹⁾, the above explanation has been substantiated first by establishing the existence of the interrelationship between the development of two polymorphic forms of mullite from an Indian kaolinite with the geometry of the 1253 K DTA peak. By the XRD analysis along with the DTA they concluded that both polymorphs of mullite specially form during 1253 K peak formation.

K. Srikishna and G. Thomas⁽³²⁾ investigated the kaolinite-mullite reaction series in single crystal kaolinite characterized by transmission electron microscopy (TEM). The 1253 K exotherm was due to the formation of a spinel phase. At this temperature the mullite crystallites have also been observed with the spinel phase.

Another recent work⁽³³⁾ of the formation of mullite from single phase aluminosilicate gel has been performed using XRD. In situ measurements of conversion and separate infrared spectra data indicate that the amorphous single phase precursors form crystalline mullite at temperature as low as 1213 K (940°C).

Chibowski et al⁽³⁴⁾ found that physically adsorbed water remain on the surface up to 398 K, indicating most experimental surface energy values contain a film water component that decreases the value.

2.7 Review of previous works on Bijoypur white clay

Bijoypur white clay was discovered in February, 1957. The clay was beneficiated (washing and elutriation) and was chemically analyzed. It was found that through washing, most of the free silica and iron oxide present in the clay was removed and the washed clay was considerably upgraded and enriched in alumina. The process of elutriation, further, had reduced the content of free and fine silica in the washed clay and enriched the clay slightly in alumina content^(19,35). The infrared absorption analysis⁽³⁶⁾ of Bijoypur clay has shown that the clay is composed of a single mineral, kaolinite. The same conclusion was also achieved by the x-ray diffraction study⁽³⁷⁾. Plastic and dry properties of beneficiated and unbeneficiated Bijoypur clay were also reported⁽³⁸⁾. In the same report the grain size distribution of washed clay as well as some fired properties of unbeneficiated and beneficiated clay were also given. They indicated that the clay was suitable for use as a China clay in the manufacture of whitewares (soft porcelain, earthenwares etc.) especially when blended with other white-burning kaolins. In our country, very few works have been reported on the electrical properties of Bijoypur clay. One attempt was made to prepare the samples by the combination of graphite mixed Bijoypur clay in the ratio of 1:5 by weight at temperature between 1073-1123 K in air at different durations under a pressure of 10^5 gm/cm². They⁽³⁹⁾ measured the conductivity, dielectric loss, dielectric

constant, loss tangent etc. over the frequency range of 1 kHz to 40 kHz. They also suggested that low loss material could be prepared if the firing duration would have increased further for future possible applications as electric materials.

Another step was reported⁽⁴⁰⁾ to make resistor with the mixture of Bijoypur clay and graphite powder in varying proportion. Also to make the resistor mechanically rigid polyvinyl alcohol was used as a binder. The prepared resistors were heat treated in an oven upto 473 K because it was found that at temperature higher than 473 K the binding property of the binder (polyvinyl alcohol) decreases. The prepared resistors had values from 400 Ohm to 500 kilo-Ohm having wattage ratio 0.25W to 0.50W and also the tolerance of the prepared resistors are from down to -2% upto +7%. The resistors were made of mixtures of Bijoypur clay and graphite having different proportions from 1:1 to 7:1. When the portion of Bijoypur clay in the mixture increases in comparison with the graphite powder, the resistance increases gradually.

References :

1. B. D. Cullity, "Elements of x-ray diffraction", 2nd ed; Addison - Wesley Publishing Inc., Phillipines, (1978)
2. Chatelier, H. Le., Bull. Soc. France mineral, [10] 204 (1887)
3. H. Frohlich, "Theory of Dielectrics," 2nd ed; Oxford University Press, London, (1958)
4. C. P. Smyth, "Dielectric Behaviour and Structure," Mc Graw Hill, New York, (1955)
5. P. Debye, "Polar Molecules," Dover, NY, (1947)
6. R. M. Fuoss, J. Am. Chem. Soc. [63] 2410 (1941)
7. W. O. Baker and W. A. Yager, J. Am. Chem. Soc. [64] 2171 (1942)
8. M. E. Baur and W. H. Stockmayer, J. Chem. Phys. [43] 4319 (1965)
9. G. Williams, Trans, Far. Soc. [61] 1564 (1965)
10. S. Yano, R. R. Rahalkar, S. P. Hunter, C. H. Wang, and R. H. Boyd, J. Polym. Sci.; Polym. Phys. Ed., [14] 1877 (1976)
11. K. S. Cole and R. H. Cole, J. Chem. Phys. [9] 341 (1941)
12. R. M. Fuoss and J. G. Kirkwood, J. Am. Chem. Soc. [63] 385 (1941)
13. C. R. Ashcraft and R. H. Boyd, J. Polym. Sci. Polym. Phys. Ed. [14] 2153 (1976)
14. B. E. Read and G. Williams, Polymer [2] 239 (1961)
15. Reply, J. Am. Ceram. Soc., 69 [8] C-201 (1986)

16. S. Mazumdar and B. Mukherjee, "Structural Characterization of the Spinel Phase in the Kaolin-Mullite Reaction Series Through Lattice Energy," J. Am. Ceram. Soc., 66 [9] 610-12 (1983)
17. K. J. D. Mackenzie, I. W. M. Brown, R. H. Meinhold, and M. E. Bowden, "Outstanding problems in the Kaolinite-Mullite Reaction Sequence Investigated by ^{29}Si and ^{27}Al Solid-State Nuclear Magnetic Resonance: I, Metakaolinite," J. Am. Ceram. Soc., 68 [6] 293-97 (1985)
18. G. W. Brindley and M. Nakahira, "The Kaolinite-Mullite Reaction Series: II, Metakaolin," J. Am. Ceram. Soc., 42 [7] 314-18 (1959)
19. G. W. Brindley and M. Nakahira, "The Kaolinite-Mullite Reaction Series: III, The High Temperature Phases," J. Am. Ceram. Soc., 42 [7] 319-24 (1959)
20. A. J. Leonard, "Structural Analysis of the Transition Phases in the Kaolinite-Mullite Thermal Sequence," J. Am. Ceram. Soc., 60 [1-2] 37-43 (1977)
21. I. W. M. Brown et al, "Outstanding Problems in the Kaolinite-Mullite Reaction Sequence investigated by ^{29}Si and ^{27}Al Solid-State Nuclear Magnetic Resonance: II, High Temperature Transformation of Metakaolinite," J. Am. Ceram. Soc., 68 [6] 298-301 (1985)
22. G. W. Brindley and M. Nakahira, "The Kaolinite-Mullite Reaction Series: I, J. Am. Ceram. Soc., 42 [7] 311-314 (1959)
23. Patrick S. Nicholson and Richard M. Fulrath,

"Differential Thermal Calorimetric Determination of the Thermodynamic Properties of Kaolinite," J. Am. Ceram. Soc., 53 [5] 237-240 (1970)

24. A. K. Chakraborty and D. K. Ghosh, "Reexamination of the Kaolinite-to-Mullite Reaction Series," J. Am. Ceram. Soc., 61 [3-4] 170-73 (1978)

25. Kiyoshi Okada and Nozomu Otsuka, "Characterization of the Spinel Phase from $\text{SiO}_2\text{-Al}_2\text{O}_3$ Xerogels and the Formation Process of Mullite," J. Am. Ceram. Soc., 69 [9] 652-56 (1986)

26. Akshoy Kumar Chakravorty and Dilip Kumar Ghosh, "Crystallization Behaviour of Al_2O_3 in the Presence of SiO_2 ," J. Am. Ceram. Soc., 70 [3] C-46-C-48 (1987)

27. D. W. Hoffman, R. Roy and S. Komarneni, "Diphasic Xerogels, A New Class of Materials : Phases in the System $\text{Al}_2\text{O}_3\text{-SiO}_2$," J. Am. Ceram. Soc., 67 [7] 468-71 (1984)

28. K. Okada, Comment on, "Diphasic Xerogels, A New Class of Materials: Phases in the system $\text{Al}_2\text{O}_3\text{-SiO}_2$," J. Am. Ceram. Soc., 68 [3] C-85 (1985)

29. A. K. Chakravorty and D. K. Ghosh, Comment on, "Diphasic Xerogels, A New Class of Materials : Phases in the System $\text{Al}_2\text{O}_3\text{-SiO}_2$," J. Am. Ceram. Soc., 69 [8] C-202-C-203 (1986)

30. Sridhar Komarneni and Rustum Roy, "Reply," J. Am. Ceram. Soc., 69 [8] C-204 (1986)

31. Akshoy Kumar Chakravorty and Dilip Kumar Ghosh, "Synthetic and 980°C Phase Development of Some Mullite Gel,"

J. Am. Ceram. Soc., 7 [4] 978-987 (1988)

32. K. Srikrishna and G. Thomas, "Kaolinite-Mullite Reaction Series : A TEM Study," J. Mater. Sci. (UK), 25 [1B] 607-13, (1990)

33. D. X. Li and W. J. Thomson, "Mullite Formation Kinetics of a Single Phase Gel," J. Am. Ceram. Soc., 73 [4] 964-969, (1990)

34. Chibowski, Emol, Staszczuk and Piotr, "Determination of Surface Free Energy of Kaolinite," Clays Clay Miner., 36 [5] 455-461 (1988)

35. M. Qudrat-I-Khuda, M. Alim Biswas and A. K. Basak, "Investigations on Some Clays of East Pakistan Part I - Beneficiation of Bijoypur (Mymensingh) Clay," Pak. J. Sci. and Ind. Research, 1 [1] 43-48 (1964)

36. M. A. Biswas and A. K. Basak, Pak. J. Sci. and Ind. Research (Dhaka) [4] 118 (1961)

37. M. Nazrul Islam, "White Clay (Kaolin) Deposits of Bijoypur Area, Netrakona District, Bangladesh, vol. 4, part 3, (1985)

38. M. Alim Biswas and Shamim Jahangir Ahmed, "Investigation of Some Clays of East Pakistan, Part II - Plastic, Dry and Fired Properties of Bijoypur (Mymensingh) Clay of Whiteware Bodies," Pak. J. Sci. and Ind. Research, 1 [2] 81-87 (1964)

39. R. I. Sharif, Matiur Rahman Mian and Nurul Haque Mian, "Some Electrical Properties of Graphite mixed Bijoypur Clay

Materials Part-I," Bangladesh J. Sci. Ind. Res. XVII [1-2]
26-33 (1982)

40. J. Rahman and M. Z. Haque, "Preparation of Resistor by
Locally Available Bijoypur Clay," Dhaka University Studies, B,
33(2) : 179-181 (1985)

CHAPTER - III

3.1 Collection of BWC

The location of the BWC has been shown in fig 1.1 (cf: sec 1.3.1). The BWC is collected from the mine at Bijoypur area in the district of Netrokona. To collect the sample, in the form of hard lumps, the overburden of about 5 m thickness is removed.

3.2 Method of BWC washing

The method of washing of BWC as adopted in the laboratory scale is based on the principle of washing in a slow stream of water. The arrangement used for washing BWC is shown in fig 3.1. It consists of four large beakers (each with a capacity of about 8 litres) arranged in series so that each one lies a little below the level of the preceding ones. Each beaker has a drain tube near its upper edge, the tube being bent at right angles almost reaches the bottom of the beaker next to it. Such an arrangement maintains a constant flow of water and efficiently washes away the clay particles. The clay suspension, to be washed, is placed in the first beaker and the clay washed away in the suspension is collected from the last beaker.

3.2.1 Procedure


Half a kilogram of BWC lumps is manually crushed into coarse powder and is allowed to soak under water in a large vessel for about a week. Well-soaked BWC on thorough blunging in sufficient water is completely disintegrated and fine BWC particles together with the coarse particles of

impurities formed a thick suspension, which is then transferred gradually to the first beaker of the washing apparatus, situated at the top most position with respect to the other beakers. A steady stream of tap water is turned on. The rate of flow of water is so adjusted that the BWC suspension is sufficiently diluted and the BWC particles are efficiently carried away leaving behind the impurities at the bottom of each beaker and finally the last beaker contains the washed BWC suspension.

The impurities, in order of their size and weight, collected in different beakers and thus the BWC on washing yielded four fractions coarse sand, fine sand, BWC mixed with fine sand and the washed BWC.

3.3 Drying and pellet preparation

The beaker containing the washed clay suspension (4th beaker) is kept for about 3 days for settling. After settling water is removed and the beaker is initially allowed to dry in the sun and finally the BWC is dried in an electric oven at about 378 K. This dried sample is labelled as washed BWC.

The dried BWC sample is then ground  and is allowed to pass through 200 mesh. About .002 kg of this is then placed inside the die punch (fig 3.2). The BWC pellets of diameter .005 m are obtained with 2000 psi, 3000 psi and 3500 psi pressures by using a hydraulic pressure unit. The thickness of the pellet sample depends on the pressure applied. After removing the sample from the die punch its edges are then

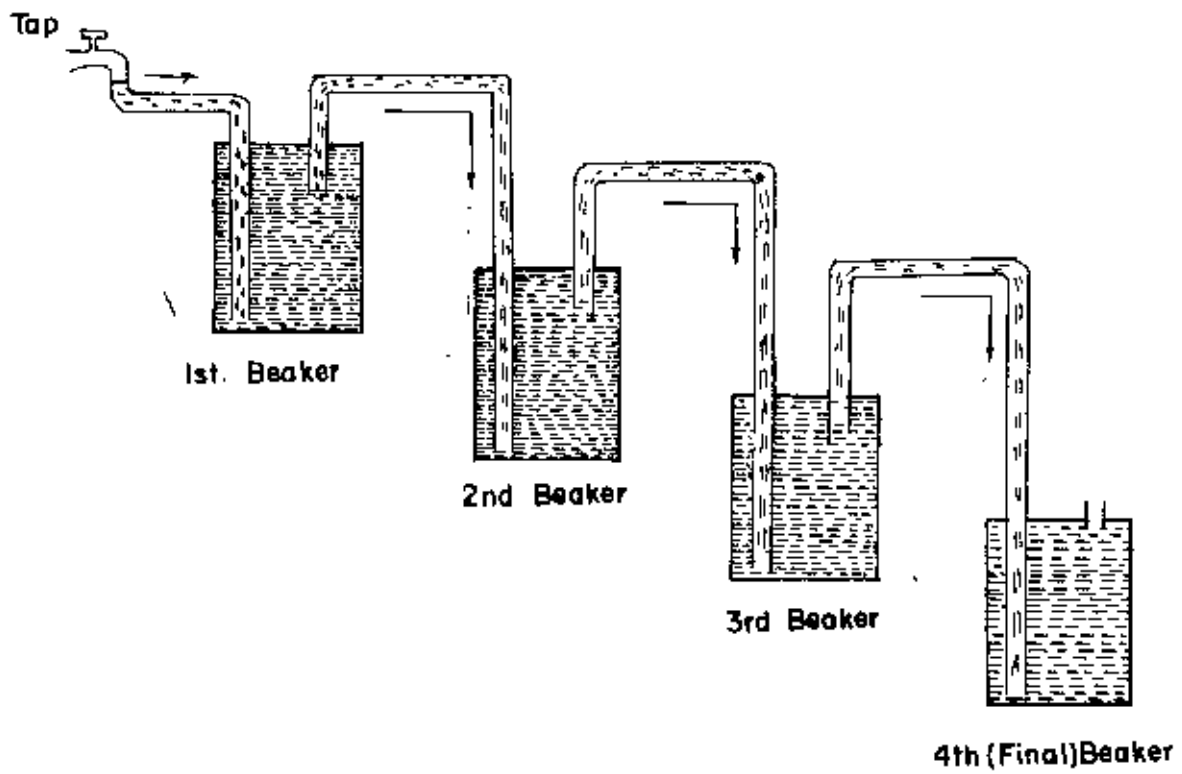


FIG 3-1 CLAY WASHING .

polished by a metallographic polisher (cf: sec. 4.4.2) and finally the polished sides are painted with silver deg to make electrodes for electrical contact. Some of the prepared samples are heat treated in a high temperature furnace (Department of Metallurgy, Bangladesh University of Engineering and Technology, Dhaka) at 773 and 1273 K. The different samples are designated as followed :-

Sample A : Raw BWC (as collected). [A1 - 2000; A2 - 3000 and

Sample B : Washed BWC. [B1 - 2000; B2 - 3000 and B3- 3500 psi]

Sample C : Washed BWC heat treated at 773 K. [C1-2000; C2-3000
and C3-3500 psi]

Sample D : Washed BWC heat treated at 1273 K. [D1-2000;
D2-3000 and D3-3500psi]

All the experiments are carried out on such samples.

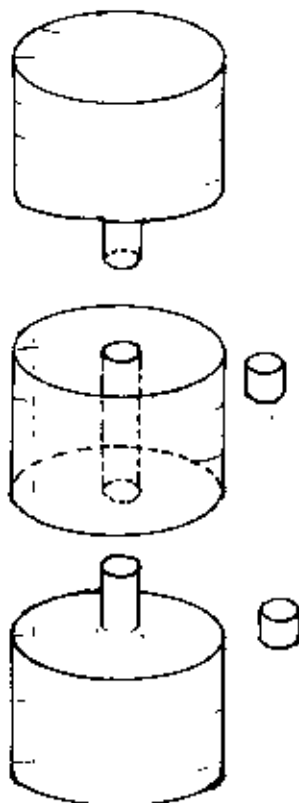


Fig 3.2 Die punch

CHAPTER - IV

4.1 X-ray diffractometer (XRD)

X-ray diffractometer (model JDX-8P) of JEOL LTD., Tokyo, Japan is used in this study.

Target is $\text{CuK}\alpha$ and the wavelength of x-ray radiation is 1.5418 \AA

4.1.1 X-ray investigation of the samples

4.1.1.1 Working procedure for taking XRD pattern

Samples are crushed into fine powder using mortar and pestle and the powder is sieved through 200 mesh sieve. Then x-ray diffractograms of different types of samples are recorded using the above mentioned diffractometer in the Department of Metallurgy, Bangladesh University of Engineering and Technology, Dhaka. Four XRD patterns are collected for BWC samples A, B, C and D.

4.1.1.2 Formula for the calculation of interplanar spacing

The Bragg equation for the first order diffraction is written as

$$d_{hkl} = \left[\frac{2 \sin \theta}{\lambda} \right]^{-1}$$

where, d_{hkl} is the interplanar spacing

θ is the angle of diffraction

λ is the wavelength of the x-ray radiation used for diffraction (i.e., $\lambda = 1.5418 \text{ \AA}$).

4.2 Polarizing microscopy

4.2.1 Polarizing microscope

In this study, a Reichert Metavert reflected polarized

light microscope of C. Reichert Optische Werke A. G., Austria is used. The eye piece lens system, fitted to the microscope body, is of the binocular type having a 10X magnification. This together with the different objectives produces an overall magnification ranging from 25X - 1000X. The illumination of the microscope is provided with a 6V, 15W low-voltage halogen bulb. The bulb is contained in a well ventilated housing with a circular opening for the emission of light. The photograph of the microscope is shown in fig 4.1.

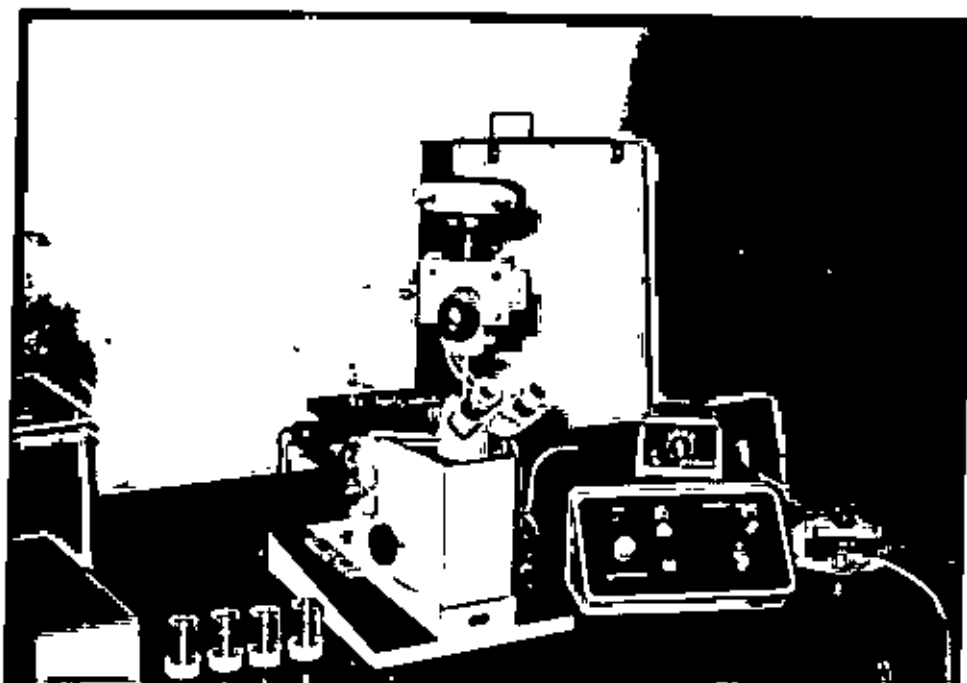


Fig 4.1 The Reichert Metavert reflected polarized light microscope.

4.2.2 Procedure

The samples, after polishing, are placed on the stage of the microscope. In the surface microscopy the pellet is

placed horizontally on the stage so that the reflected polarized light from the pellet surface can enter into the objective.

Fuji color film is used in this study. An automatic exposure time is programmed for the intensity of the reflected light. Exposure time is varied by using the various speed of films. Different areas are chosen to see the variation of the surface quality.

4.3 DTA apparatus

DTA apparatus consists of a thin wall refractory specimen holder made of sintered alumina with two adjacent cubical compartments of exactly the same size .01 m in length, (fig 4.2) one for the reference (inert) material and the other for the test material. The specimen holder is placed in the cavity of the heating block, which is made of fine grained refractory cement. This block is heated with a uniform heating rate using an electric furnace (9"x6"x9" deep). The input of current into the furnace is secured through the secondary of a variac transformer, which controls the current. Fine chromel-alumel wires (28 gauge) are used for thermocouples. A cold junction is used for thermocouples leads and the e.m.f. is recorded almost continuously, while the temperature of the inert material is measured at 3 minutes interval. It is essential to use perfectly dry materials as otherwise errors will be introduced in the analysis. Approximately 0.1g anhydrous alumina is used in the reference cup and the sample

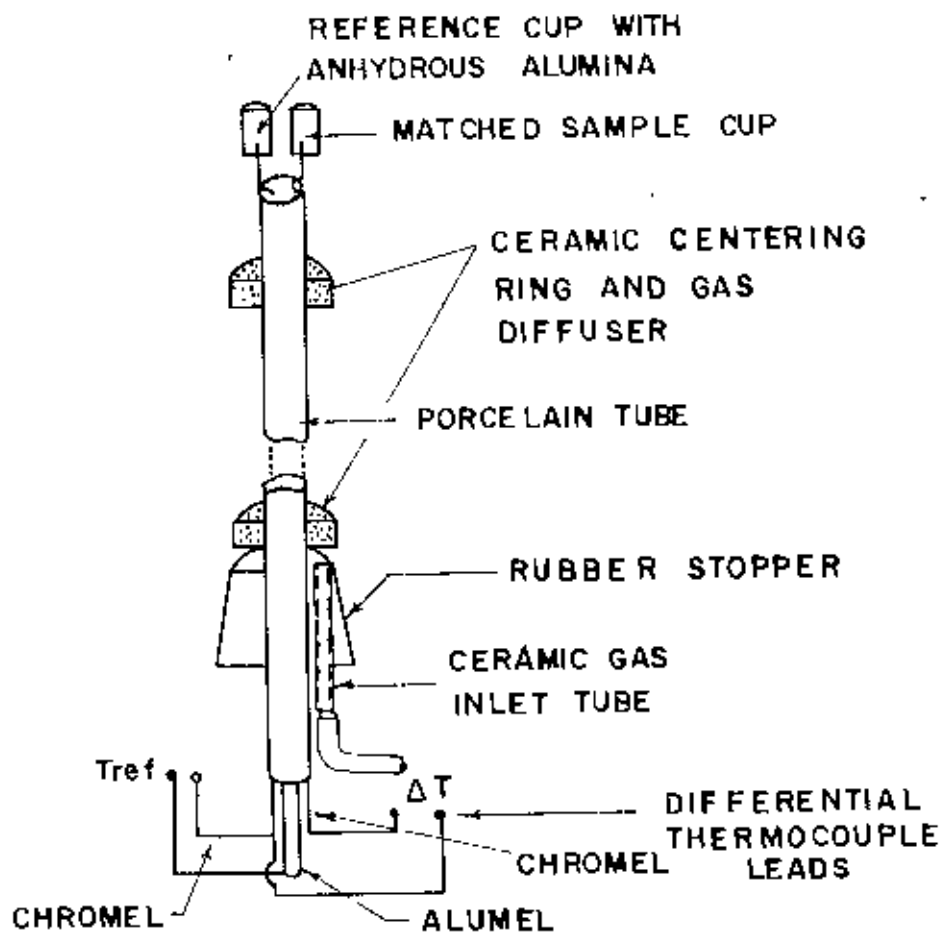


Fig. 4-2 DTA thermocouple assembly.

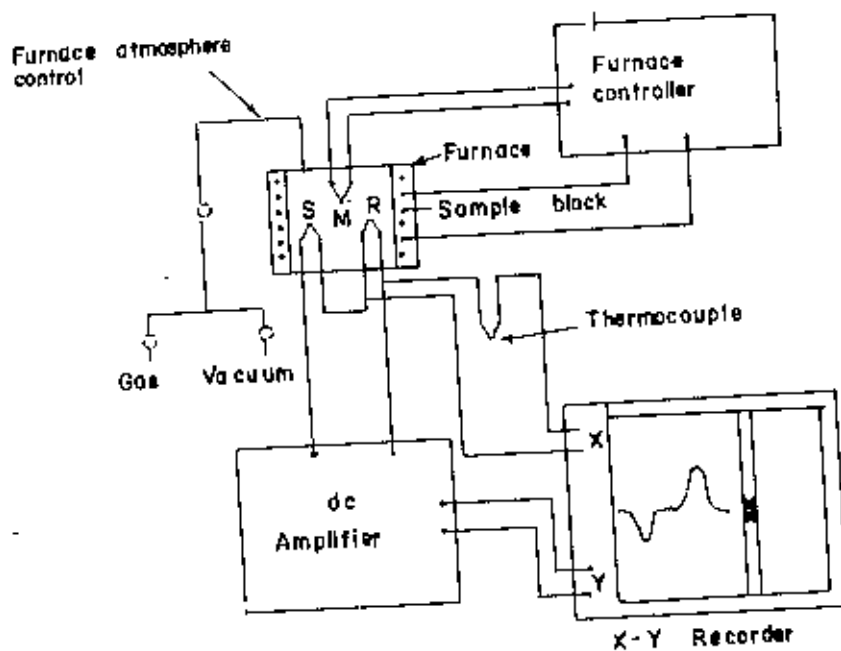


Fig. 4-3 Block diagram of a differential thermal analysis equipment, (S) sample thermocouple, (R) reference thermocouple, (M) monitor thermocouple.

weights varies over a range 0.05g to 0.125g, depending on their packed density. A heating rate of 10 K per minute (average) of the furnace is conveniently kept, and this gives satisfactory results in most cases. A block diagram of DTA apparatus is shown in fig 4.3.

The thermal analysis runs generally for 1 to 1.5 hours. Thermal analysis curves are obtained by plotting heating temperature and the difference between the temperatures of the test and the reference materials. From these traces the reaction temperature could be determined.

Melting and boiling points are indicated usually by a sharp endothermic peak. The temperatures of sublimation and decomposition were similarly given by exothermic peaks and in some cases, typical exothermic curves afforded useful information about the structural changes taking place in the material.

All experiments are run at atmospheric pressure in a continuous flow of purified inert gas. Gases are normally purged into the furnace chamber at the lower end through a purification train in which oxygen and water are removed by heated copper wool and exhausted from the top into a condensate trap for collecting the condensable volatile products.

4.3.1 Working procedure of DTA

When a sample and a standard inert reference material (e.g., Aluminium oxide, Al_2O_3) are heated or cooled at a

constant rate at the same environment, their temperature differences are measured as a function of time or temperature (as shown by the curve in fig 4.4). The temperature of the reference material, which is thermally inactive, rises uniformly when heated while the temperature of the sample stops rising when an endothermic reaction (e.g., fusion) occurs, because the heat supplied from outside is consumed by the reaction or varies differently due to evolution of heat during phase transitions or chemical reactions. And when the reaction is over, the sample temperature is much different from that of the ambient, and then the rate of increase of the sample temperature changes rapidly to catch the rate of rise of reference material temperature. The temperature difference ΔT is detected, amplified and recorded. The exothermic and endothermic reactions are generally shown in the DTA trace as positive and negative deviations respectively from a base line. So, DTA gives a continuous thermal record of reactions occurring in a sample.

The temperature at the sample holder is measured by a thermocouple, the signal of which is compensated for the ambient temperature and fed to the temperature controller. This signal is compared with the program signal and the voltage applied to the furnace is adjusted. Thus the sample and reference material are heated or cooled at a desired rate. The temperature in the sample holder is digitally displayed and is recorded on the recorder.

4.4 D.c. electrical measurements

4.4.1 Keithley electrometer

A digital Keithley electrometer (model 614 of Keithley Instrument Inc., Cleveland, Ohio, U.S.A.) is used for resistance measurement. The Keithley 614 electrometer is a versatile instrument which measures a wide range of d.c. voltage, current, resistance and electric charge. This electrometer can measure current as low as 10^{-14} amp. Voltage sensitivity is $10 \mu\text{V}$ to 20V with an input impedance of greater than 5×10^{13} Ohms. Resistance sensitivity of this model is from 1 Ohm to 2×10^{11} Ohms using the constant current technique.

4.4.2 Polisher

A metallographic specimen polisher type MSP-2 of Shimadzu Scientific Instrument Company Ltd. Japan, is used to polish the samples. CAMBIMENT special silicon carbide grinding paper with grit numbers 320, 400 and 420 are used.

4.4.3 Die

Die is the shaping unit of powder specimen. Die may be of different shape and size depending on the required specimen dimension. To prepare samples of required dimension, a die is designed and fabricated as shown in fig 3.2. Two steel bars of same diameter (.05 m) are used for the fabrication of the die. A circular hole (female) of diameter .01 m and thickness .005 m is dug on to one of the bars using a lathe machine and the other steel bar is cut to fit the inner dimension of the female which acts as male. Two cylindrical bars of length

.005 m and diameter .01 m are also made between which sample powder is to be placed for pressing.

4.4.4 Specimen chamber with an inbuilt heater

Specimen chamber and the heater are designed and fabricated in the workshop of Bangladesh University of Engineering and Technology, Dhaka. A schematic diagram of the chamber alongwith its accessories is shown in fig 4.5. This unit is basically consists of three main parts, namely, the iron tube, the sample holder and the electric heater.

An iron tube having inner diameter of .06 m and of length .3 m is used. The lower end of the tube is closed by welding a circular piece of iron sheet. At the upper end of the tube one flat iron sheet (.1 m x .1 m) with a circular hole (diameter .06 m) at its centre is welded. Another iron sheet with a hole of the same dimension is welded to an iron tube of diameter .06 m and of length .05 m. A rubber gasket is placed in between the two iron sheets. The upper portion can be fixed to the lower portion by screws. The top opening is closed tightly with a perspex stopper. Two copper leads (electrodes) which hold the specimen holder, two leads for heater connection and the thermocouple are passed through the perspex stopper.

A thick layer of mica sheet is placed on to the inside wall and bottom of the iron tube for electrical insulation.

A nicrome heating coil is wound around the outer wall of a pyrex tube of diameter .04 m and of length .1 m. The coil

is covered with China clay. This heater is placed at the bottom of the specimen chamber and the heater terminals are connected to the leads passing through the stopper. For this experiment a Chromel-Alumel thermocouple is used.

4.4.5 D.c. resistivity measurement

4.4.5.1 Experimental procedure

(i) Direct method

A Keithley 614 electrometer (cf: sec. 4.4.1) is used for the direct measurement of resistance at different temperatures. For raising temperature, the chamber of the specimen is heated by the inbuilt electric heater within the specimen chamber. Resistance is measured at every 0.1 millivolt increase of thermocouple reading from room temperature to 673 K depending on different samples. This operation is repeated for different samples. The experimental arrangement is shown in fig 4.6.

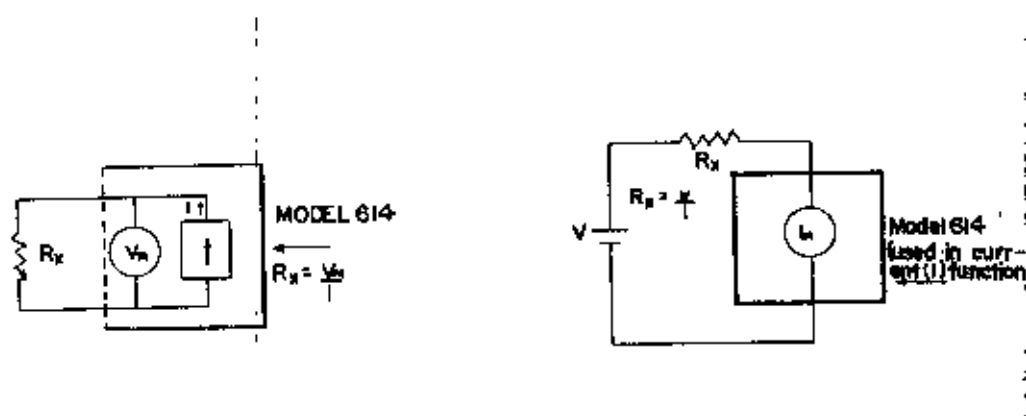


Fig 4.6(a) Constant current method employed by the model 614

(b) Technique for measuring resistance $> 10^{11}$ Ohm

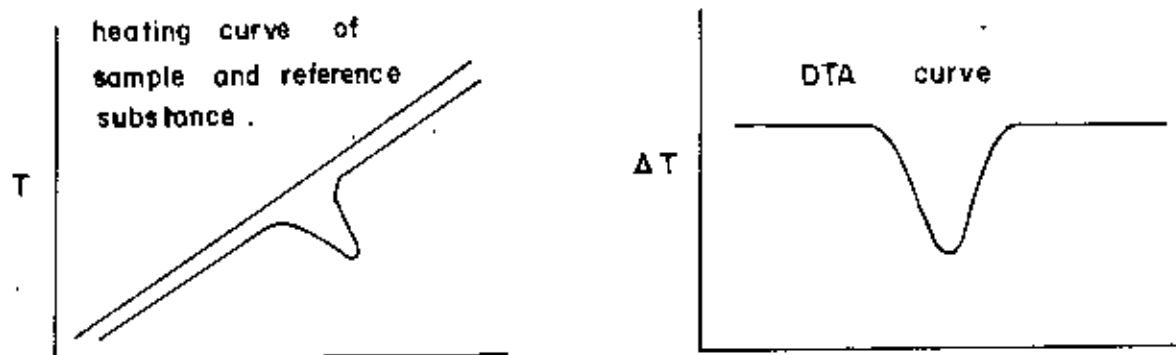


Fig. 4.4 Typical DTA trace

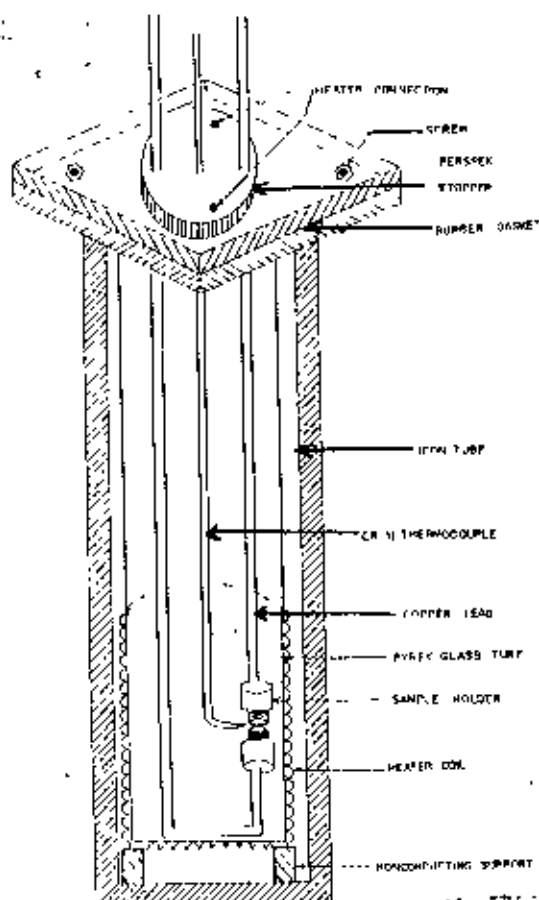


FIG. 4.5 THE SPECIMEN CHAMBER WITH BUILT HEATER

(ii) I-V method

Since clay is highly resistive, the direct method of measuring the conductivity is not the best way to choose because in that case the voltage across the specimen is not known. The Keithley electrometer is connected parallel to measure the voltage drop across the resistance R. A constant current d.c. power supply is used to supply desired voltage. Firstly, the voltage drop across the resistance is recorded by varying the total voltage with the aid of the T.P.S. From these set of readings the voltage drop across the specimen is then found out by subtracting the voltage across resistance from the total voltage and finally the current across the specimen is calculated by using the following relation :

$$I_s = \frac{V_R}{R} \dots\dots\dots(1)$$

where, V_R = voltage across the resistance (R)

R = resistance in series with the specimen

I_s = current through the specimen

From these sets of data the various curves are drawn.

4.4.5.2 Precautions

Precautionary measures are necessary at every step of any such measurement. First of all it is ensured that the chamber of the specimen holder is dried otherwise error would be introduced in the readings. The sealing is checked from time to time for the confirmation that no moisture from

atmosphere entered into the chamber. The measurements have to be done carefully so that the specimen did not touch the body of the chamber. Heating is done carefully for the temperature variation so that the rate does not exceed 0.4 K/min for ensuring that the temperature of the specimen and the thermocouple are approximately the same. The chamber is properly screened to avoid pick ups. Continuous care is taken against any abrupt disconnection of power supply.

4.4.5.3 Working formula

The resistance of the specimens is obtained from the data of the I-V method by the relation :

$$r_s = \frac{V_s}{I_s} \dots\dots\dots(2)$$

where, V_s = voltage drop across the specimen,
 I_s = current through the specimen and
 r_s = resistance of the specimen.

Resistivity ρ is calculated from the measured resistance of the sample, from the thickness of the specimen and the area of electrodes by using the following relation :

$$\rho = r_s \cdot \frac{A}{d} \dots\dots\dots(3)$$

where, r_s = resistance of the specimen,
 d = thickness of the specimen and
 A = area of the electrodes.

Then, the curves $\log_{10} \rho$ vs. $1/T \text{ K}^{-1}$ drawn.

4.5 A.c. electrical measurements

Transformer ratio-arm bridge, a audio-frequency bridge, which is very convenient to use in a.c. measurements is shown schematically in fig. 4.7. This bridge uses inductive ratio arms to compare the unknown directly with standard components. The voltage transformer is energised by an oscillator connected to its primary winding and develops one voltage V_1 between the unknown impedance Z_u and the neutral (earthed) line, and a second voltage V_2 , 180° out of phase with the first, across the standard Z_s . The currents I_1 and I_2 flowing through Z_u and Z_s are then V_1/Z_u and V_2/Z_s respectively. When these currents are equal they combine, on account of their phase difference, to produce zero core flux in the current transformer, and the detector indicates a null. The circuit has two big advantages: (a) impedances between the unknown and earth merely shunt the low resistances of the voltage and current transformers and do not affect the bridge balance, so that long screened leads and guarded electrodes can be used; (b) the voltage transformer can be tapped very accurately to obtain decade ratios, so that only a few standards are required. The principal drawback is that full sensitivity is restricted to the small frequency range for which the transformers are designed.

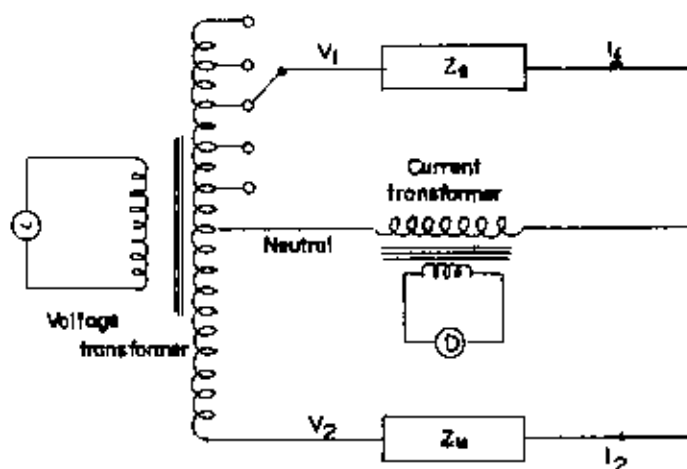


Fig 4.7 A simplified circuit diagram of a transformer-ratio-arm bridge.

Below about 20 Hz transformers become very inefficient and more specialised bridges are necessary. Below about 10^{-2} Hz bridge balancing also becomes a very slow business, because the period of each cycle is so long that one has to wait a long time after each readjustment of the bridge to see the resulting change in the amplitude of the output signal at the detector. The frequency range can be extended down to about 10^{-3} Hz, however, by balancing the bridge during just part of a cycle using a phase-sensitive detector.

At high frequencies, bridges can still be used provided that special precautions are taken to eliminate the effects of stray inductances which become very large, but it is usually better to adopt a resonance method above 10^6 Hz.

4.5.1 Instruments used for a.c. conductance and dielectric measurement

The a.c. bridge used for the present measurement is of ANDO ELECTRIC CO. LTD., TOKYO, JAPAN (Fig 4.8). Its photograph

92028

is shown in (fig 4.9).

The whole system is composed of the following units.

(i) Type WBG-9 oscillator (AS-76182)

This apparatus is an oscillator suited for use as the signal source for a dielectric loss measuring set. The oscillator frequencies are 30, 50, 60, 110, 330, 1k, 3k, 10k, 30k, 100k, 300k, 1M and 3M Hertz. This apparatus is used in conjunction with a type BDA-9 null detector, for the measurement on the basis of synchronous selection.

(ii) Type TR-10C dielectric loss measuring set

This unit is used for the variation of the capacitance and conductance components transformer ratio-arm bridges are mounted inside it for matching the frequency range.

(iii) Type BDA-9 null detector

(iv) Type TO-19 thermostatic oven (AS-20669)

This device is a thermostatic oven for measurement of temperature characteristics of various dielectrics, which provides variable temperature from 203 K (using liquid CO₂) to 473 K. The temperature is regulated by a PID controller. Also this device allows easy mounting of measurement electrode of specimen with plug in facilities.

(v) Type SE-43 electrode (AS-20646)

It is a three terminal electrode used for mounting the specimen. It is kept into the thermostatic oven for connection of the specimen during measurement.

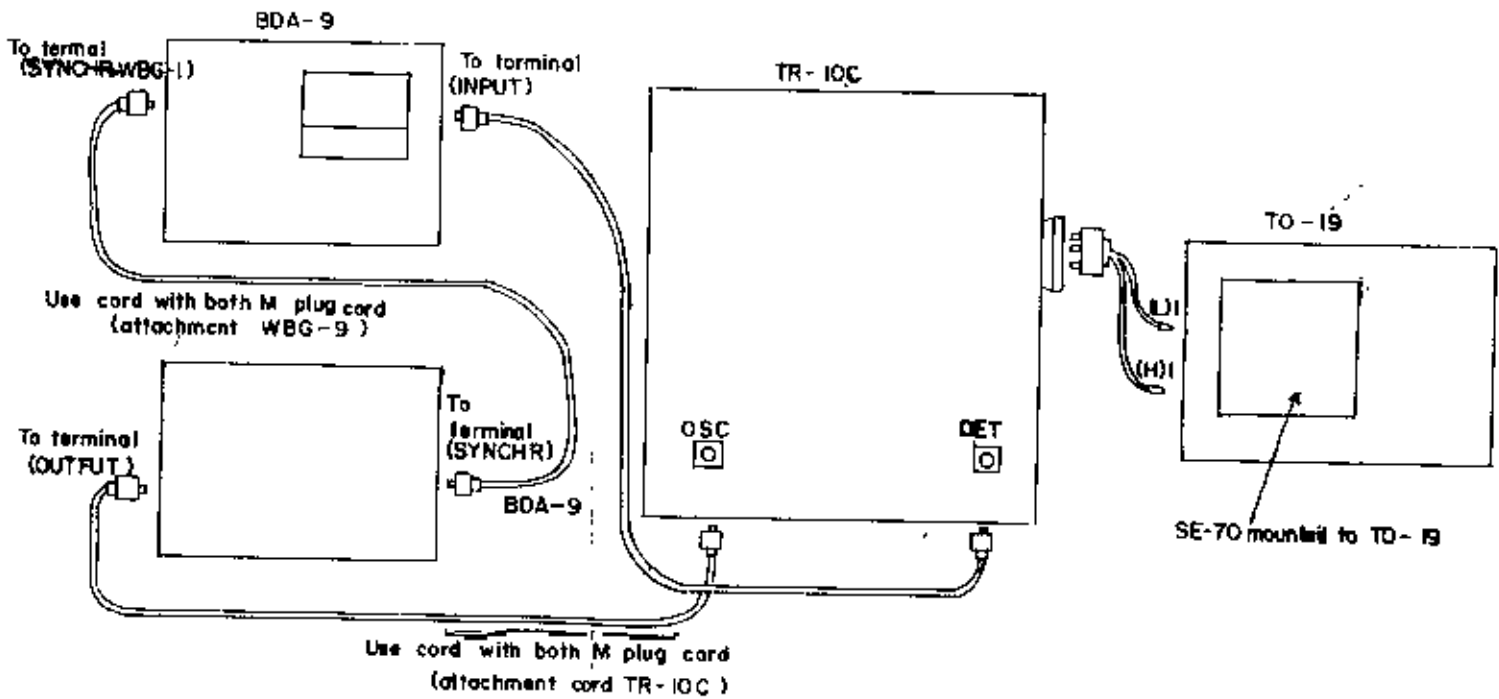


Fig 4.8 Electrical connections of dielectric loss measuring system.

Electrical specifications and characteristics of the dielectric loss measuring system:

- i) Measuring frequency (f)
 - 30 Hz, 50 Hz, 60 Hz, 110 Hz, 330 Hz, 1 kHz, 3 kHz, 10 kHz, 30 kHz, 100 kHz, 300 kHz, 1 MHz, 3 MHz.
- ii) Capacitance (Cx)
 - a) Measurement range : 1 to 200 pf
 - b) Minimum scale interval : 0.01 pf
 - c) Measurement accuracy : $\pm 3\%$ at 15 pf and over $\pm 1\%$ for specimens having the thickness 0.5 to 1.5 mm.
- iii) Conductance (Gx)
 - Measurement accuracy
 - $\pm (5\% + f.3 \times 10^{-14} s)$

where f is the measuring frequency in kHz and 0.3 for any frequency below 330 Hz.

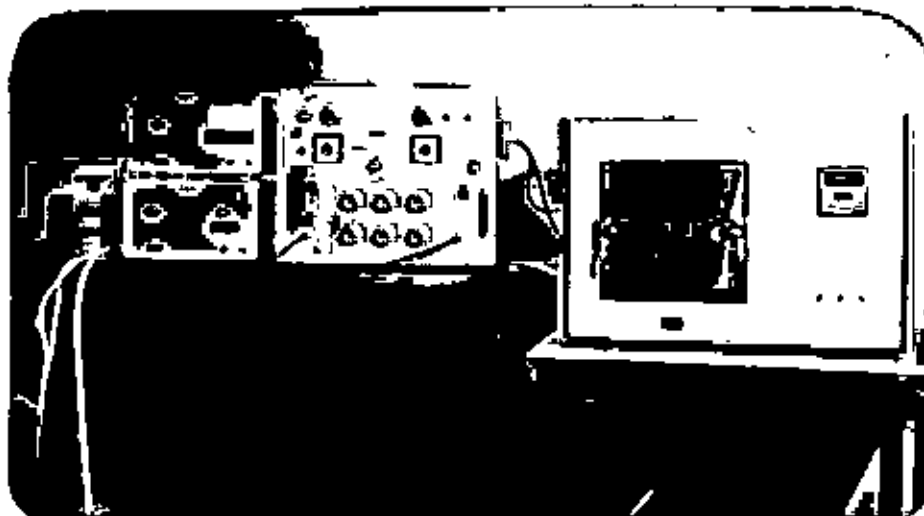


Fig 4.9 Dielectric loss measuring system
 (i) Upper left : Null detector
 (ii) Lower left : Oscillator
 (iii) Middle : Dielectric loss
 (iv) Right : Thermostatic oven

iv) $\tan \delta$

a) Measurement range

1×10^{-2} to 1×10^{-1}

Provided that $\tan \delta$ should be calculated by $\tan \delta = G_x / C_x$ and f , C_x and G_x should be in the respective ranges shown before.

b) Measurement accuracy

$\pm(10\% + 2 \times 10^{-2}$ in terms of $\tan \delta$) at f of 330 Hz to 100 kHz.

v) Characteristics and requirements for specimens

a) Applied voltage : 10V max, 1V min.

b) Thickness : 2×10^{-4} to 2×10^{-2} m.

c) Temperature variable range : 203-473 K

d) Temperature stability : ± 0.5 K

The unit of the conductance has been changed from mho to Siemens (S).

4.5.2 A.c. conductance and dielectric measurement

4.5.2.1 Experimental procedure

For a.c. measurement a transformer ratio-arm bridge is used which has been discussed in section 4.5.1. Three transformer ratio-arm bridges are used for three different frequency ranges. One is used for the measurement range from 30 Hz - 1 kHz, the second one is for the range from 1 kHz - 1 MHz and the rest one is for 1 MHz - 3 MHz range.

Measurement on these bridges are made in the normal manner, an initial balance known as zero balance is obtained at each frequency by trimming (without the specimen being connected) and from the conductance ratio-arm the value of R_0 is obtained. The specimen leads are then connected to the bridge terminals and a final balance is obtained by adjusting the knobs in the conductance (G_x) arm and capacitance (C_x) arm. The final balance is known as measuring balance. At measuring balance position from the conductance ratio-arm the value of R' is obtained. Thus conductance G_x of the specimen is obtained by multiplying $(R' - R_0)$ by G_x . Simultaneously, value of the capacitance is obtained from the capacitance scale. This capacitance value is required for dielectric constant and dielectric loss factor, $\tan \delta$ calculation. The thermostatic oven is used as heating system. A particular

temperature is maintained during the performance of frequency variation measurement of conductance and capacitance. The same procedure is followed for different higher temperatures. Temperature is raised from room temperature to 498 K by adjusting the thermostatic oven.

4.5.2.2 Precautions

Precautionary steps are taken at every part of the measurement. First of all it is ensured that there should not be any short circuit path. The chamber of the specimen holder is kept dry otherwise error would be introduced in the readings. Accurate zero balance should be reached every time so that accurate measurement may be obtained. The pointer of the null detector should not turn more than 70 degree so that the internal amplifier become saturated.

4.5.2.3 Working formula

During the observations for different frequencies of a specimen a particular temperature is maintained. The calculations are performed using the observed values of conductance (G_x) and capacitance (C_x) at different frequencies and temperatures by the following relations.

For a.c. conductivity,

$$\sigma_{ac} = \frac{d}{A} G_x \dots\dots\dots (4.1)$$

where, G_x = conductance.

For dielectric constant,

$$\epsilon' = C_x \frac{d}{\epsilon_0 A} \dots\dots\dots(4.2)$$

where, C_x = capacitance of the specimen,

ϵ_0 = permittivity of free space

and for dielectric loss tangent,

$$\tan \delta = \frac{G_x}{\omega C_x} = \frac{G_x}{2 \pi f C_x} \dots\dots\dots(4.3)$$

where, f = linear frequency.

CHAPTER - V

5.1 XRD analysis

The XRD patterns of samples A, B, C and D are presented in fig. 5.1. These are represented respectively by diffractograms A, B, C and D. The 2θ , d_{hkl} , and the constituent compounds are depicted in tables 6.1, 6.2, 6.3, 6.4 in appendices.

The XRD pattern of the sample A (as collected BWC), diffractogram A, shows the presence of silica, kaolinite, aluminium oxide, magnesium oxide, potassium aluminium silicate hydroxide, etc. Small amount of oxides of potassium, calcium, manganese, sodium, etc. may also be present. Because of the limitation of the XRD technique to detect presence of any compound less than a few percent, these are not appeared in the XRD pattern of BWC.

The XRD pattern of the sample B (washed BWC), diffractogram B, shows the presence of all the constituent compounds those are present in the raw BWC but the peak intensities of the different constituent compounds has varied drastically indicating the change in the percentage composition of the constituent compounds due to washing of raw BWC. The major change occurs in the case of kaolinite and silica peak intensities. It is observed that the kaolinite peak intensity has increased whereas those of silica decrease significantly.

The XRD pattern of the samples C (after heat treatment at 773 K of washed BWC), diffractogram C, gives the signature of the presence of all the constituent compounds that are present in the washed BWC. It is observed that there is a drastic decrease of the peak intensities of kaolinite whereas the peak intensities of silica remain nearly same.

The XRD pattern of the sample D (after heat treatment at 1273 K of washed BWC), diffractogram D, reveals the presence of silica (quartz, low), mullite precursor, aluminium oxide, γ -alumina, potassium aluminium silicate. Among these, mullite precursor and γ -alumina are the new phases appeared due to heat treatment at 1273 K. It also shows the absence of detectable amount of kaolinite, iron oxide, magnesium oxide and other constituent compounds.

The XRD analysis of the different samples revealed that the amount of the main ingredients of BWC the kaolinite (7.03, 3.56 and 2.32 Å) increases and that of silica (4.23, 3.32 and 2.44 Å) decreases after washing the raw BWC (diffractograms A and B). On heat treatment at 773 K (diffractogram C) and at 1273 K (diffractogram D), the reflections for silica still persist in the form of quartz (low) whereas the XRD reflections for kaolinite are absent in the final product thereby indicating a major transformation of the kaolinite to its high temperature phases (diffractogram D) such as

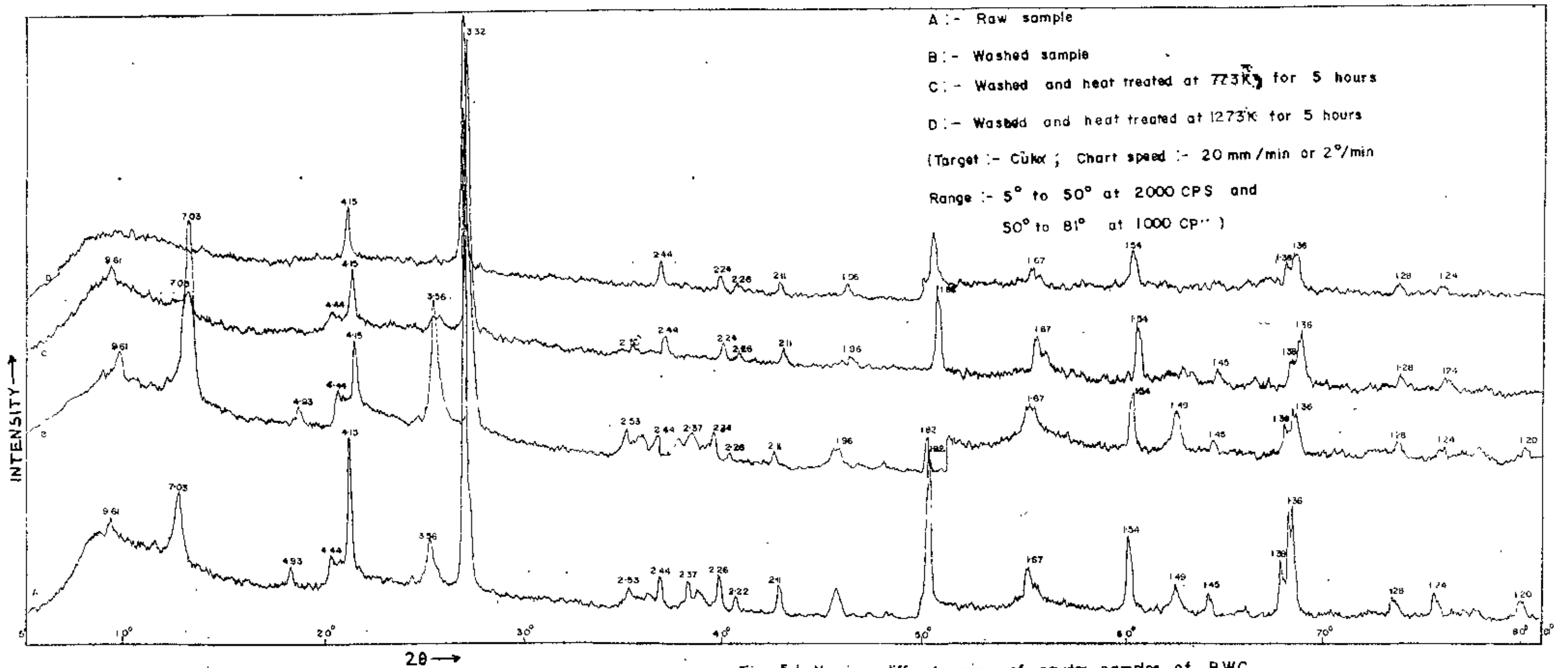


Fig: 5.1 X-ray diffractograms of powder samples of BWC

meta-kaolinite, mullite, etc. Apart from these two phases, the other constituents may also be present in small amount.

As found from the XRD analysis of the BWC samples A, B, C and D (diffractograms A, B, C and D), alumina (2.12, 1.44 and 1.39 Å) transforms to γ -alumina (2.39, 1.98 and 1.39 Å), aluminium silicate (4.42, 4.34 and 1.44 Å) persists as it is in less amount in the final phase. Potassium aluminium silicate hydroxide (9.61, 3.55 and 1.99 Å) is not present in the BWC after heat treatment at 1273 K. Potassium aluminium silicate (4.15, 2.25 and 1.53 Å) appears only in the 1273 K heat treated BWC. It seems from the diffractograms that iron oxide (4.92, 2.53 and 1.48 Å), magnesium oxide (2.11 and 1.49 Å) decrease to below detectable limit after heat treatment at 1273 K.

Thus, it is seen from XRD analysis of BWC and its modified forms that after 1273 K heat treatment a metakaolinite and/or γ -alumina-mullite might have formed. A sufficient amount of silica in the form of quartz (low) is also present. These kind of transformations in this temperature region have been reported by several authors^(1,2,3,4).

5.2 DTA analysis

The DTA traces of the samples B and C (powder form) are shown in the fig. 5.2. For comparison a DTA trace of pure

kaolin^(b) is also shown in the figure. It is observed that an endothermic peak is appeared at 853 K. This endotherm is at lower temperature than that of the pure kaolin. This endotherm may be due to the evolution of the water of crystallization, i.e., the expulsion of water from mineral lattice and thereby forming precursor metakaolinite material. This fact becomes apparent from the DTA, as seen in the figure for the BWC sample heat treated at 773 K (sample C) in which there^{is} no endotherm at 853 K. In fact it is our intention to do the DTA study upto 1273 K but due to lack of instrumental facility it could not be possible to do the experiment at higher temperatures.

5.3 Polarizing microscopy

Microphotographs of different samples are presented in fig 5.3. It is observed that the surface structure changes significantly on washing, heat treatment and pressure of pellet preparation. It can be seen that porosity in the pellets decreases with the increase of pellet preparation pressure. It is clearly seen that formation of cluster results due to heat treatment at higher temperature. This may be an indication of decomposition and some structural change that might have taken place in the BWC.

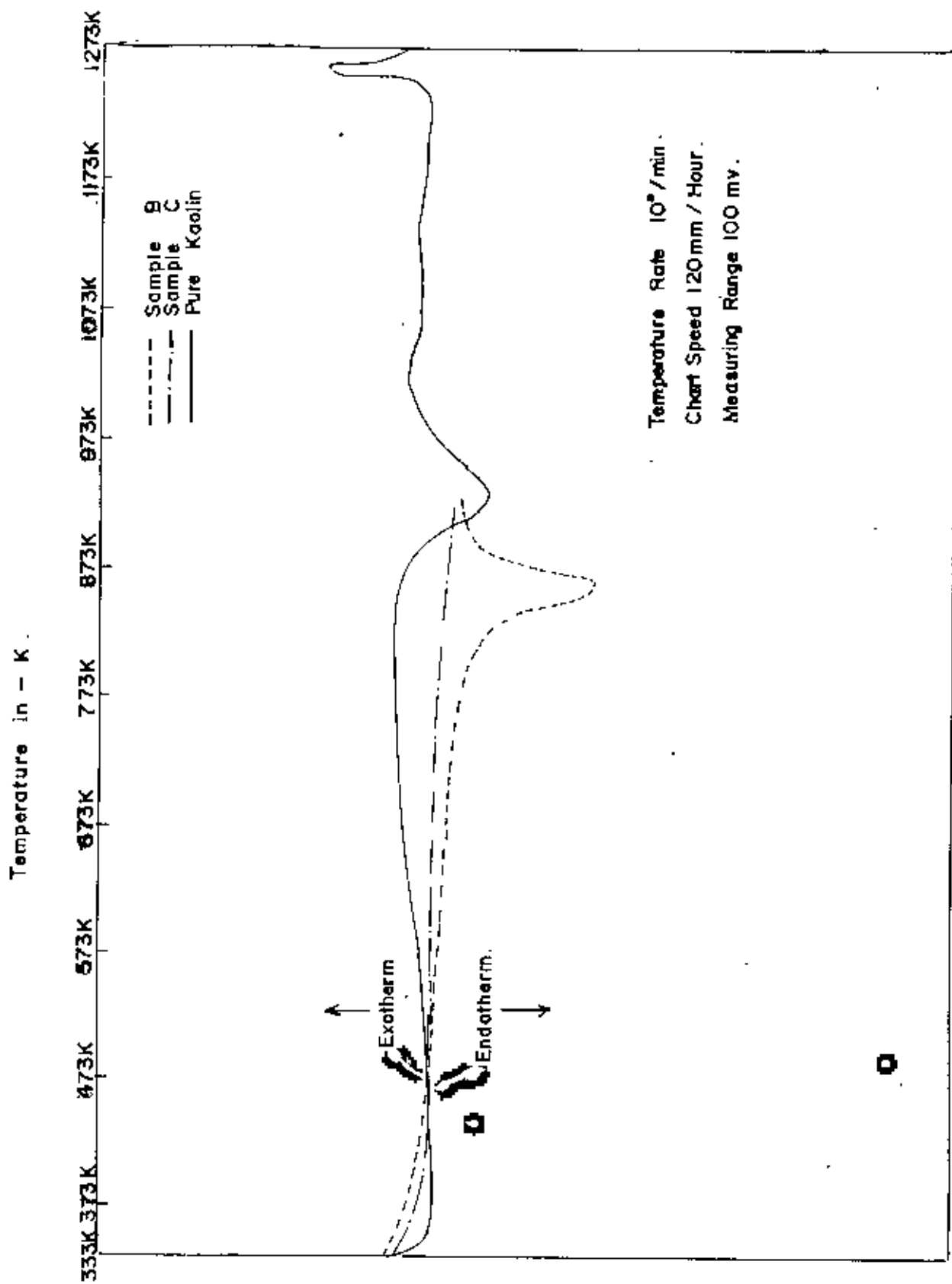
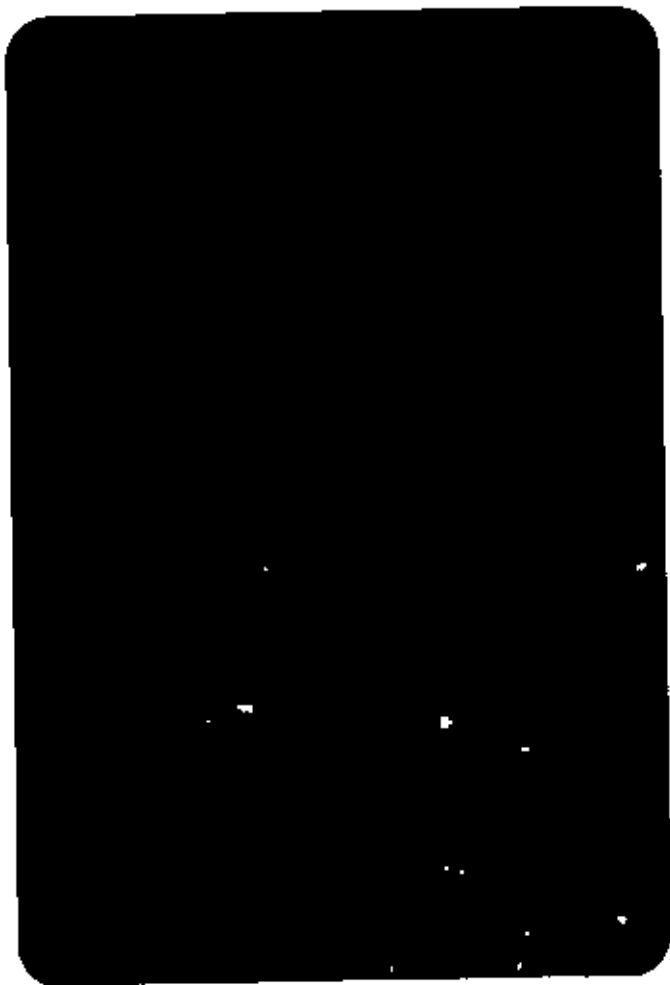
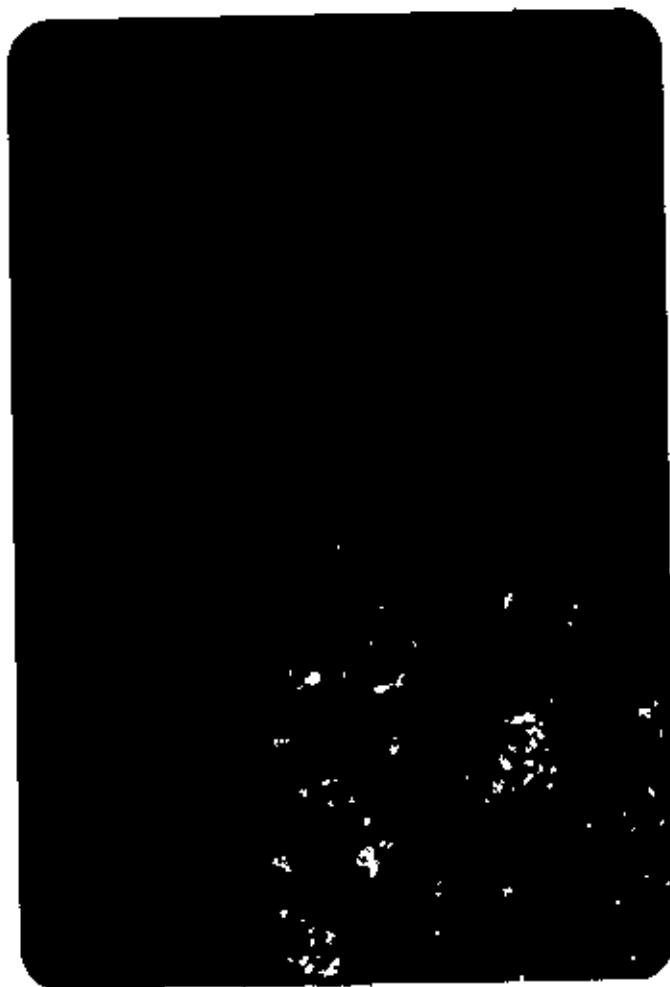


FIG. 5.2 DTA of Kaolin and BWC Samples.



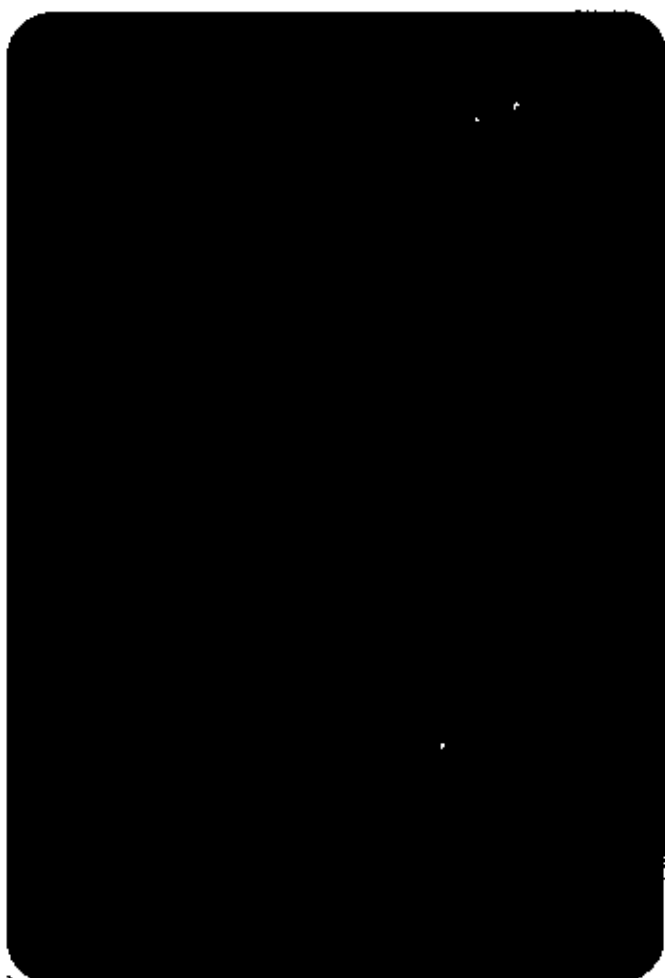
(a)



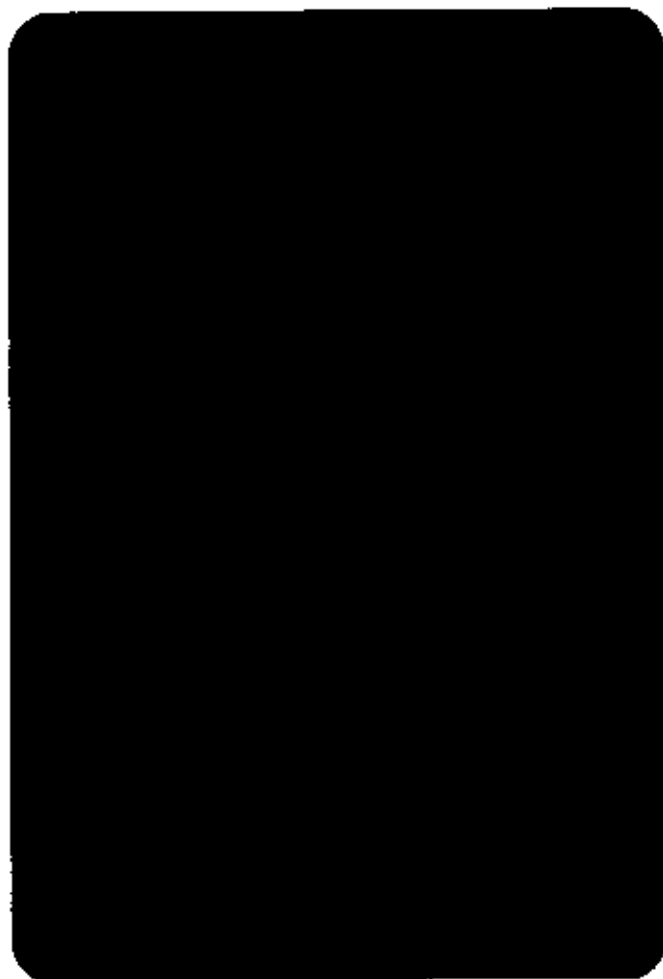
(b)



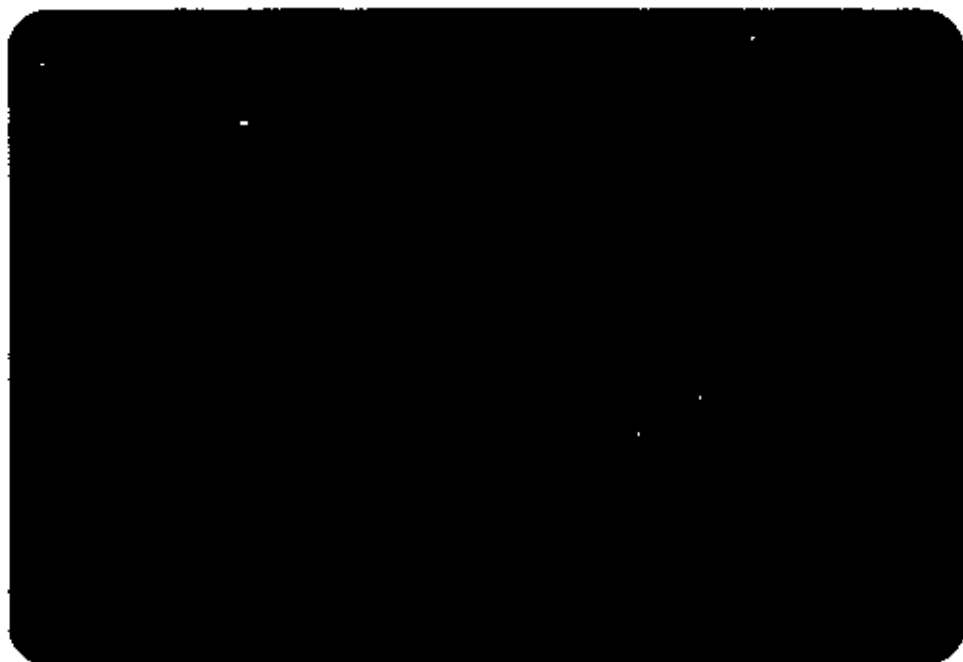
(c)



(d)



(e)



(f)

Fig. 5.3 Microphotographs of samples (a) A 3, (b) B 1, (c) C 3, (d) D 1, (e) D 2, (f) D 3.

5.4 D.c. electrical measurements

To perform any electrical measurement on solids, it is necessary to make good electrical contacts (non-blocking contact electrode) because the electrode-material contact plays an important role in understanding the material properties. In this purpose at the out-set, the I-V characteristics are studied and the results are presented below.

5.4.1 Current-voltage (I-V) characteristics

Since all the samples show similar behaviour, a set of representative I-V characteristic curves for sample D for pressures 2000, 3000 and 3500 psi and temperatures 303, 373, 423, 473 and 523 K are presented in fig. 5.4. It is observed that the I-V curves fit to a relation $I = V^n$, where n is the power factor. It is seen that first three temperature curves have different slopes at low, intermediate and high voltage regions while there are two different slopes in the remaining two higher temperature curves for 2000 and 3000 psi samples. But it is observed that there are only two different slopes for all temperatures in 3500 psi sample. The n values for all the samples are depicted in table 5.1.

From the n values, it is seen that the low voltage region is Ohmic and the intermediate and high voltage region follow a square law and a $I \propto V^2$ with traps respectively. It is

Table 5.1 : Values of power factor n for sample D

Pressure in psi	n values below 423 K	n values above 423 K
2000	0.95	1.46
	2.16	-
	3.22	3.22
3000	0.70	1.42
	2.30	-
	3.01	3.01
3500	1.46	1.46
	3.23	3.23

seen that the Ohmic region is not present in the high temperature curves of 2000 and 3000 psi samples. There are also two slopes over the voltage range employed for all temperatures in the 3500 psi sample which correspond to the region containing traps. The above results suggest that the space-charge-limited (SCL) conduction is operative in these materials.

At low voltages the I-V characteristics are Ohmic which may be related to adsorbed water, water of crystallisation etc. Over the intermediate and high voltage ranges the SCL conduction may be due to the higher concentration of the injected free carriers than that of the carriers⁽⁶⁾ due to the presence of water in the clay, the amount of which can be changed or expelled by heat treatment or application of pressure. It is clearly seen that temperature affects the SCL

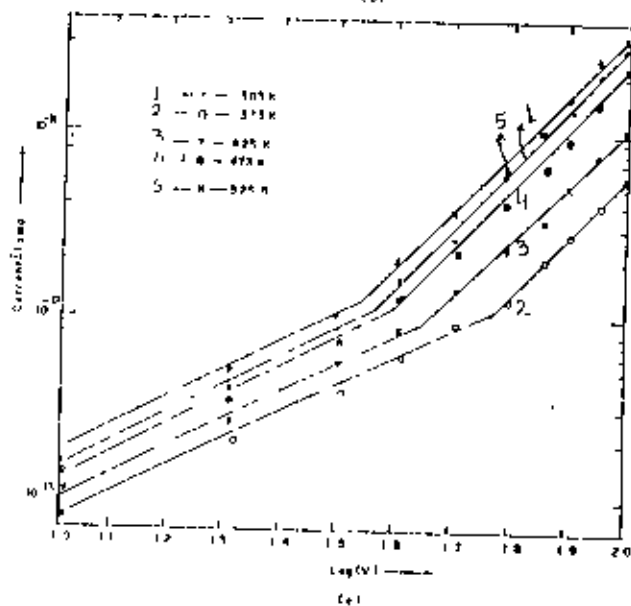
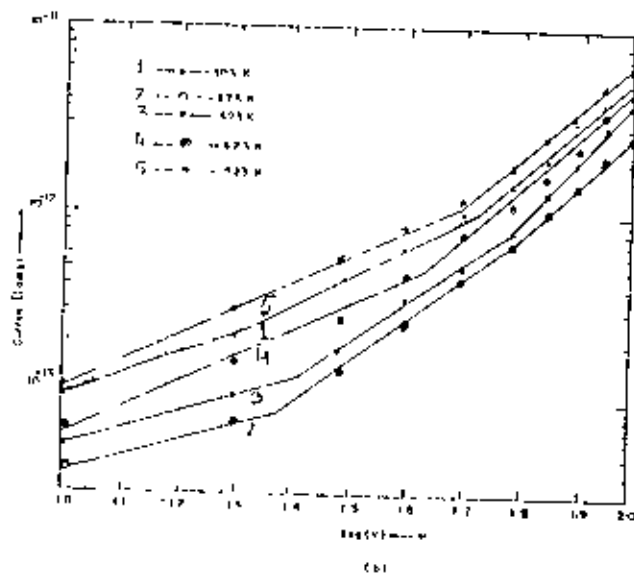
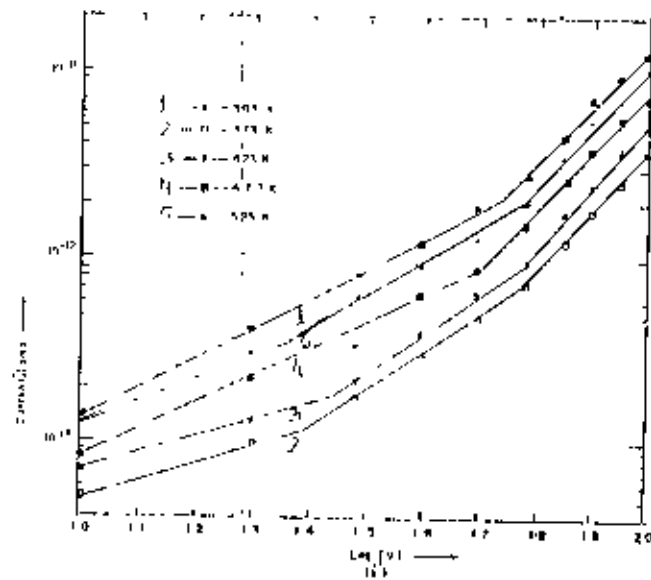


Fig. 5-4 $\log |V|$ against I at different temperatures for washed BWC (heat treated at 1273 K) (a) 2000 psi (b) 3000 psi (c) 3500 psi.

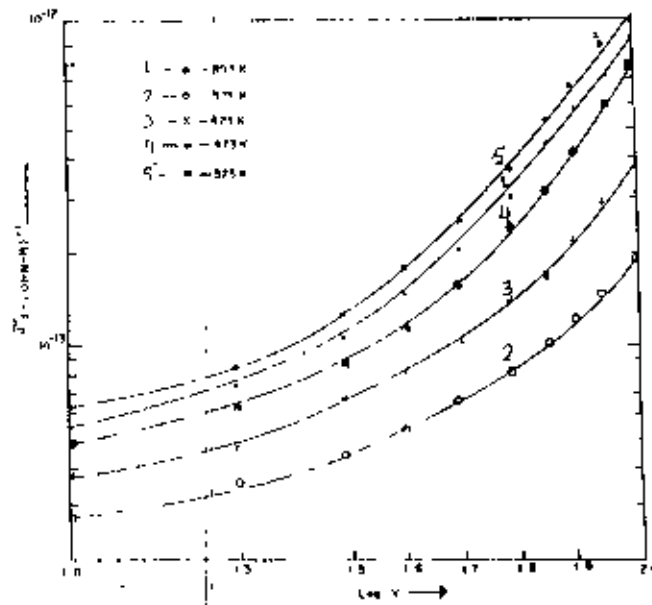
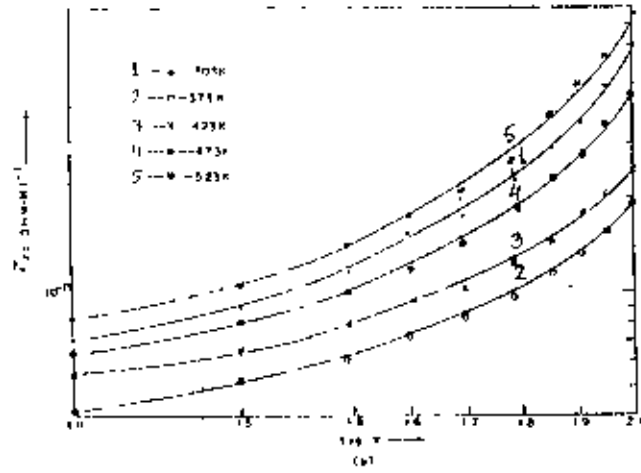
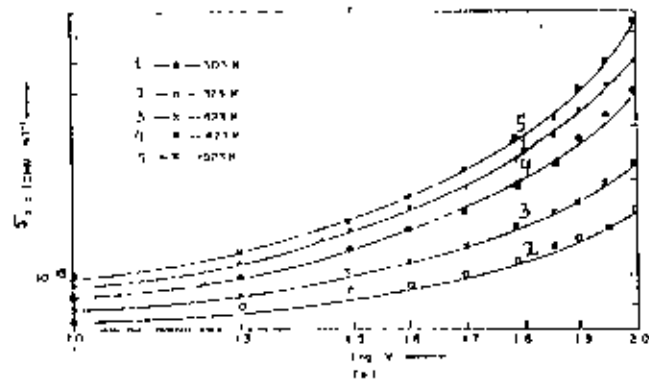


Fig. 5-5 Log V against d d.c. at different temperatures for washed BWC (heat treated at 1273 K) (a) 2000 psi (b) 3000 psi (c) 3500 psi

conduction behaviour which manifests the presence of the shallow traps in the material. Porosity plays an important role in deciding the concentration of the trap centers with other kinds of centers in a material. The absence of the Ohmic region in the 3500 psi sample may be due to less porosity (low trapping center) compared with that in the less pressurized samples⁽¹⁾, resulting higher concentration of free carriers than that of the carriers related to water in the material even at the low voltages.

In fig 5.5 shown are the σ_{ac} vs. voltage curves of the sample D for different temperatures and different pressures. It is observed that σ_{ac} varies exponentially with the applied voltage in all the samples for all temperatures and pressures. The variation of σ_{ac} with applied voltage increases progressively from low to high pressure samples. These observations also suggest that porosity decreases with pressure.

5.4.2 D. c. electrical resistivity

Generally clay absorbs water and that affects the electrical properties. To see the effect of water, d.c. resistivity (ρ_{dc}) of sample D (pressure 3500 psi) ~~is~~ measured for three successive cycles. This is shown in fig. 5.6. It is observed that after the first cycle of the measurement the resistivity of the sample becomes almost

stable with higher resistivity and on further heating no appreciable change in the resistivity is noticed.

It is found that the room temperature resistivity is higher for washed samples and increases on heat treatment from 10^{11} to 10^{12} Ohm-m. The effect of pressure of pellet preparation on the ρ_{dc} is found to be small.

The d.c. electrical resistivity, ρ_{dc} , of all BWC samples is measured over the temperature range 300 to 673 K. The plots of $\log \rho_{dc}$ against $1/T$ are shown in fig. 5.7. A common feature is observed in all the curves. It is seen in these curves that there is an initial decrease in the ρ_{dc} upto 313 K in samples A and B and upto 323 K in samples C and D and then starts increasing upto 383 K in all the samples and again ρ decreases with increasing temperature.

The initial decrease in ρ may be due to the motion of hydroxyl ions and other species present. This initial decrease and then rise of electrical resistivity is a behaviour of solid electrolyte. The increase in ρ above 313 K may be attributed to the compensation effect between evaporating absorbed water molecules and the migratory ions and/or electrons, i.e., the hydroxyl ion source decreases drastically as water molecules evaporated out. Above 383 K the decrease of ρ with increasing temperature may be due to the increased movement of adventitious ions and / or electrons

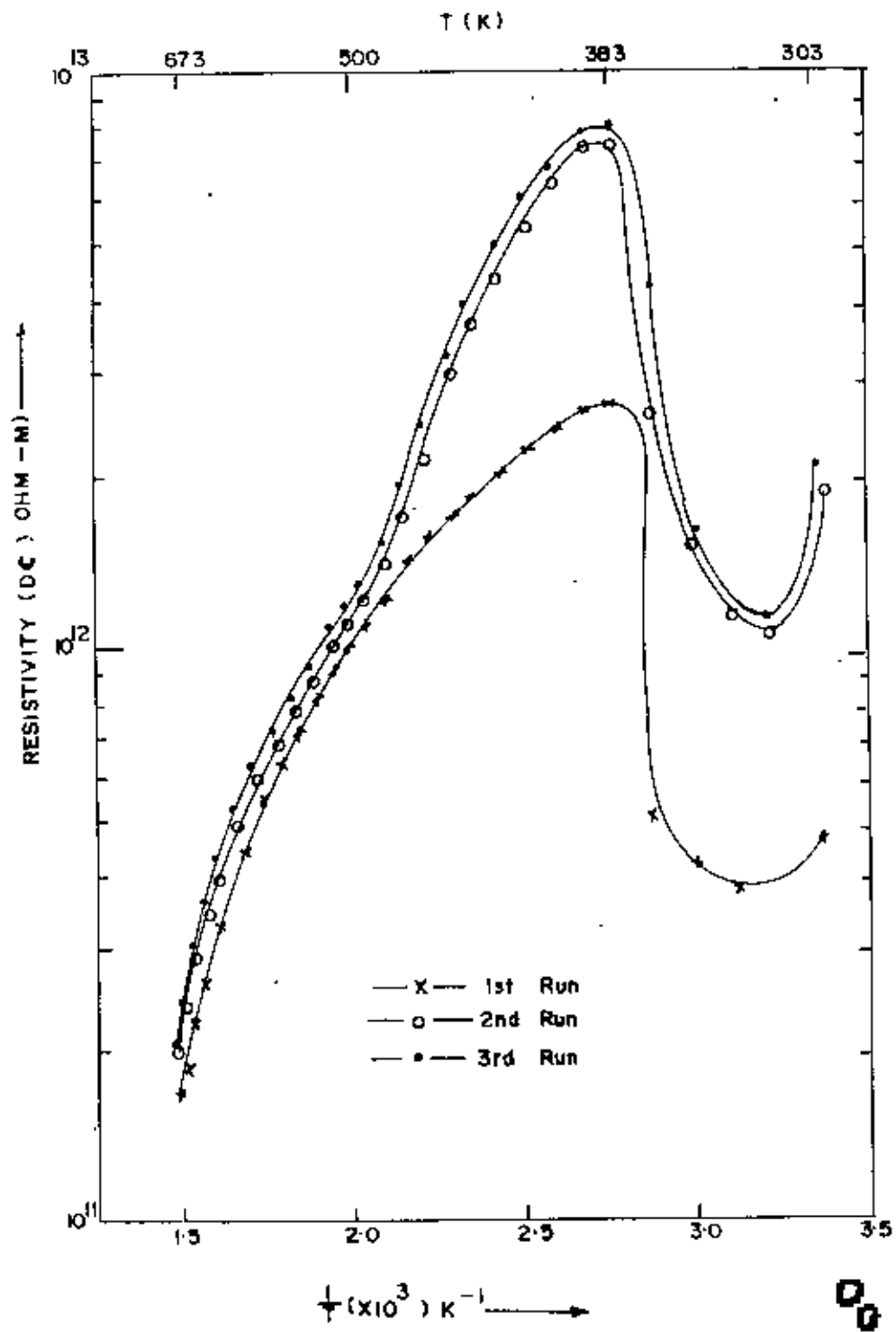


Fig. 5-6 DC Resistivity versus inverse temperature of washed and 1273.K heat treated sample (3500 psi)

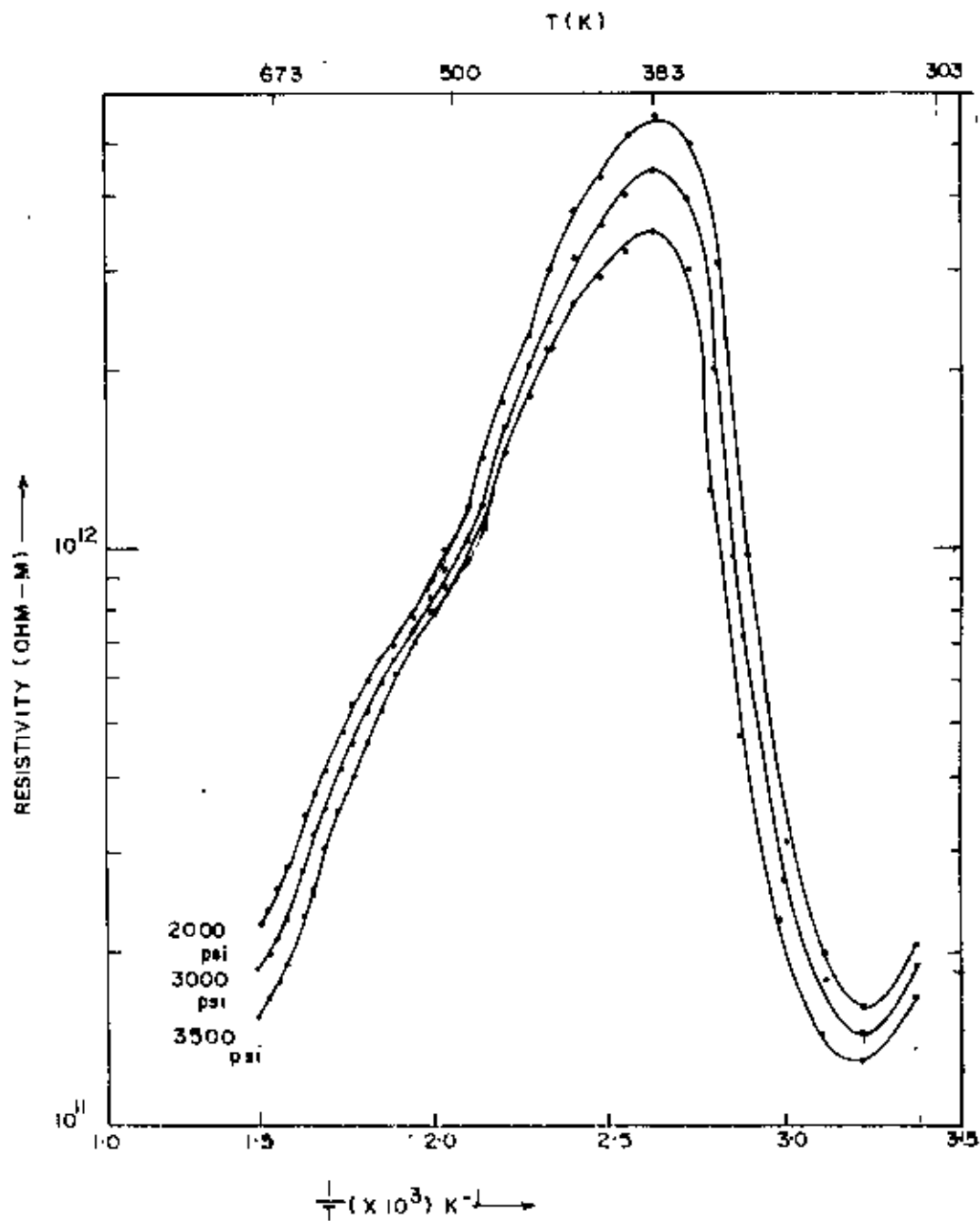


Fig. 5-7(a) Resistivity versus inverse temperature of row (as collected) sample.

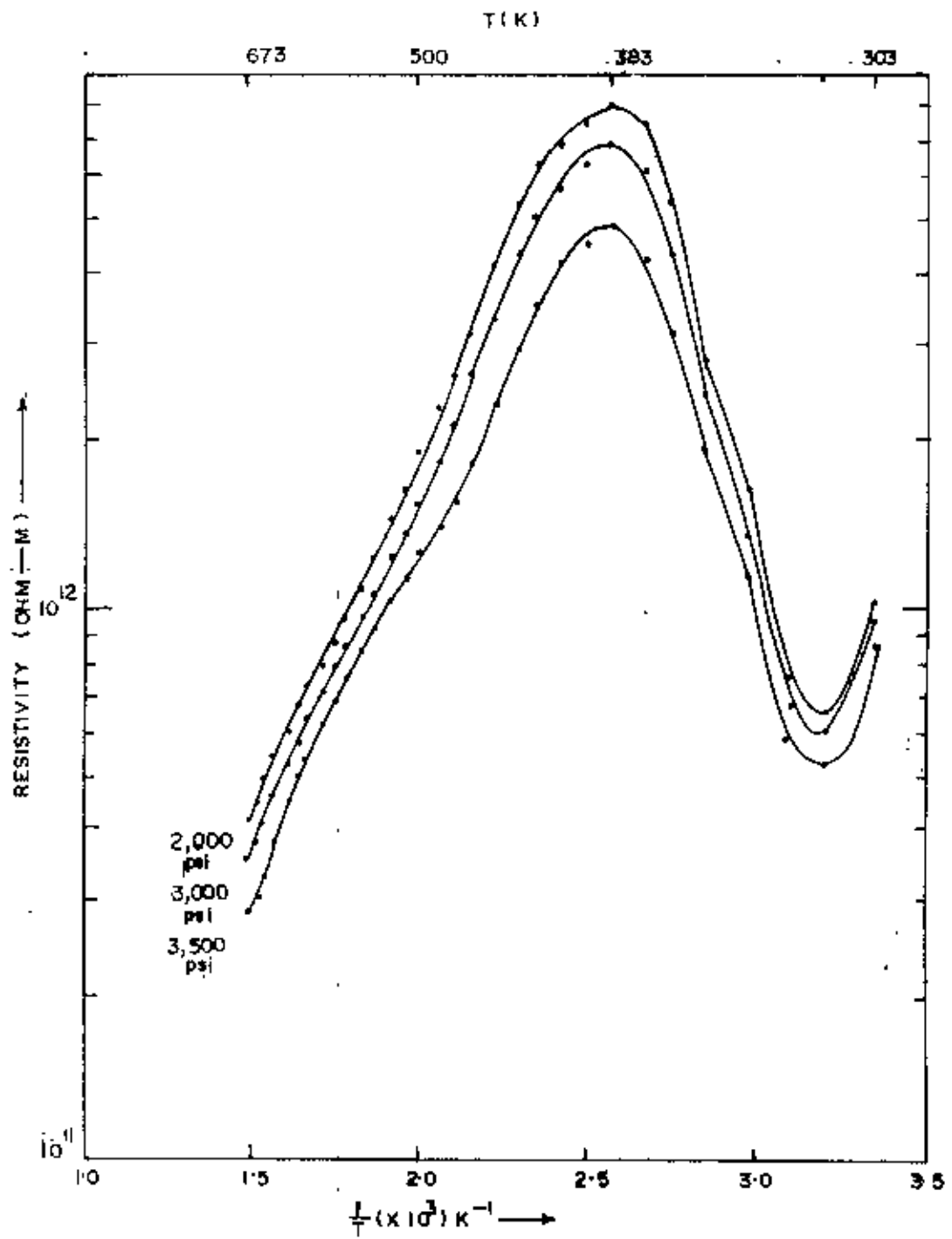


Fig. 5-7 (b) Resistivity versus inverse temperature of washed sample.

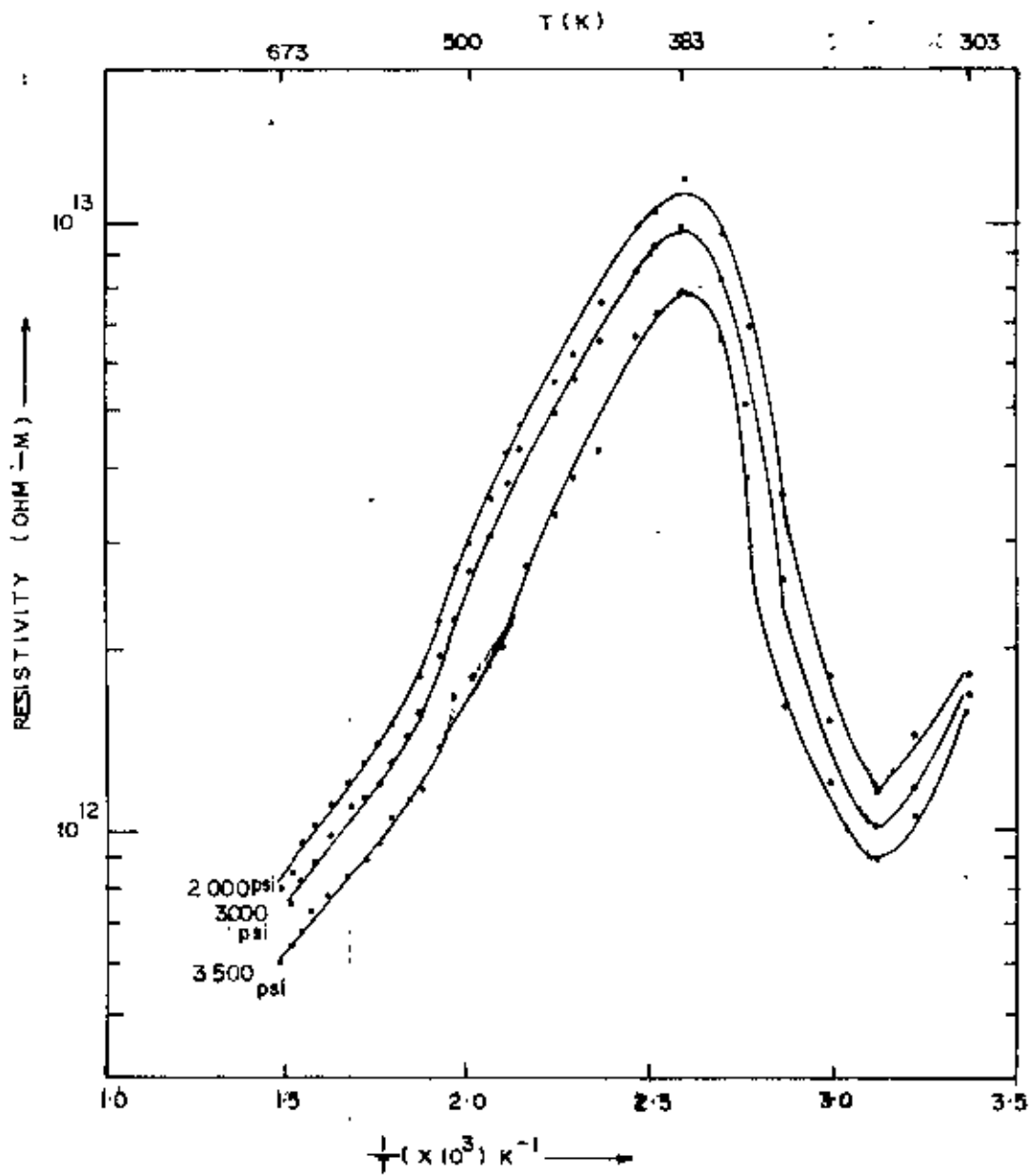


Fig. 5 7(c) Resistivity versus inverse temperature of washed and 773 K heat treated sample.

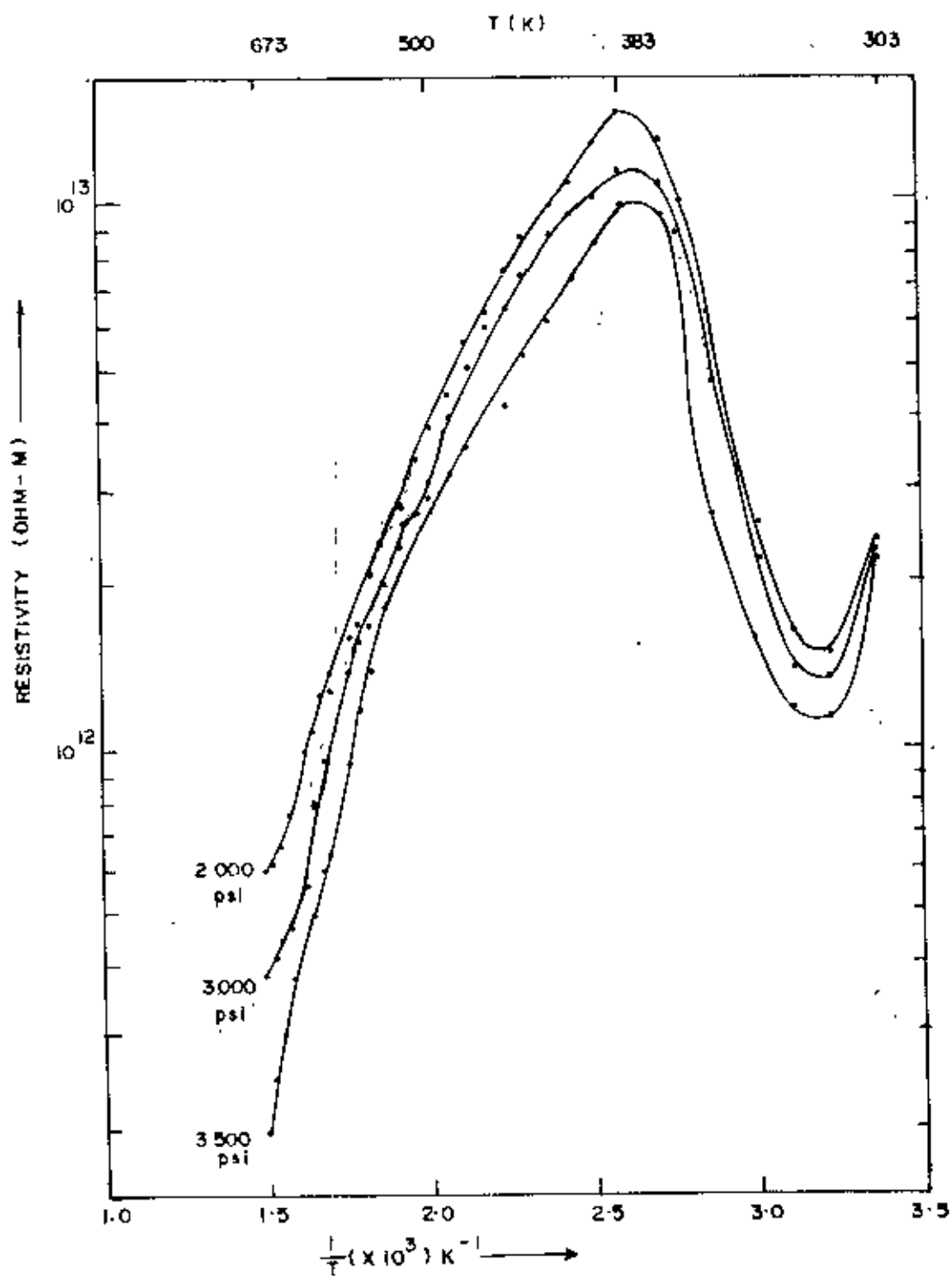


Fig. 5-7(d) Resistivity versus inverse temperature of washed and 1273 K heat treated sample.

within the bulk of the material.

It is seen that the curves fit to a straight line over the whole temperature range above 383 K for samples A, B and C whereas, in sample D, there is a considerable departure from straight line above 500 K. The activation energies are calculated from the slopes of the straight lines of $\log \rho$ vs. $1/T$ plots. The values of ρ_0 , obtained by extrapolation of the $\log \rho - 1/T$ plots to $1/T=0$, are of the order of 10^{-10} to 10^{-8} .

TABLE 5.2 : Activation energy E_r in ev and pre-exponential factor ρ_0 in Ohm-m.

Sample	Temperature range in K	Pressure 3500 psi		Pressure 3000 psi		Pressure 2000 psi	
		E_r	ρ_0	E_r	ρ_0	E_r	ρ_0
Raw: A	373 - 673	0.308	5×10^{-9}	0.278	7×10^{-9}	0.238	9×10^{-9}
Washed: B	373 - 673	0.255	7×10^{-9}	0.230	1×10^{-10}	0.227	2×10^{-10}
Washed and heat treated at 773 K: C	373 - 673	0.226	4×10^{-10}	0.211	5×10^{-10}	0.199	6×10^{-10}
Washed and heat treated at 1273 K: D	373 - 523	0.225	7×10^{-10}	0.197	8×10^{-10}	0.181	9×10^{-10}
	523 - 673	0.497	6×10^{-8}	0.411	2×10^{-9}	0.375	5×10^{-9}

The activation energies and the pre-exponential factors of all the BWC samples are summarized in Table 5.2.

The observed temperature dependence of resistivity and the activation energy calculated from Arrhenius plot suggest that thermally activated hopping conduction of carrier between localized state may be operative in these materials. However the nature of σ_{ac} variation with temperature for sample D is indicative of the variable-range hopping conduction of carriers between localized state.

5.5 A.c. electrical measurements

The a.c. electrical measurements are performed on washed BWC (sample B), BWC (washed) heat treated at 773 K (sample C) and BWC (washed) heat treated at 1273 K (sample D), prepared with 2000, 3000 and 3500 psi pressure. These measurements are carried out on all these samples at temperatures 298, 323, 348, 373 and 398 K for the frequency range 10^2 to 3×10^6 Hz. These results are discussed in the following sections.

5.5.1 A. c. conductivity

The dependence of σ_{ac} on frequency at different temperatures for samples B, C and D are presented in figures 5.8, 5.10 and 5.12 respectively. However, for one of the samples, sample D (3500 psi), measurement is extended upto 243 K.

It is observed that $\sigma_{ac} - \log f$ curves for all the

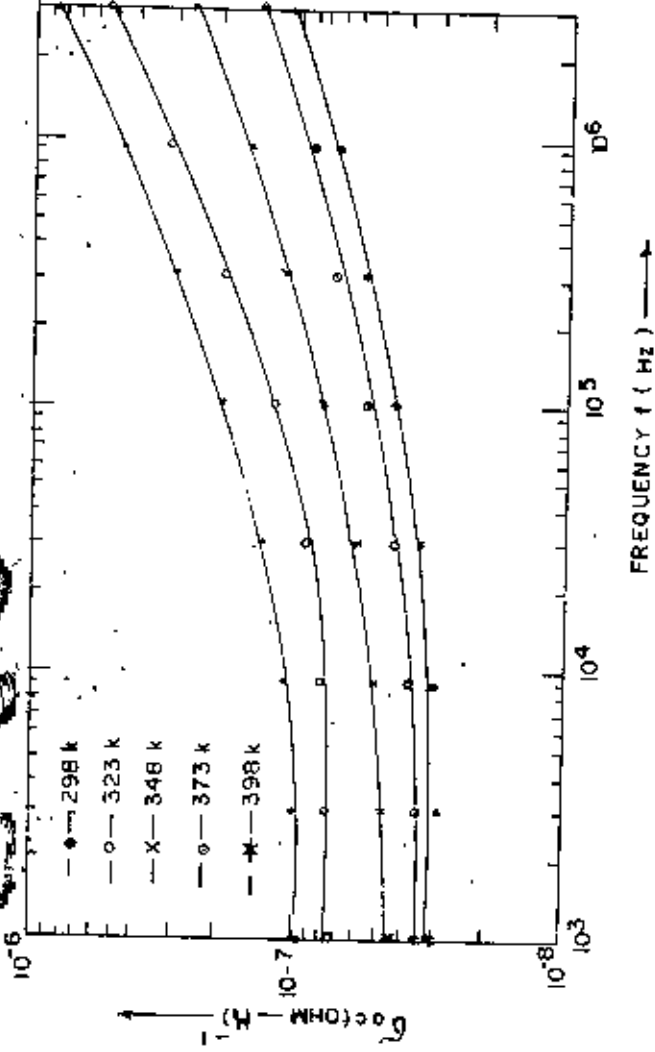


Fig. 5.8 (Z_{ac}) Versus frequency for washed sample (pressure 2000 psi) at different temperatures.

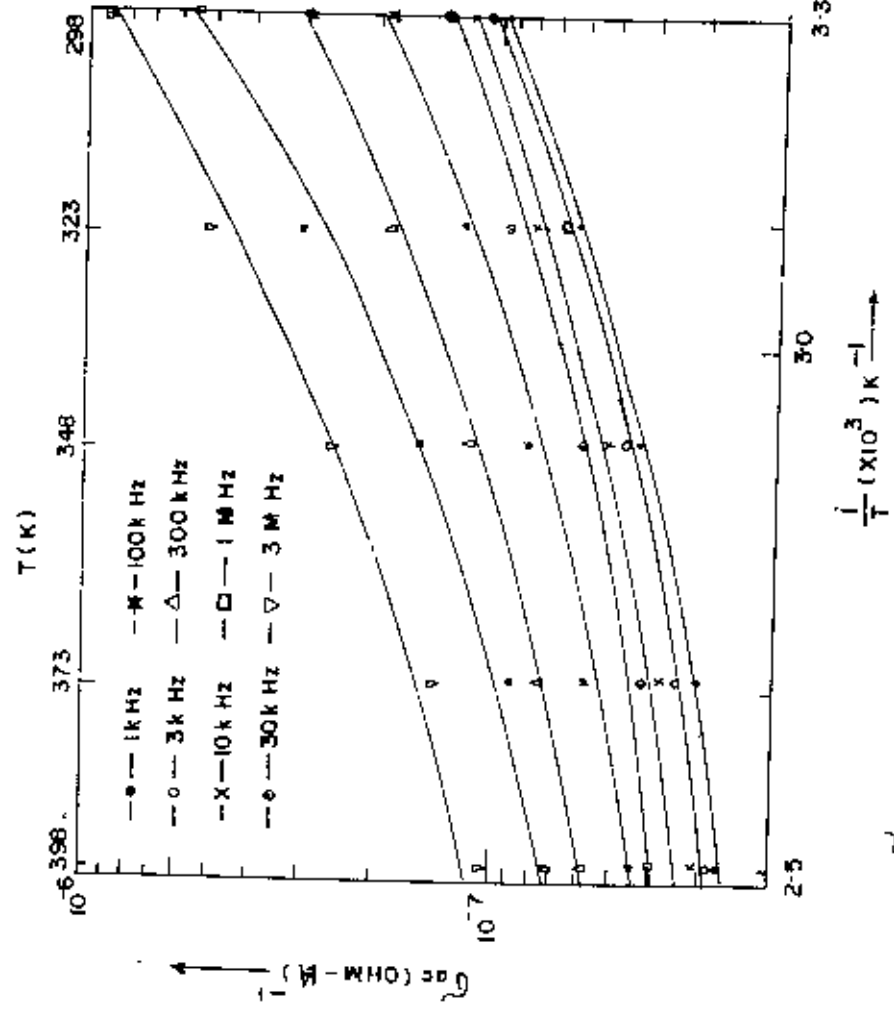


Fig. 5.9 (Z_{ac}) Variation as a function of inverse temperature for washed sample (pressure 2000 psi) at different frequencies.

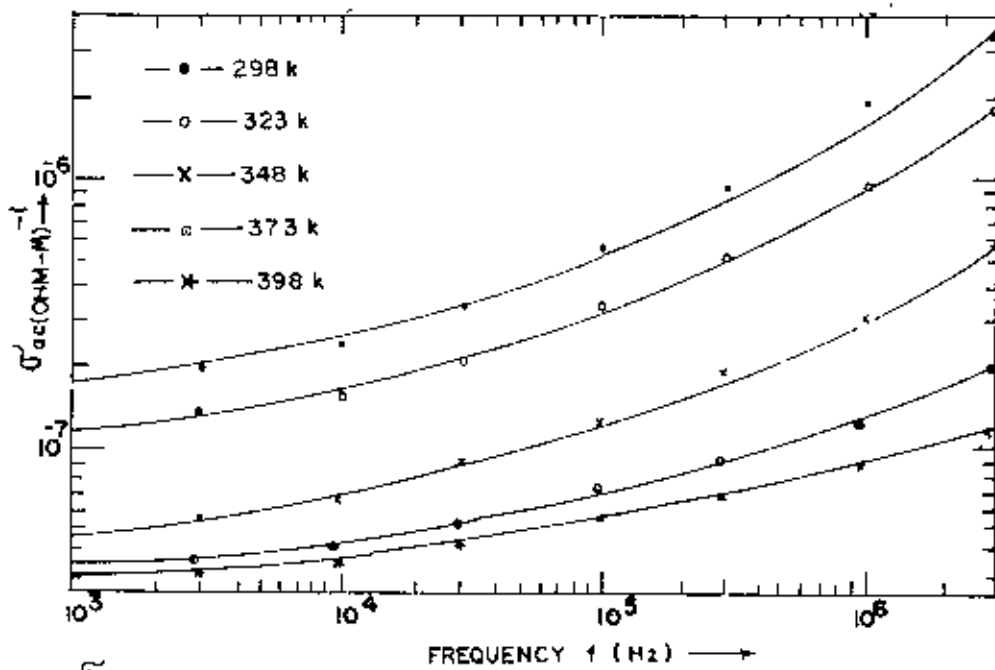


Fig. 5.8(b) σ_{ac} Versus frequency for washed sample (pressure 3000psi) at different temperatures .

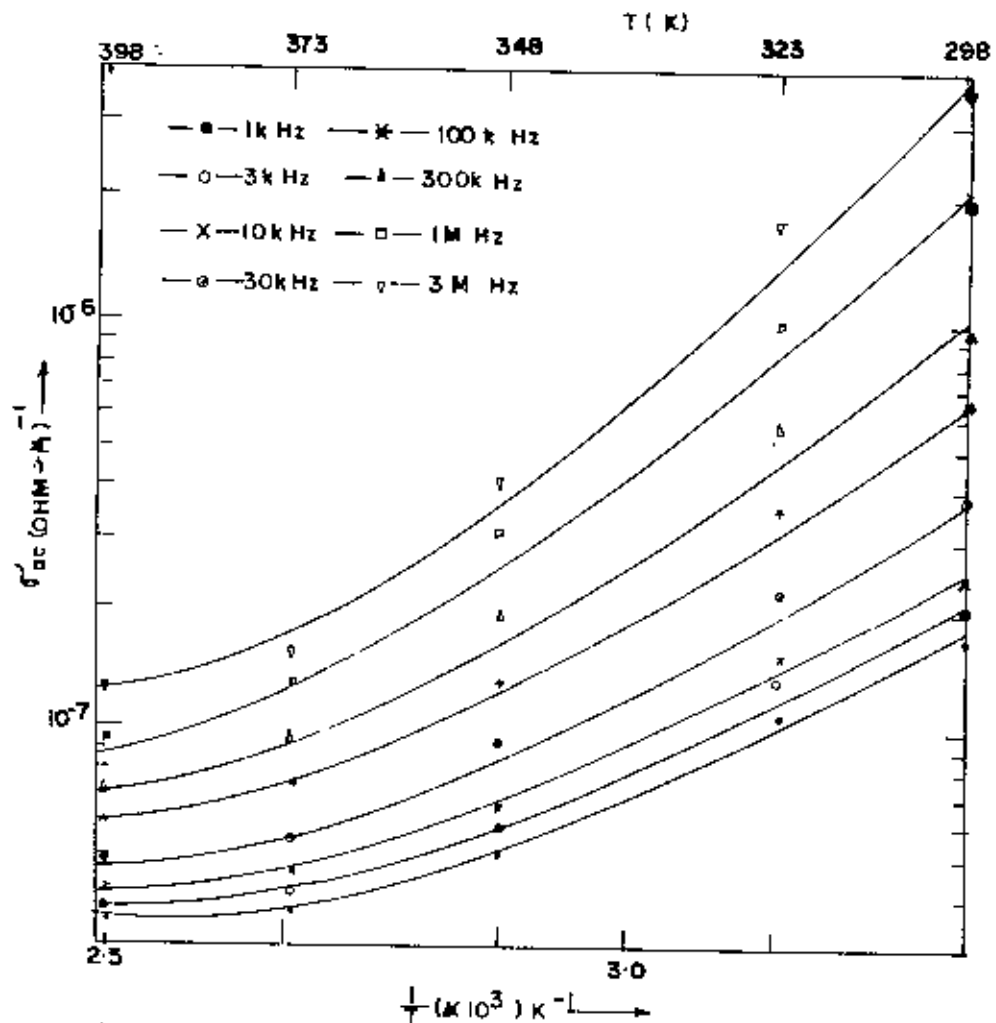


Fig. 5.9(b) σ_{ac} Variation as a function of inverse temperature for washed (pressure 3000 psi) at different frequencies.

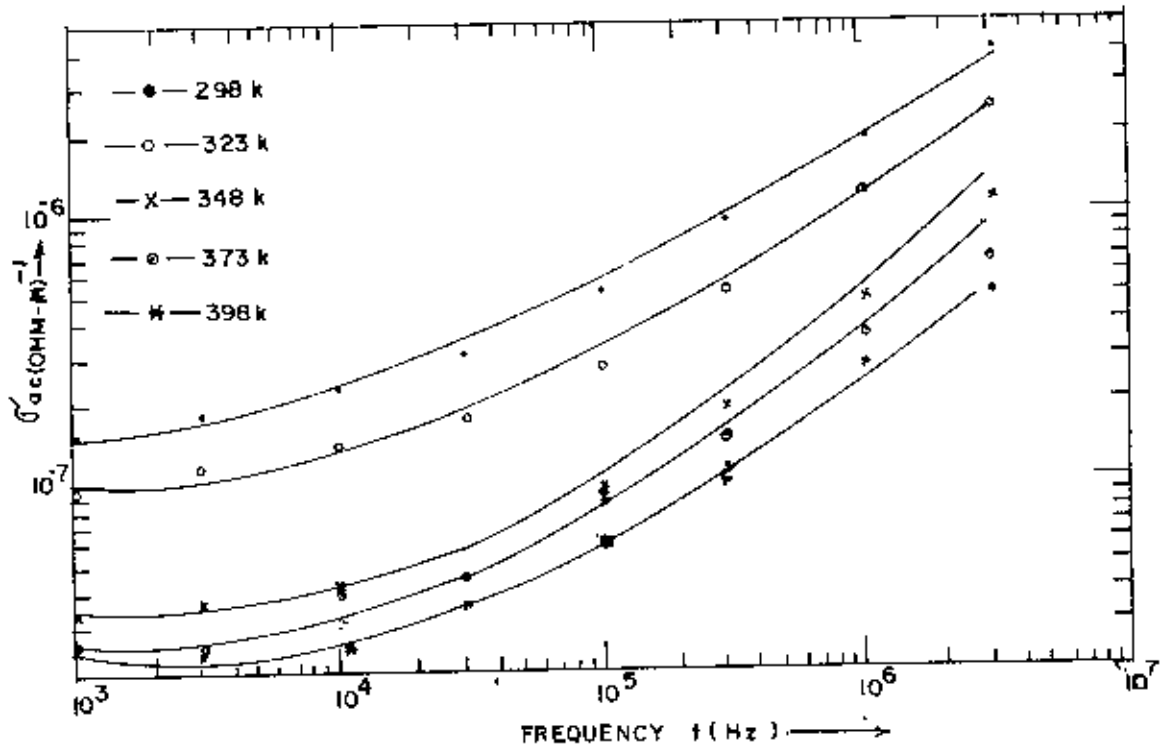


Fig 5-8(c) σ_{ac} Versus frequency for washed sample (pressure 3500 psi) at different temperatures.

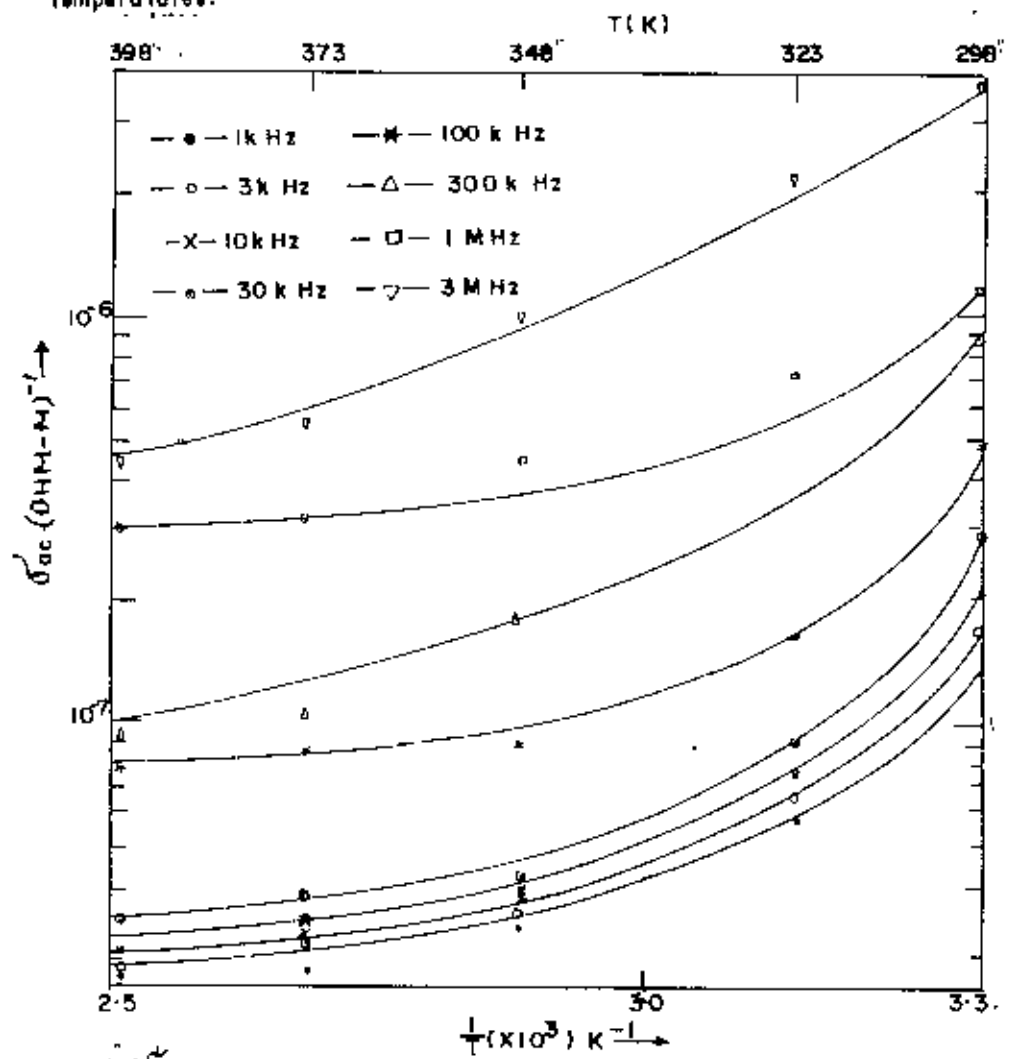


Fig 5-9(c) σ_{ac} Variation as a function of inverse temperature for washed sample (pressure 3500 psi) at different frequencies.

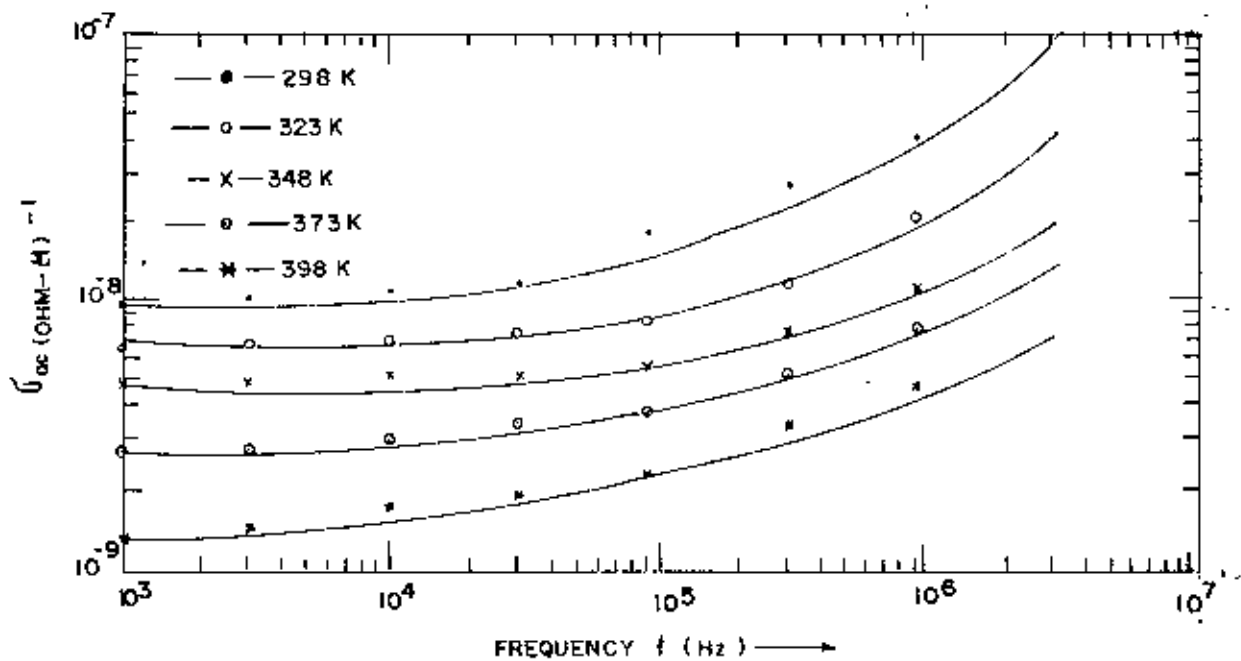


Fig. 510(a) σ_{ac} Versus frequency for washed and 773 K heat treated sample (Pressure 2000 psi) at different temperatures .

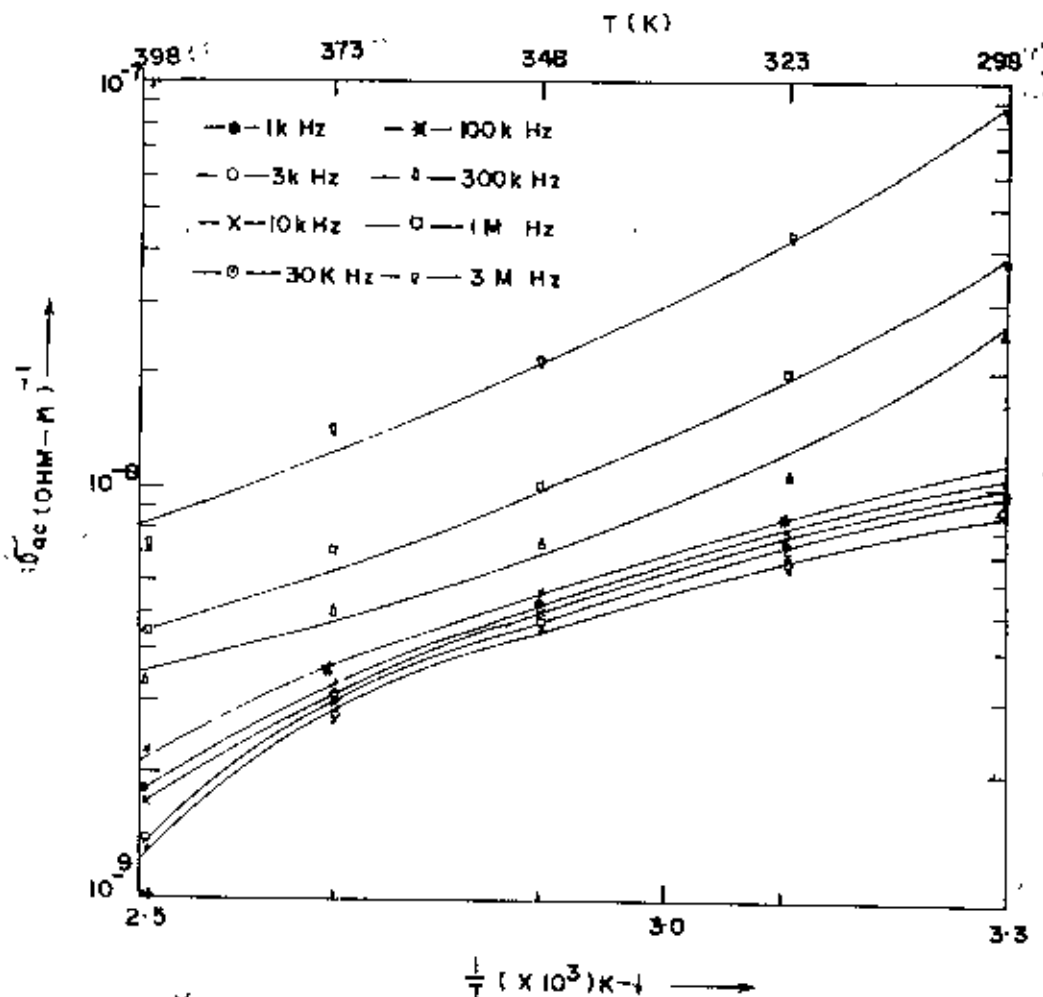


Fig 511(a) σ_{ac} Variation as a function of inverse temperature for washed and 773 K heat treated Sample (pressure 2000 psi) at different frequencies .

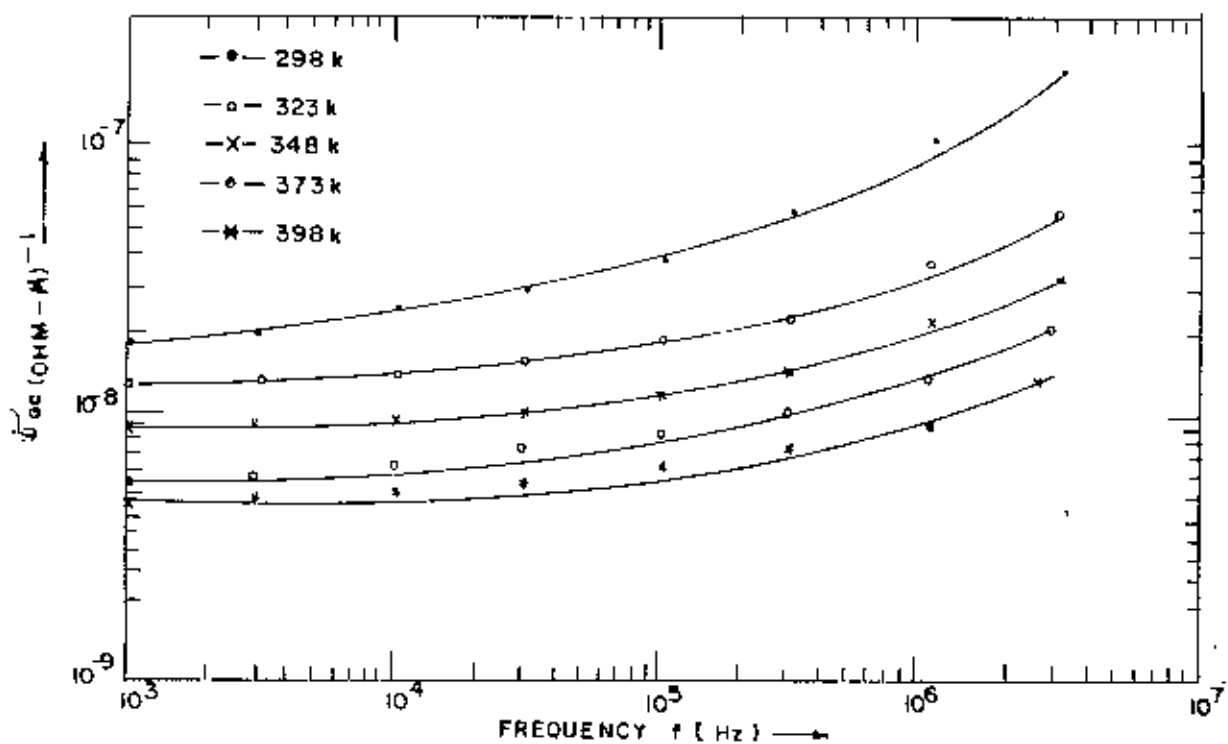


Fig. 5-10(b) σ_{ac}^{-1} Versus frequency for washed and 773 K heat treated sample (pressure 3000 psi) at different temperatures.

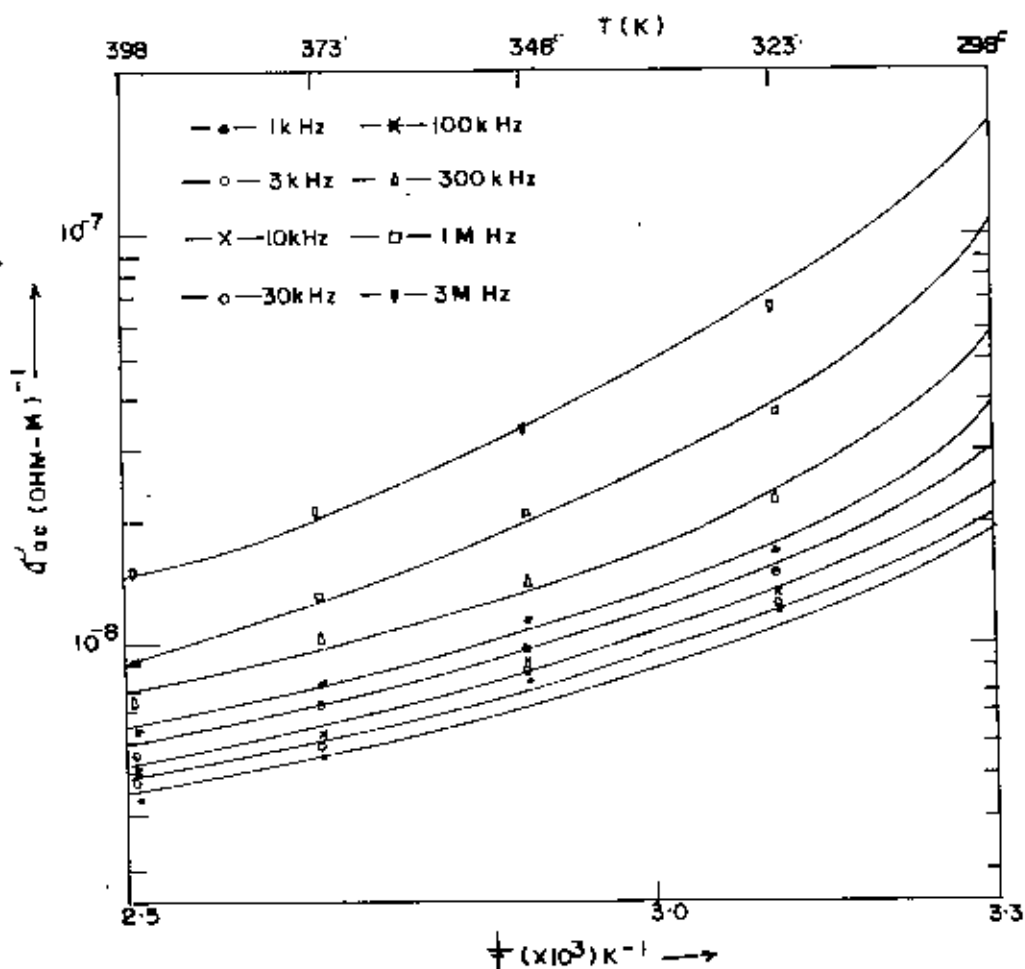


Fig. 5-11(b) σ_{ac}^{-1} Variation as a function of inverse temperature for washed and 773 K heat treated sample (pressure 3000 psi) at different frequencies.

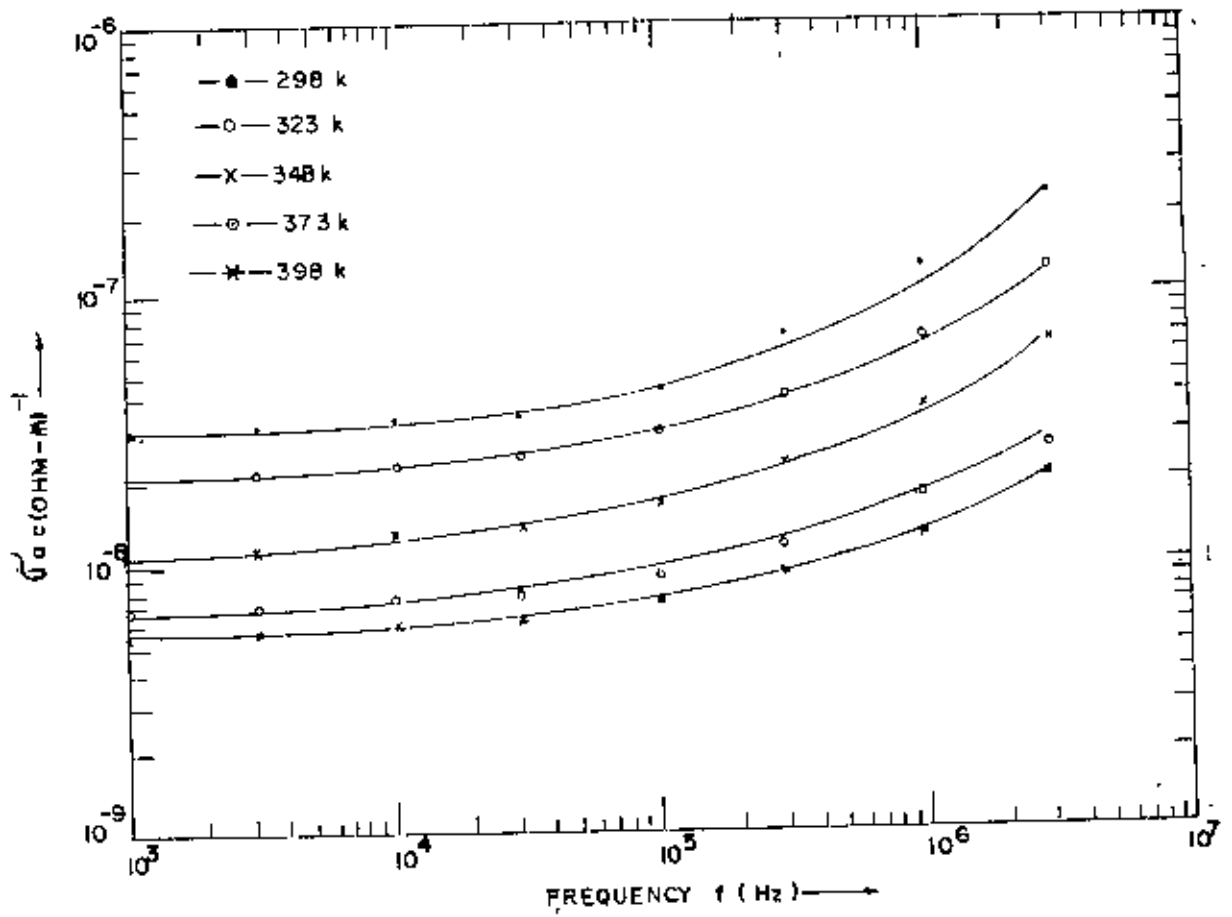


Fig. 5-10(c) σ_{ac} Versus frequency for washed and 773K heat treated sample (pressure 3500 psi) at different temperatures.

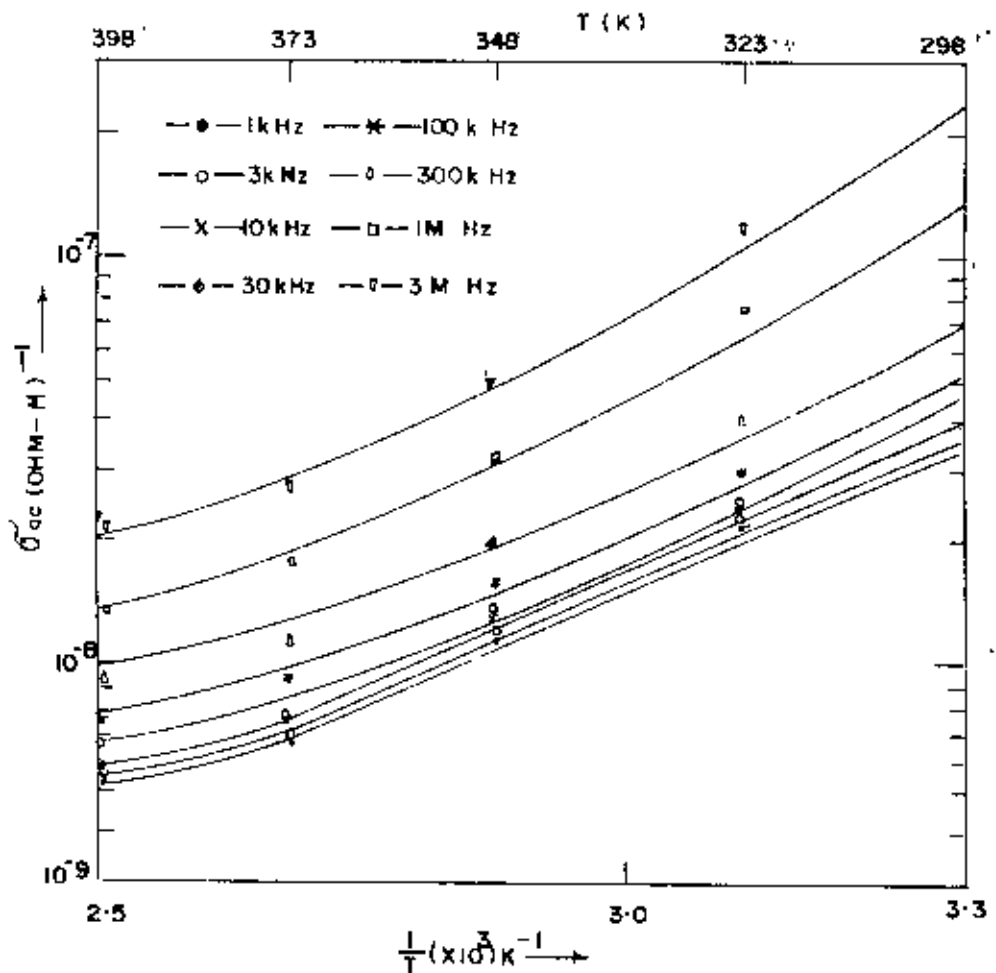


Fig. 5-11(c) σ_{ac} Variation as a function of inverse temperature for washed and 773K heat treated sample (pressure 3500 psi) at different frequencies.

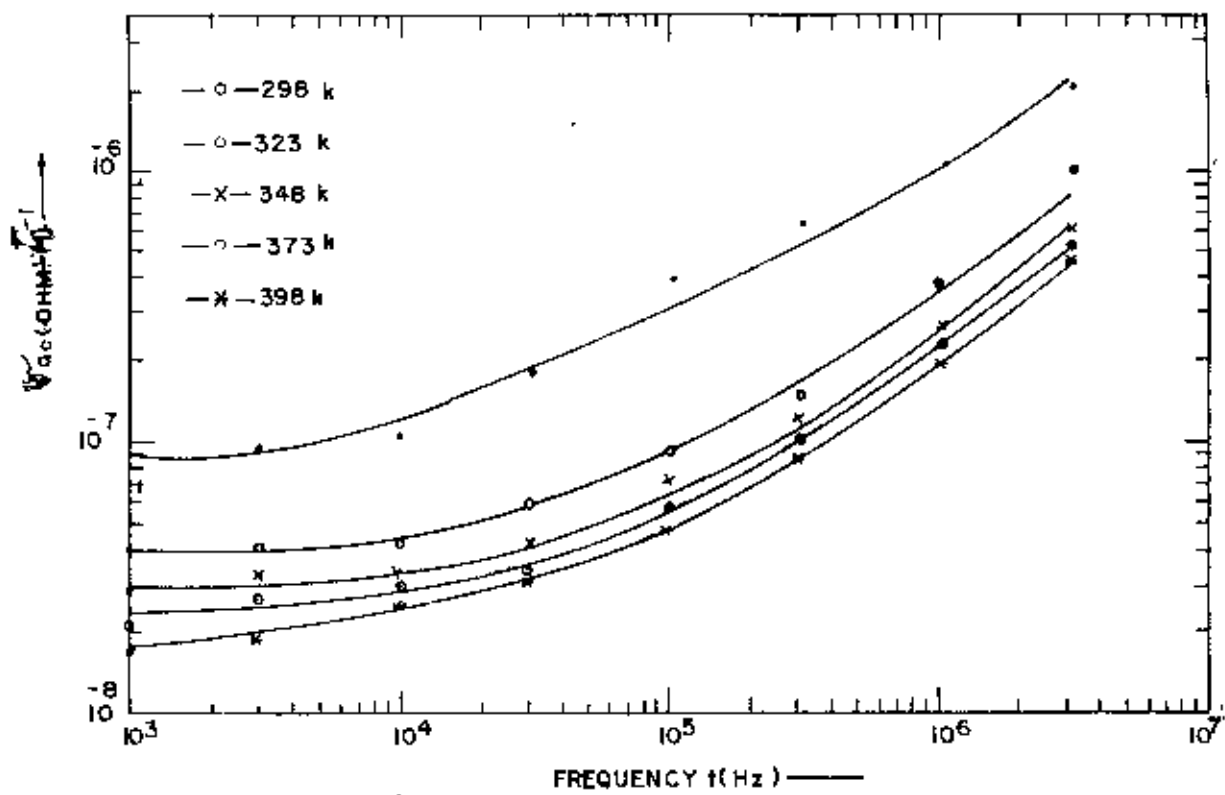


Fig 5.12.(a) σ_{ac} Versus frequency for washed and 1273 K. heat treated sample (pressure 2000 psi) at different temperatures .

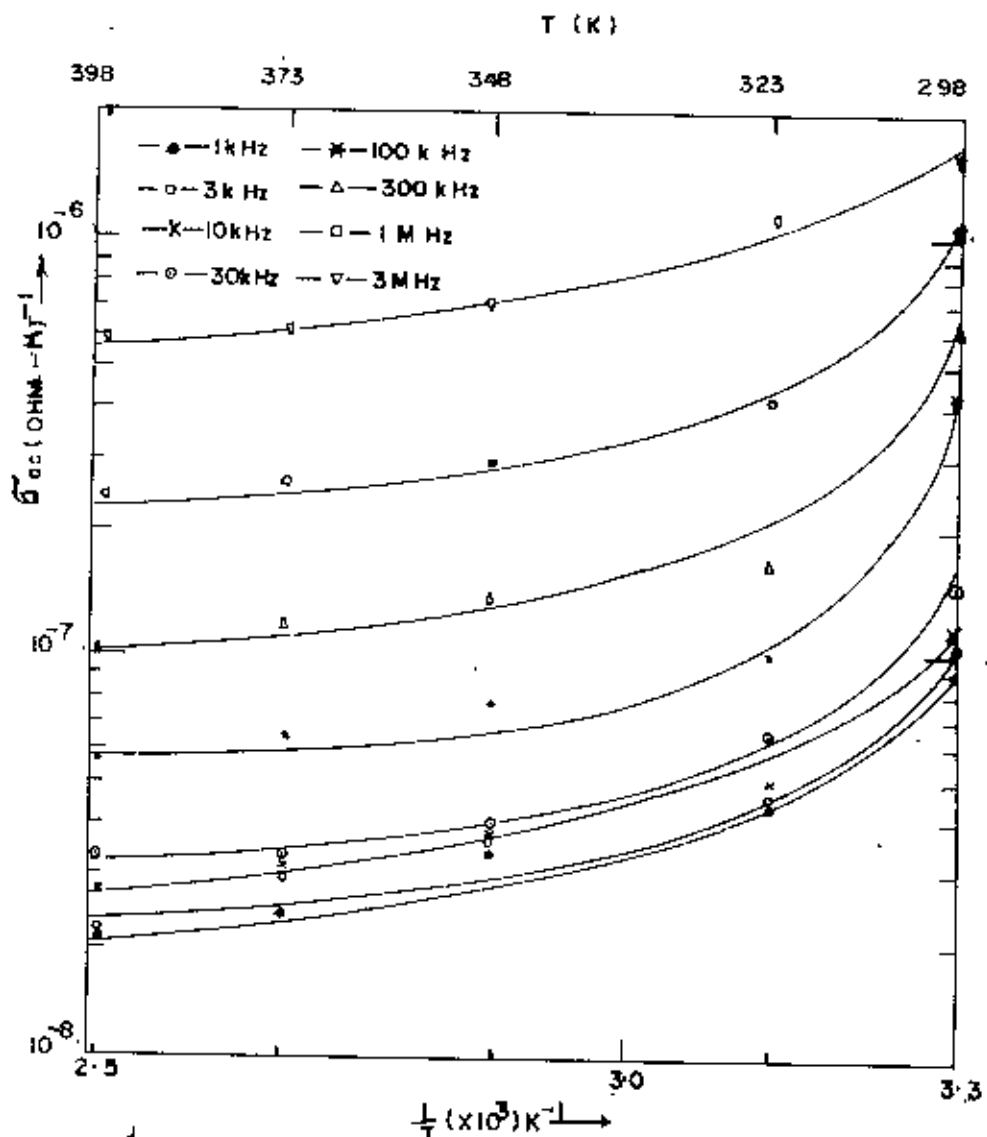


Fig 5.13 σ_{ac} Variation as a function of inverse-temperature for washed and 1273 K heat treated sample (pressure = 2000 psi) at different frequencies .

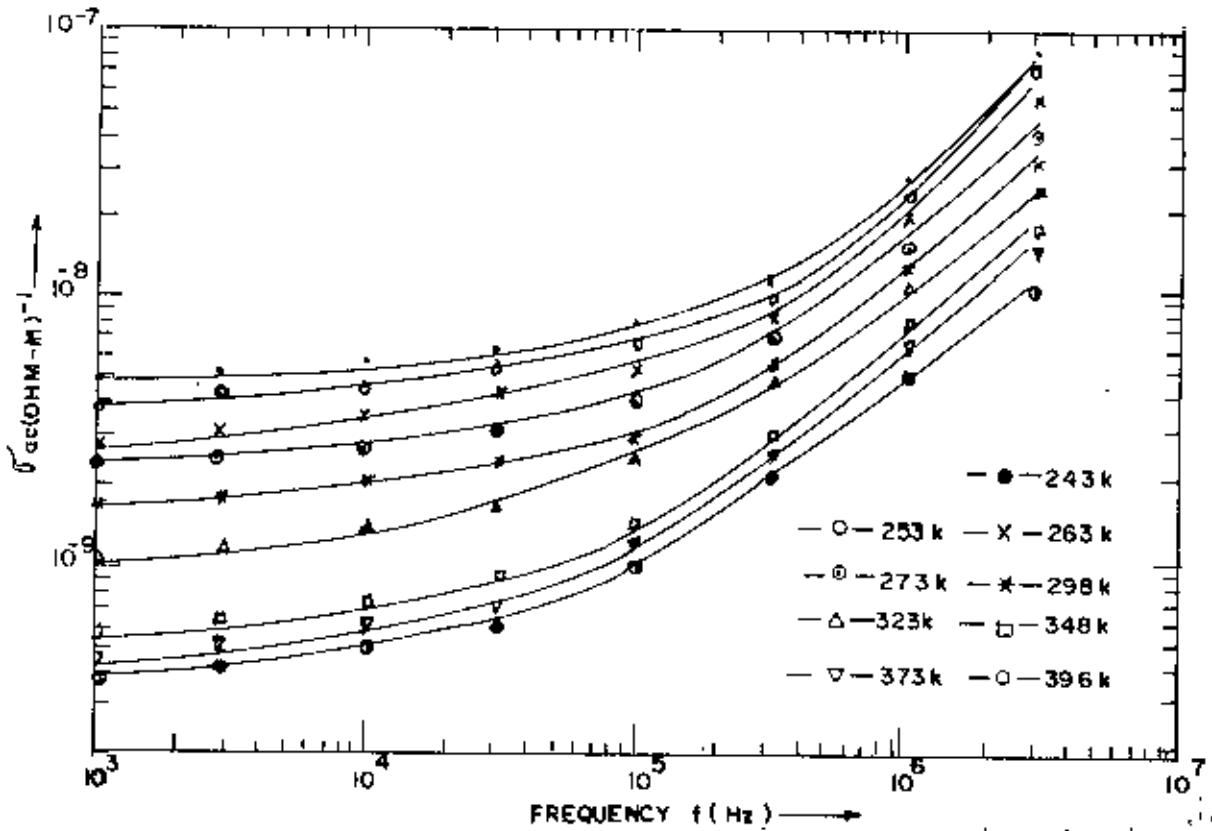


Fig. 5.12(b) Z_{ac} Versus frequency for washed and 1273 K heat treated sample (pressure 3500 psi at different temperatures.

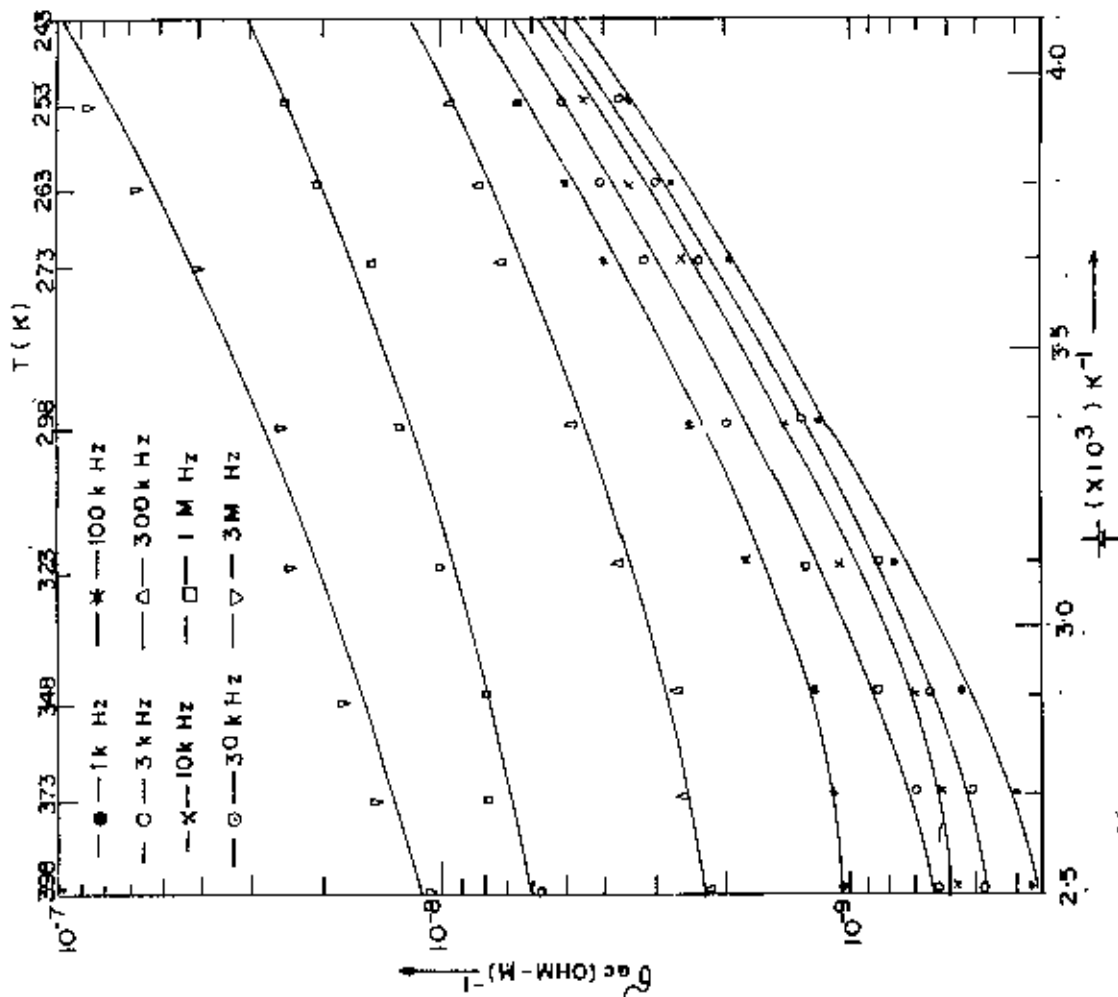


Fig. 5.13(b) Z_{ac} Variation as a function of inverse temperature for washed and 1273 k heat treated sample (pressure 3500 psi) at different frequencies.

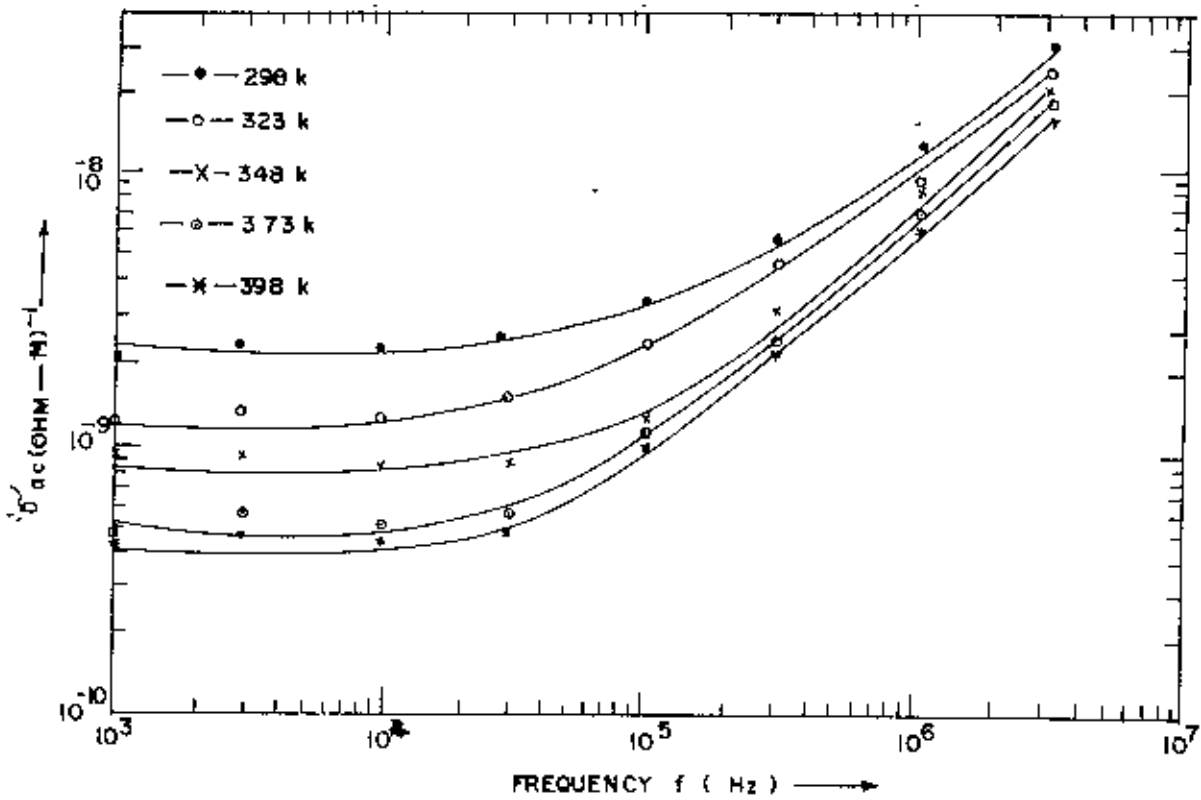


Fig 5: $\sqrt{\rho_{ac}}$ Versus frequency for washed and 1273 K heat treated sample (pressure 3000psi) at different temperatures.

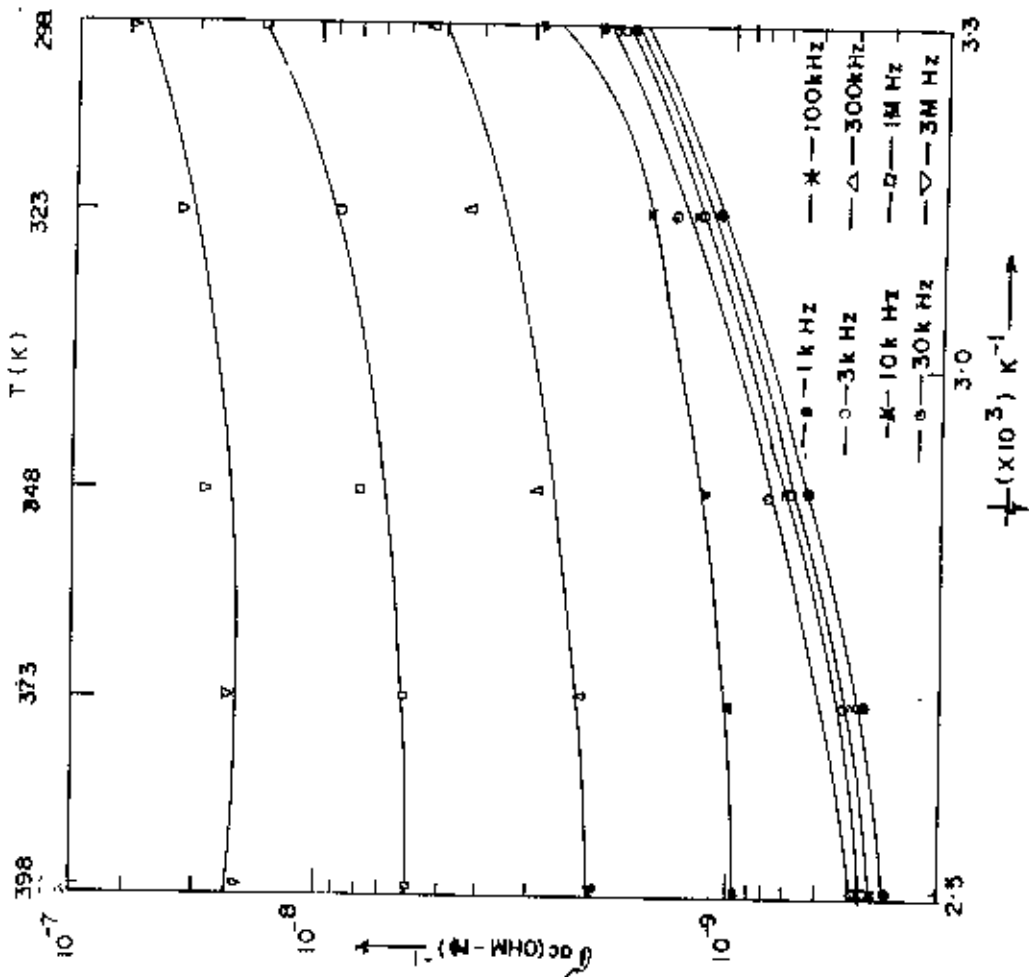


Fig 6: $\sqrt{\rho_{ac}}$ Variation as a function of inverse temperature for washed and 1273 K heat treated sample (pressure 3000psi) at different frequencies

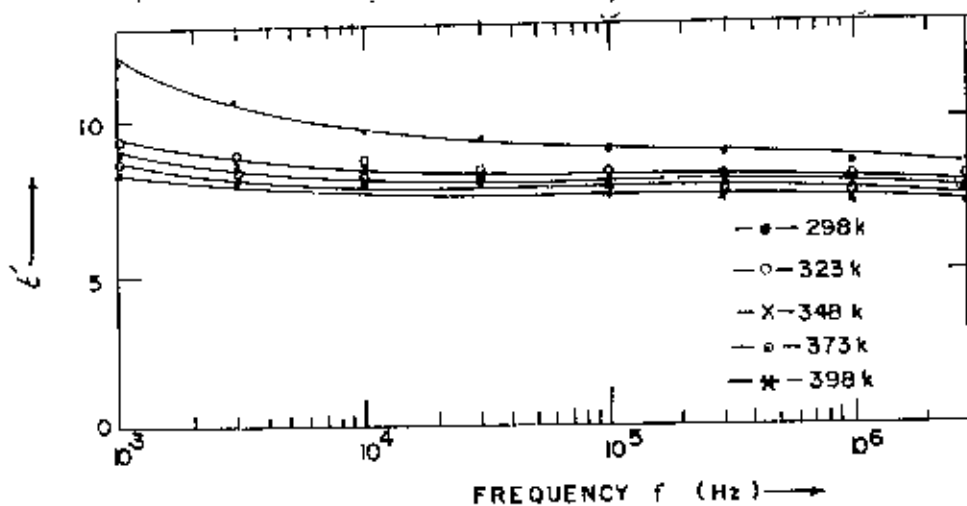


Fig. 5-14(a) ϵ'' Versus frequency for washed sample (pressure 2000 psi) at different temperatures .

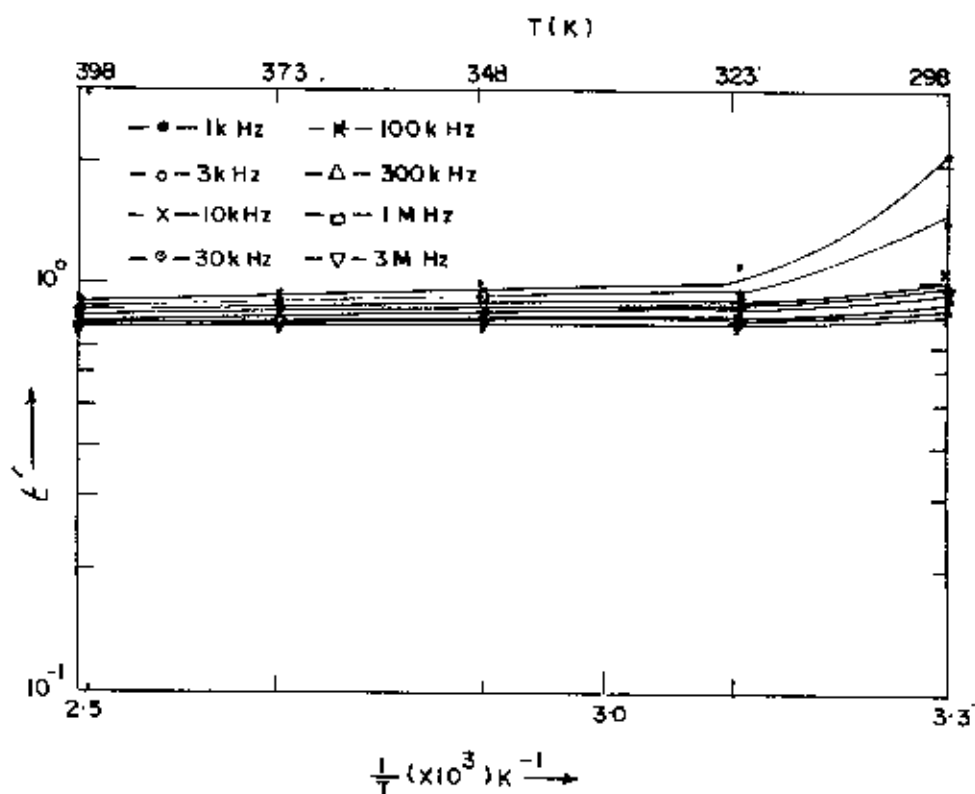


Fig. 5-15(a) ϵ'' Variation as a function of inverse temperature for washed sample (pressure 2000 psi) at different frequencies .

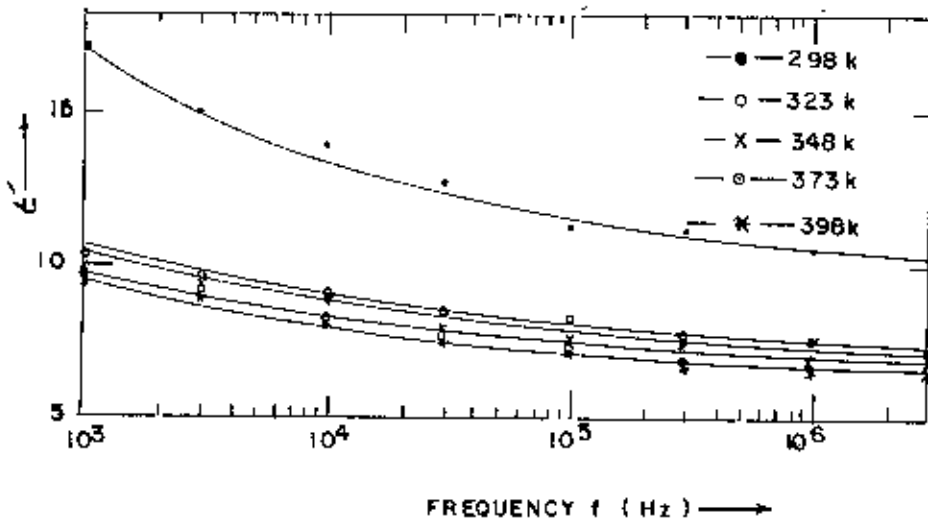


Fig 5-14(b) ϵ' Versus frequency for washed sample (pressure 3000 psi) at different temperatures.

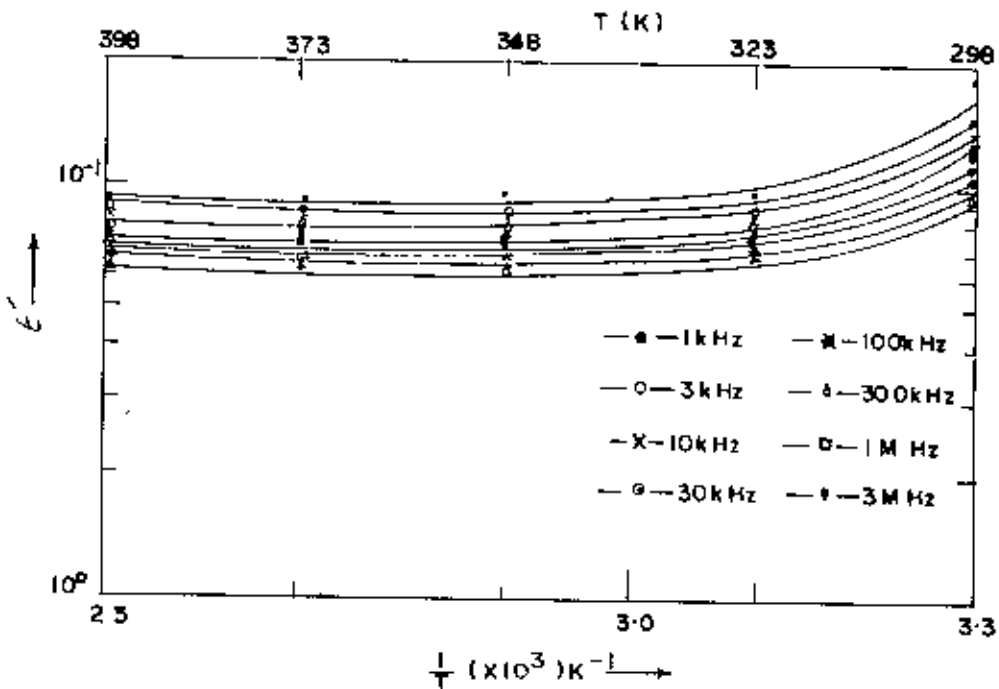


Fig 5-15(b) Variation as a function of inverse temperature for washed sample (pressure 3000 psi) at different frequencies.

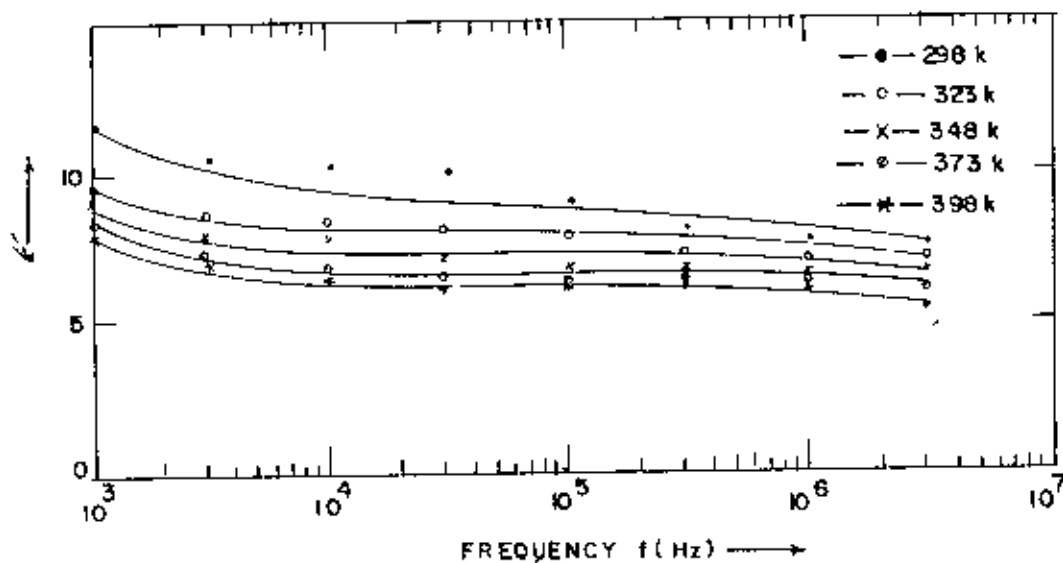


Fig 5-14(c) ϵ'' Versus frequency for washed sample (pressure 3500 psi) at different temperatures .

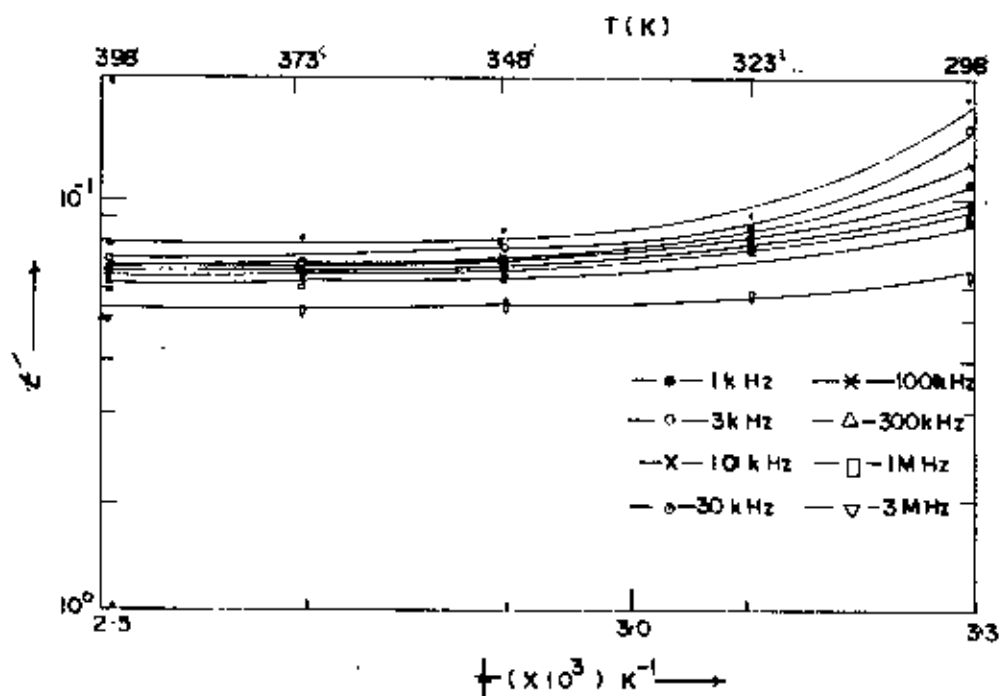


Fig 5-15(b) ϵ'' Variation as a function of inverse temperature for washed sample (pressure 3500 psi) at different frequencies.

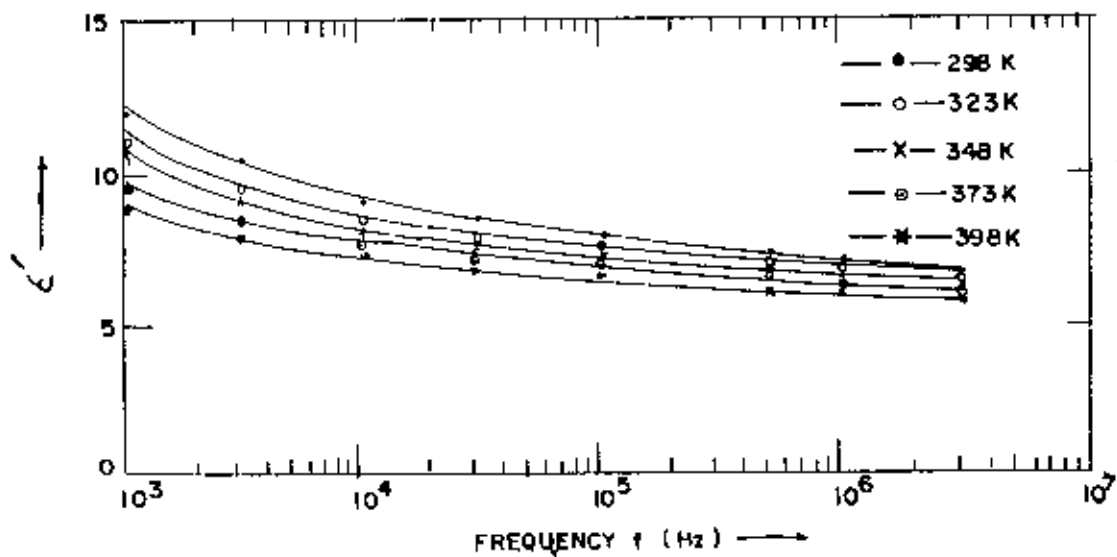


Fig 5-16(a) ϵ'' Versus frequency for washed and 773 K heat treated Sample (pressure 2000 psi) at different Temperatures .

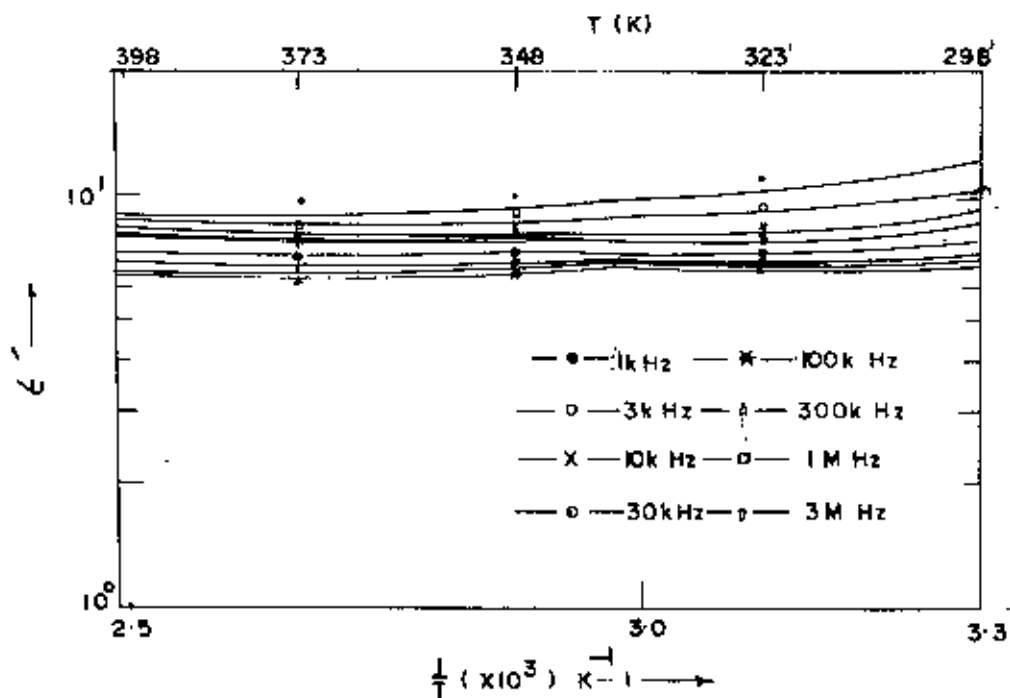


Fig.5-17(a) Variation as a function of inverse temperature for washed and 773 K heat treated Sample (pressure 2000 psi) at different frequencies .

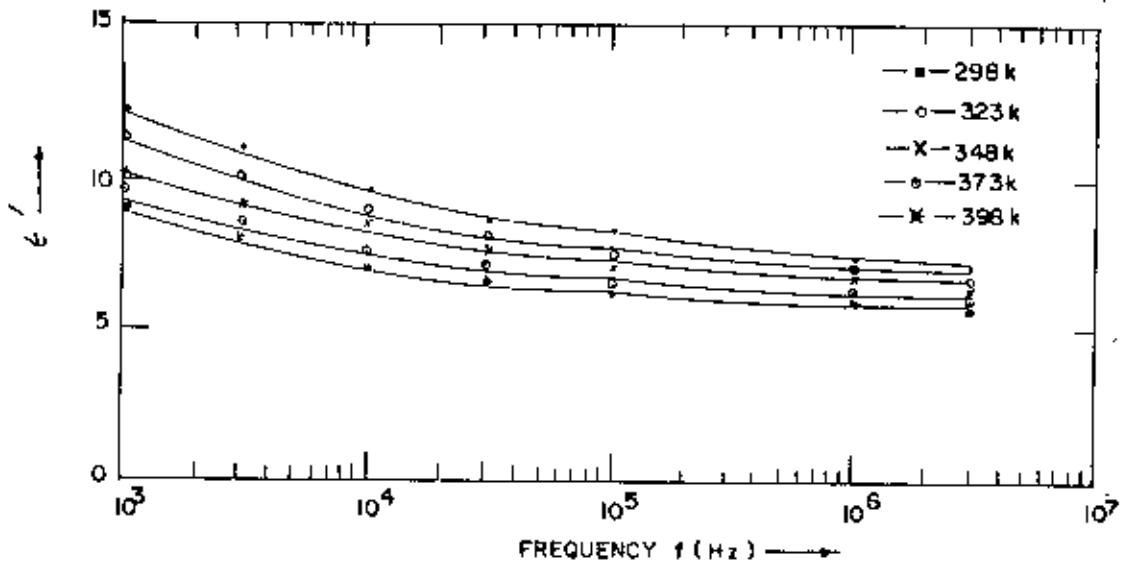


Fig. 5-16(b) ϵ' Versus frequency for washed and 773 K heat treated sample (pressure 3000 psi) at different temperatures.

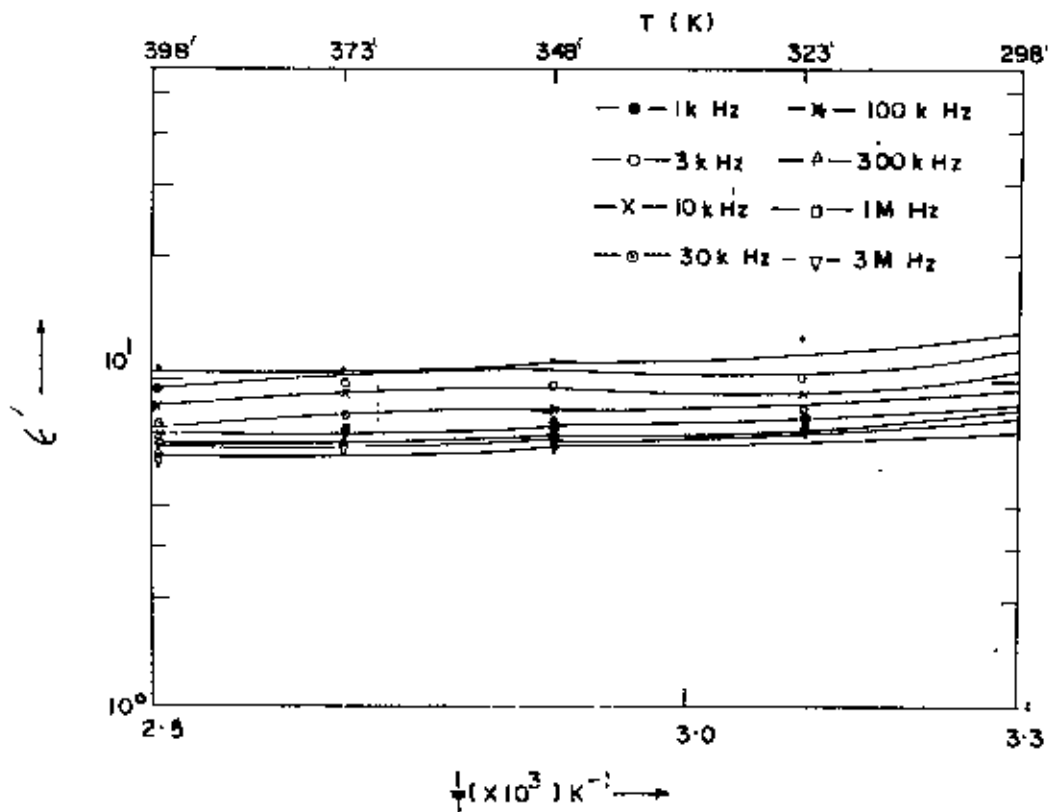


Fig 5-17(b) ϵ' Variation as a function of inverse temperature for washed and 773 K heat treated sample (pressure 3000 psi) at different frequencies.

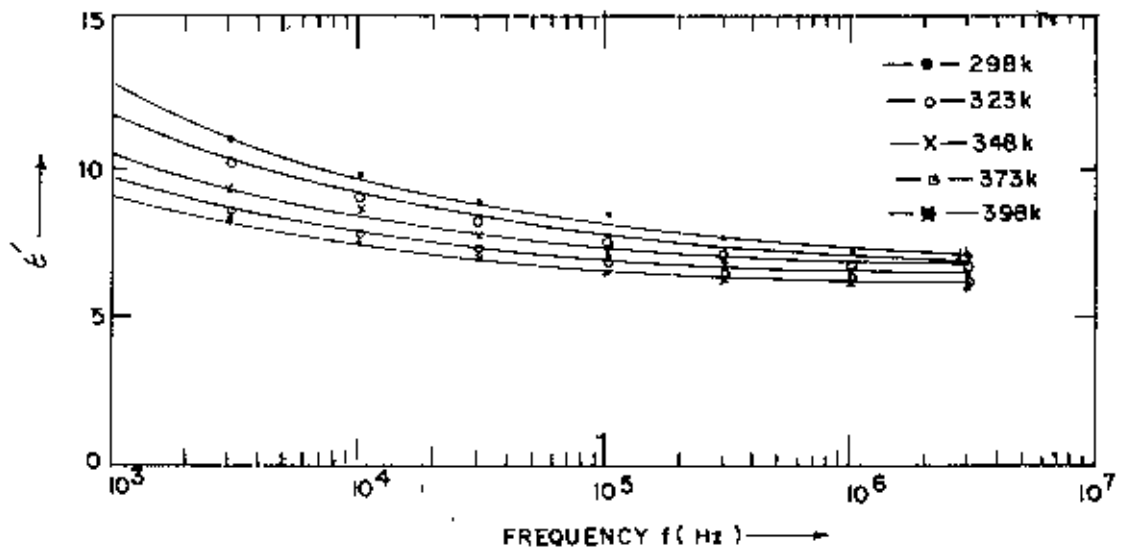


Fig. 5-16(c) ϵ'' versus frequency for washed and 773 k heat treated sample (pressure 3500 psi) at different temperatures.

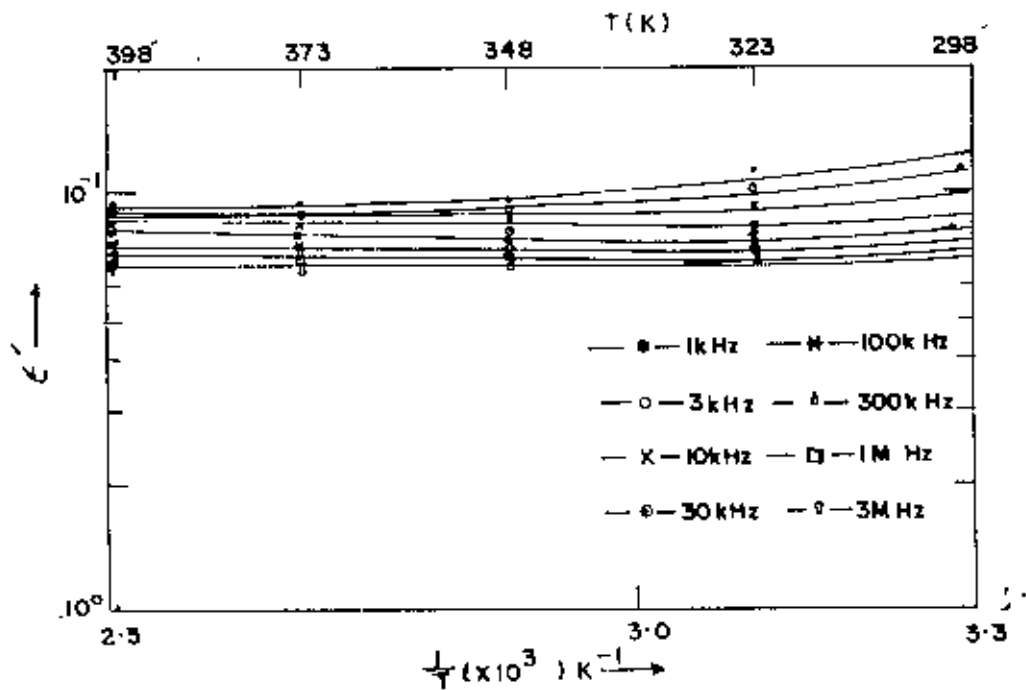


Fig. 5-17(d) ϵ'' Variation as a function of inverse temperatures for washed and 773 K heat treated sample (pressure 3500 psi) at different frequencies.

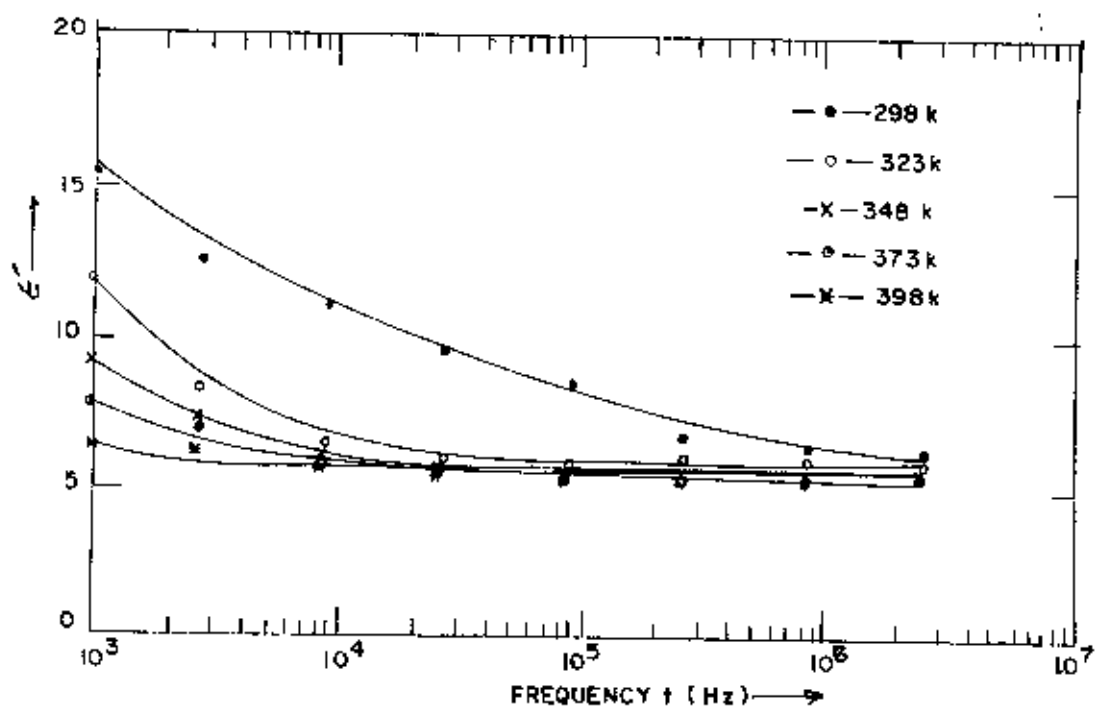


Fig. 5.18(a) ϵ'' Versus frequency for washed and 1273 K heat treated sample (pressure 2000 psi) at different temperatures.

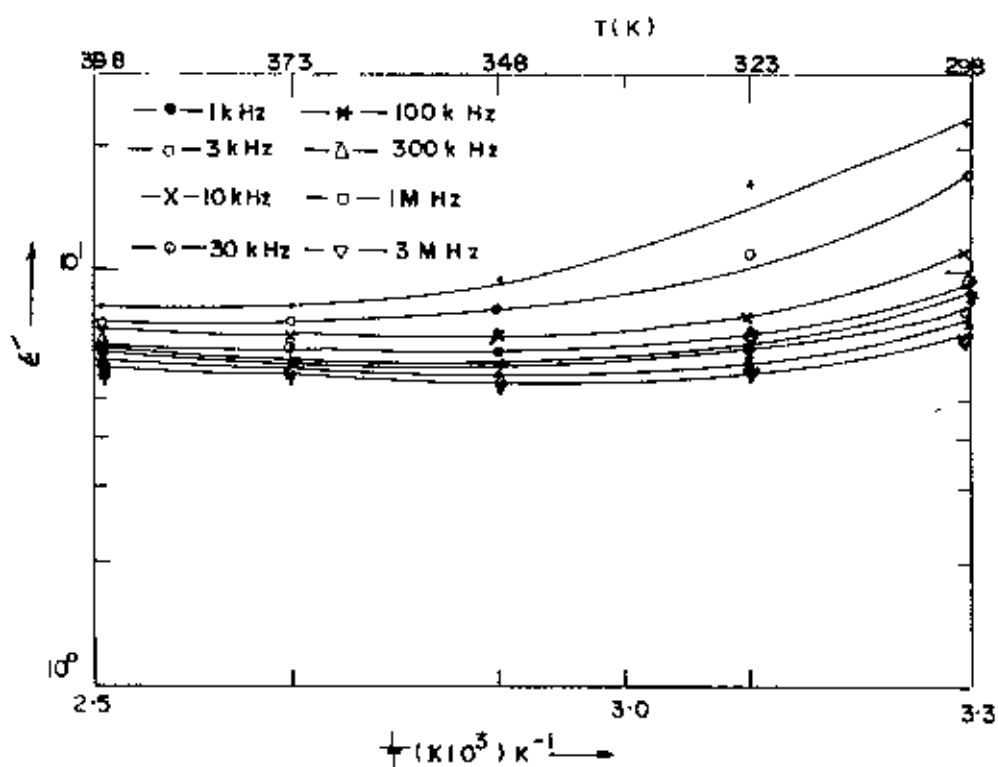


Fig 5.19(a) ϵ'' Variation as a function of inverse temperature for washed and 1273k heat treated sample (pressure 2000psi) at different frequencies.

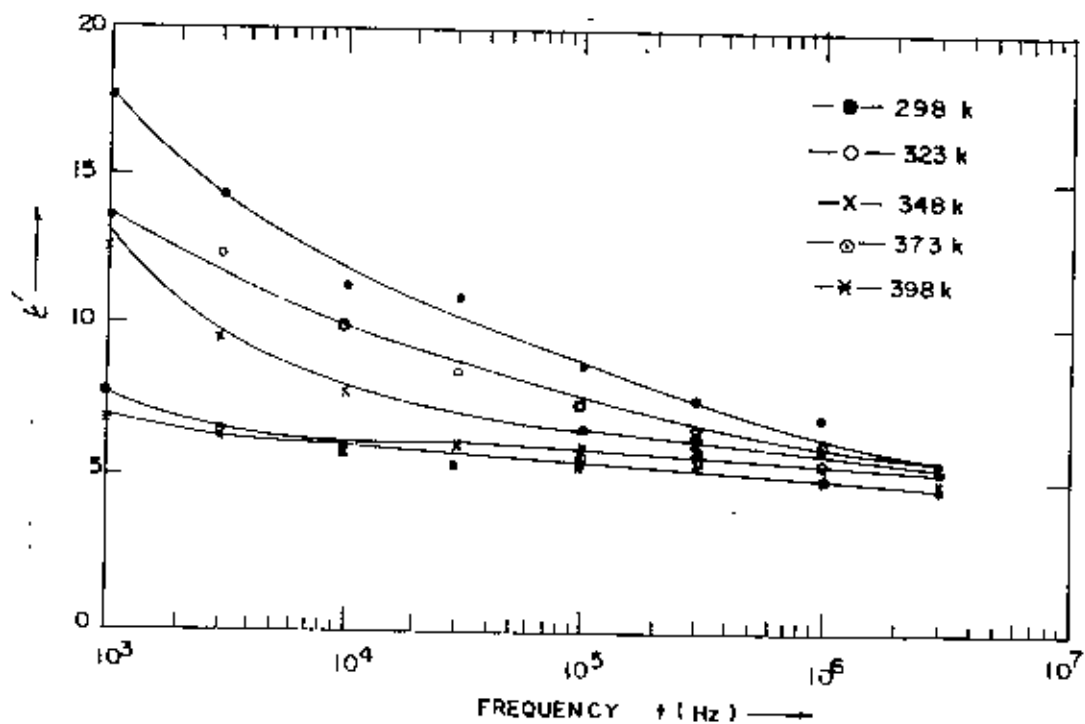


Fig 5-18(b) ϵ'' Versus frequency for washed and 1273 K heat treat treated sample (pressure 3000 psi) at different temperatures.

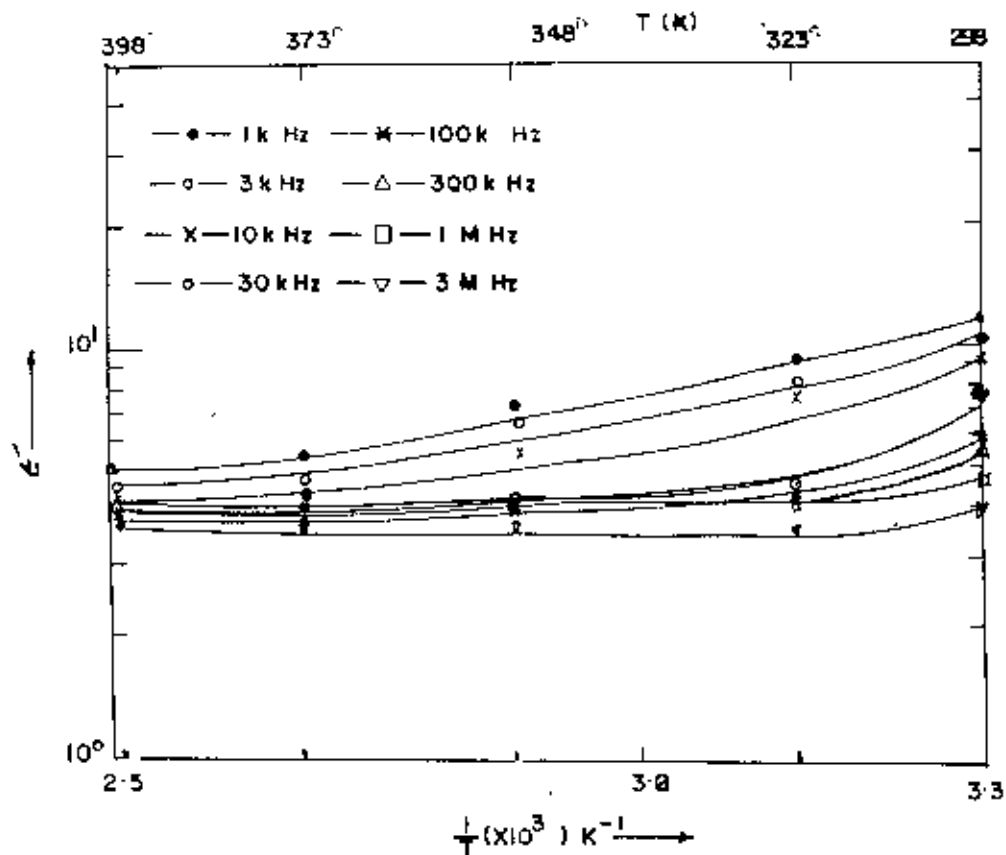


Fig 5-19(b) ϵ'' Variation as a function of inverse temperature for washed and 1273 K heat treated sample (pressure 3000 psi) at different frequencies.

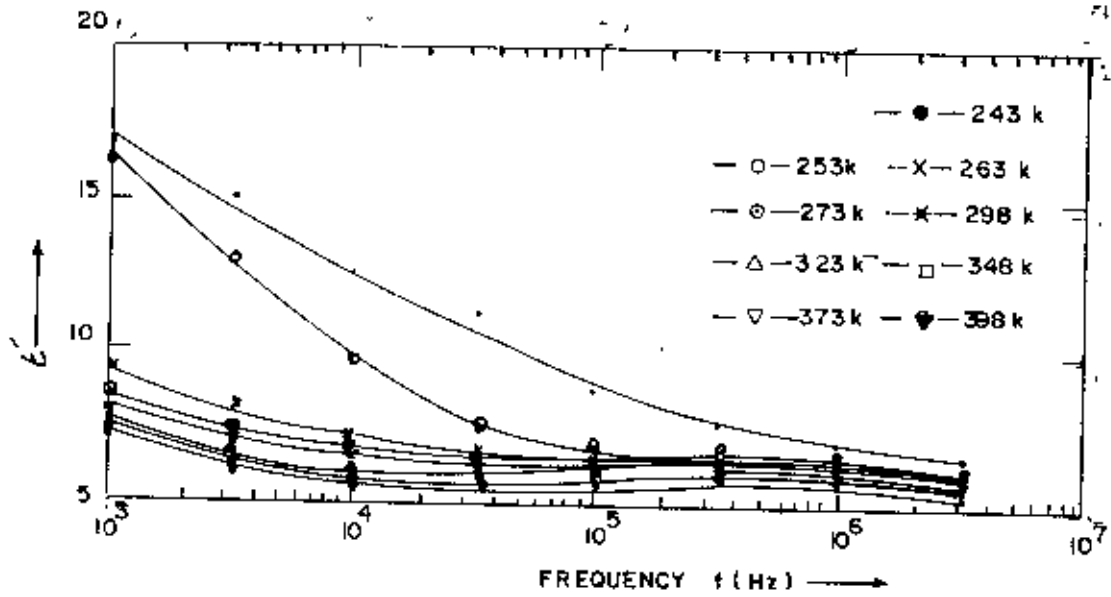


Fig. 5.18(c) ϵ'' Versus frequency for washed and 1273 K heat treated sample (pressure 3500 psi) at different temperatures.

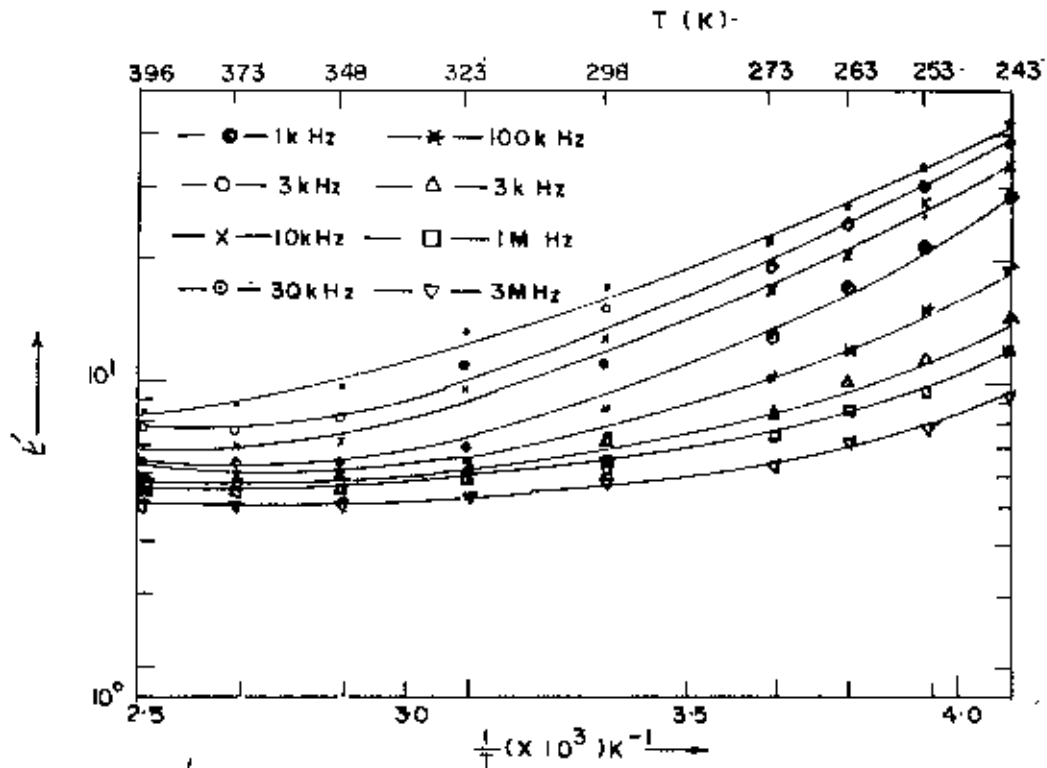


Fig. 5.18(c) ϵ'' Variation as a function of inverse temperature for washed and 1273 K heat treated sample (pressure 3500 psi) at different frequencies.

samples have similar feature. The variation of σ_{ac} with $\log f$ for all the samples at different temperature fits to a relation $\sigma(\omega) \propto \omega^n$ with $n=0.05$ to 0.1 below 10^5 Hz and $n=0.4$ to 0.9 above.

In sample B it is seen that the value of n in the higher frequency increases with the increase of pressure. In sample C the effect of pressure on the variation of σ_{ac} with frequency for different pressures is not significant. While it is more significant in sample D, resulting higher value of n with increasing pressure in the high frequency region. It is further to be mentioned that at low temperatures, the variation of σ_{ac} with frequency followed the same trend. It is apparent that the curves appear to be flatten with the increase of pressure in the lower temperatures.

The variation of σ_{ac} with inverse temperature for frequencies 1 K, 3 K, 10 K, 30 K, 100 K, 300 K, 1 M and 3 MHz for samples B, C and D is shown in figures 5.9, 5.11 and 5.13. The decrease of the σ_{ac} with temperature may likely to be due to the adsorbed water in the pores of the material. This adsorbed water acts as a source for the $(OH)^-$ groups and this OH ion compensates with clay cations as temperature increases.

5.5.2 A.c. dielectric constant

The dependence of ϵ' on frequency at different temperatures for samples B, C and D are presented in fig.

5.14, 5.16 and 5.18 respectively. It is observed that $\epsilon' - \log f$ curves for all the samples have similar features. The ϵ' decreases sharply in the frequency region upto 30 KHz and decreases slowly above. It is observed that the room temperature ϵ' is more for the sample D, i.e., ϵ' value increases on heat treatment at higher temperatures. The effect of pressure is to increase the ϵ' value by small amount in the respective samples. However, for sample D (3500 psi), the room temperature ϵ' value is observed less compared to that of the other samples. The interfacial polarization is less sensitive to rapidly changing electric field at higher frequencies which leads to a decrease in ϵ' value.

The dependence of ϵ' with inverse temperature for frequencies 1 K, 3 K, 10 K, 30 K, 100 K, 300 K, 1 M and 3 MHz for sample B, C and D is shown in fig. 5.15, 5.17 and 5.19 respectively. The general trend is to decrease sharply the ϵ' value upto 350 K and above this decreases very slowly. Since all these curves no downward inflection is exhibited. This experiment is extended upto 240 K for sample D (3500 psi). It is seen that even at low temperature ϵ' value continues to increase. This could be due to presence of adsorbed water in the capillaries within the clay. The decrease of ϵ' value with temperature may be due to the neutralization of the opposite charges constituting the dipoles thereby decreasing the number

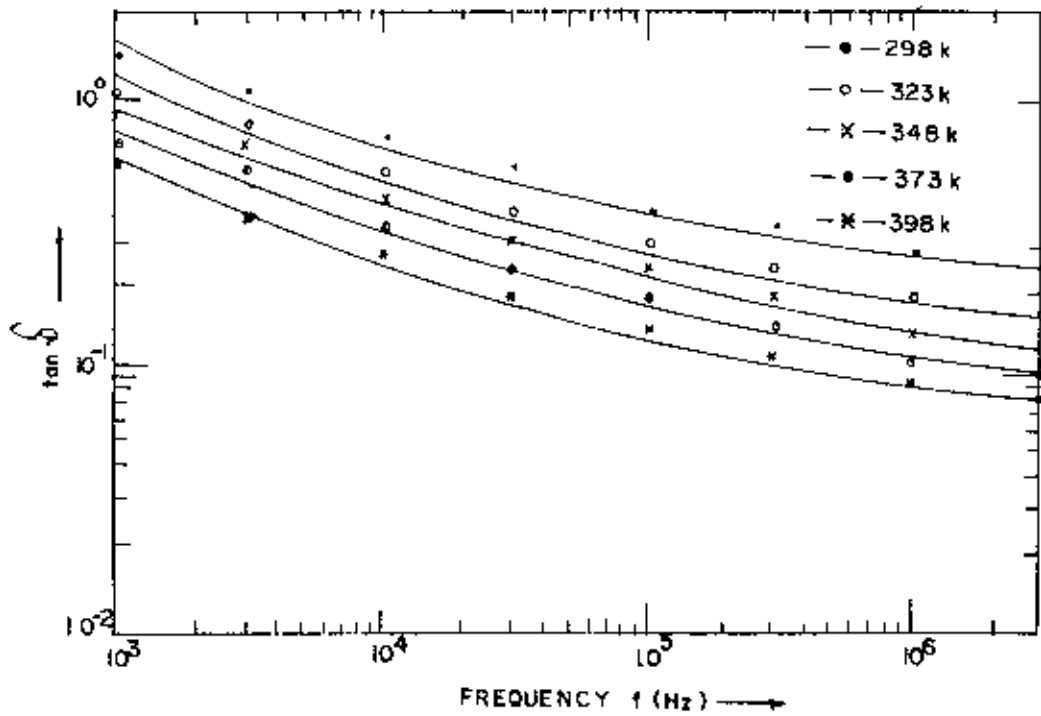


Fig- 5-20(a) $\tan \delta$ Versus frequency for washed sample (pressure 2000 psi) at different temperatures.

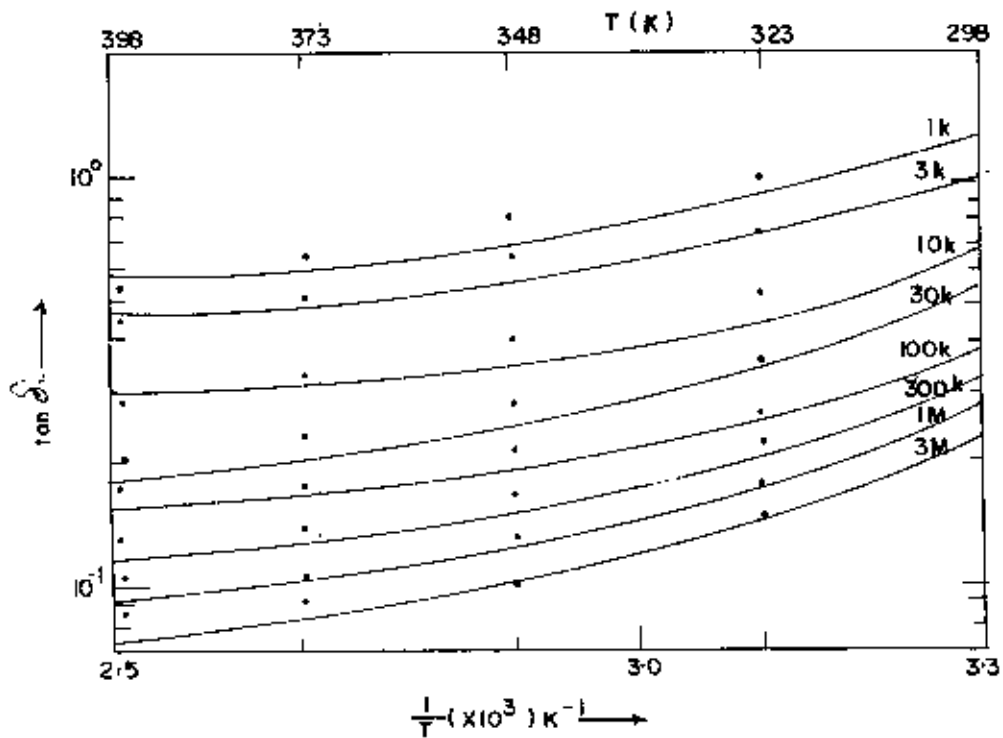


Fig- 5-21(a) $\tan \delta$ Variation as a function of inverse temperature for washed sample (pressure 2000 psi) at different frequencies.

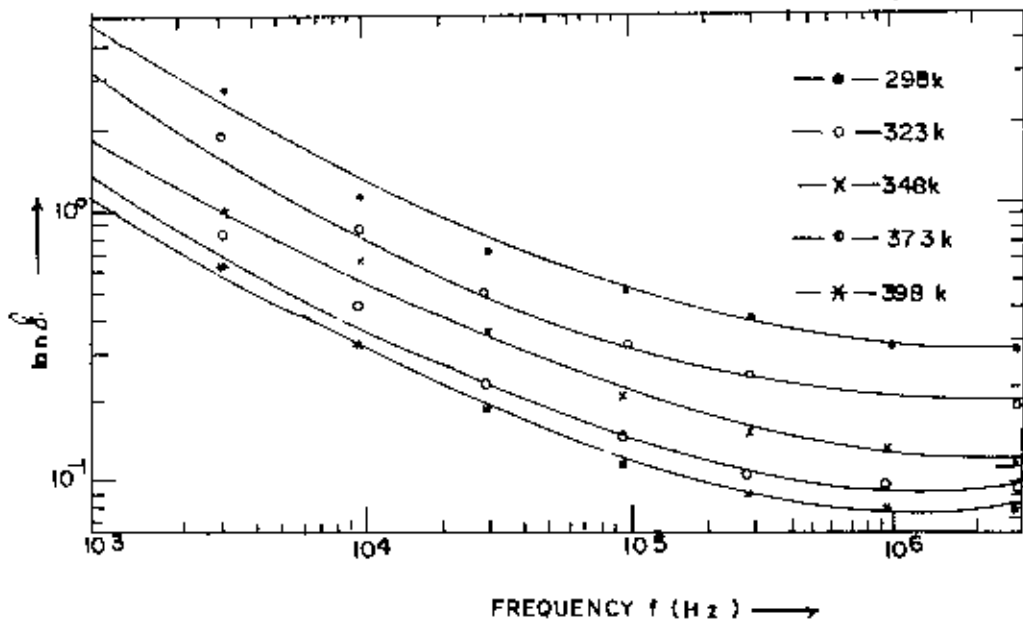


Fig. 5-20(a) $\tan \delta$ Versus frequency for washed sample (pressure 3000 psi) at different temperatures.

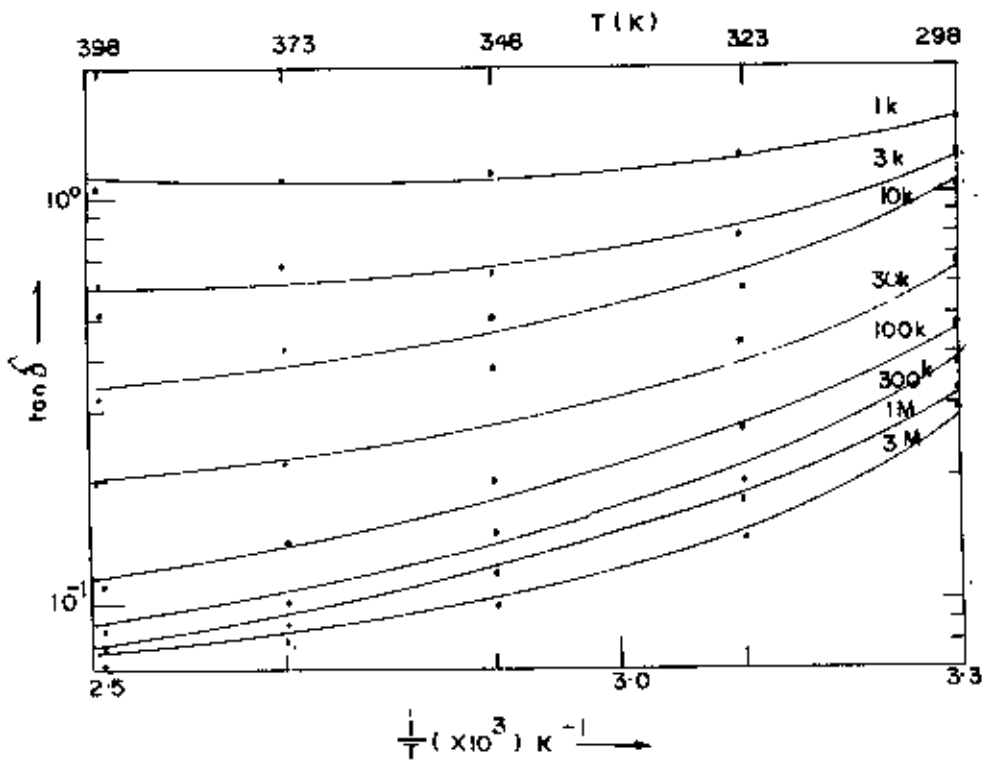


Fig. 5-20(b) $\tan \delta$ Variation as a function of inverse temperature for washed sample (pressure 3000 psi) at different frequencies.

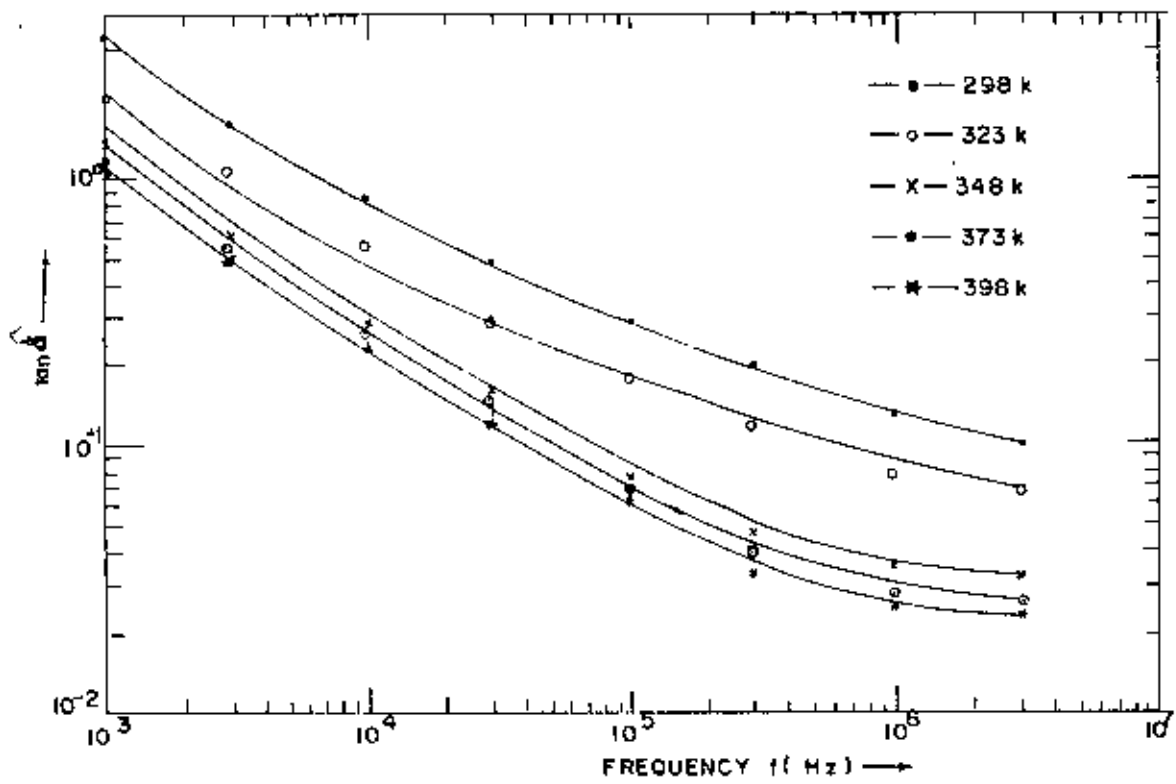


Fig. 5.20 $\tan \delta$ Versus frequency for washed sample (pressure 3500 psi) at different temperatures:

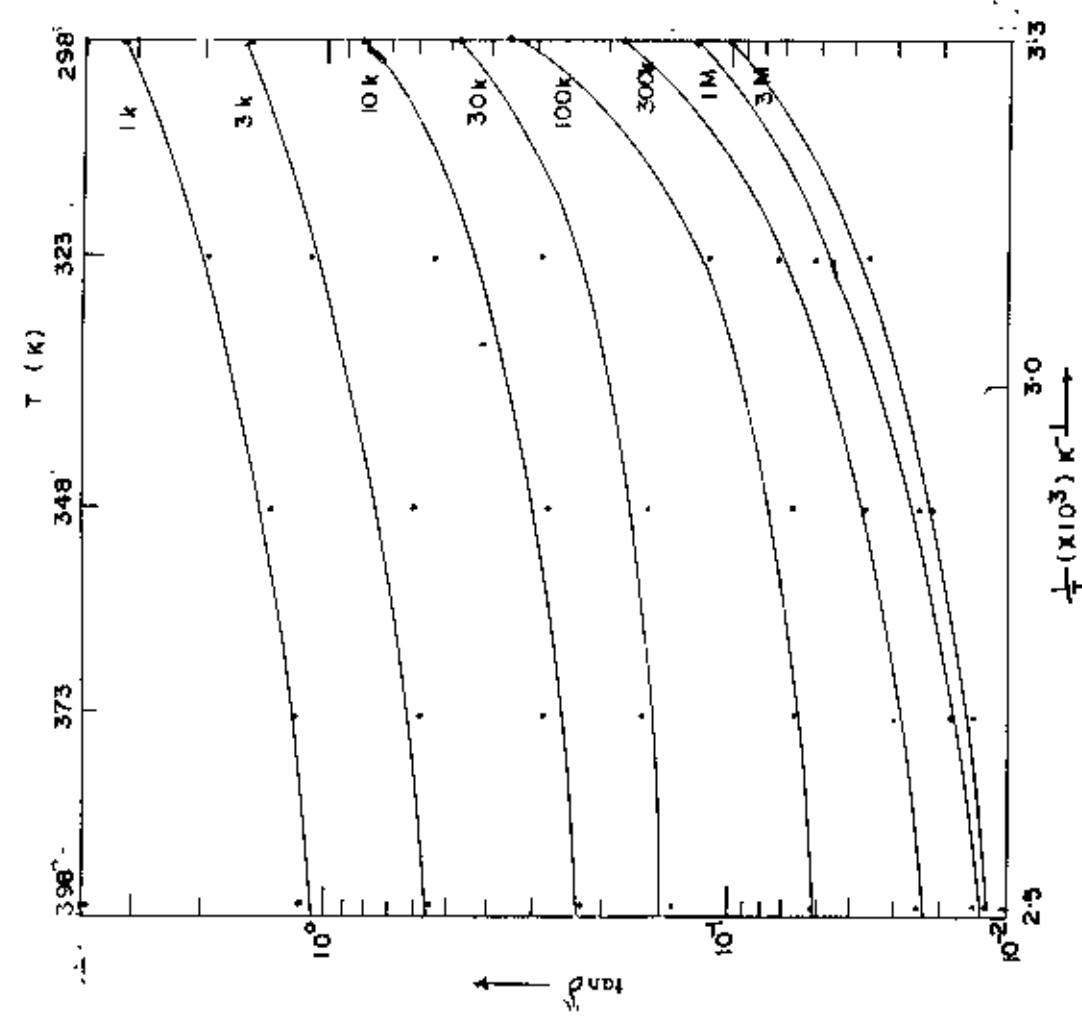


Fig. 5.21 $\tan \delta$ Variation as a function of inverse temperature for washed sample (pressure 3500 psi) at different frequencies.

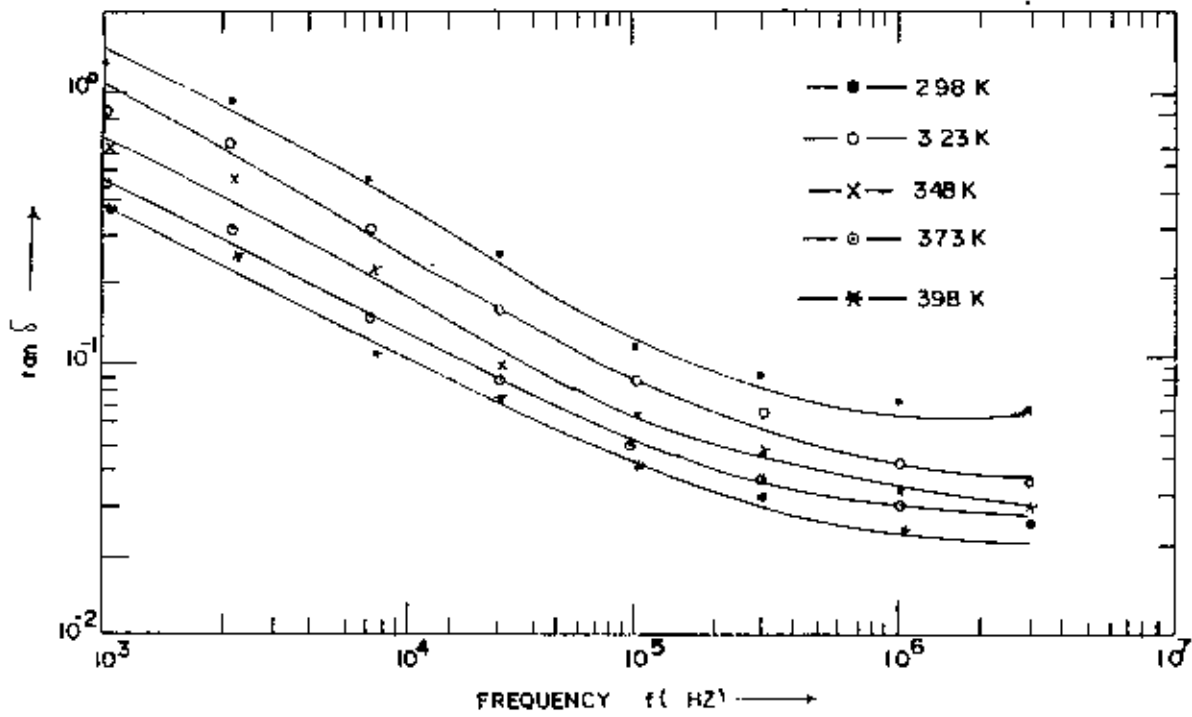


Fig 5-22(a) $\tan \delta$ Versus frequency for washed and 773 K heat treated sample (Pressure 2000 psi) at different temperatures.

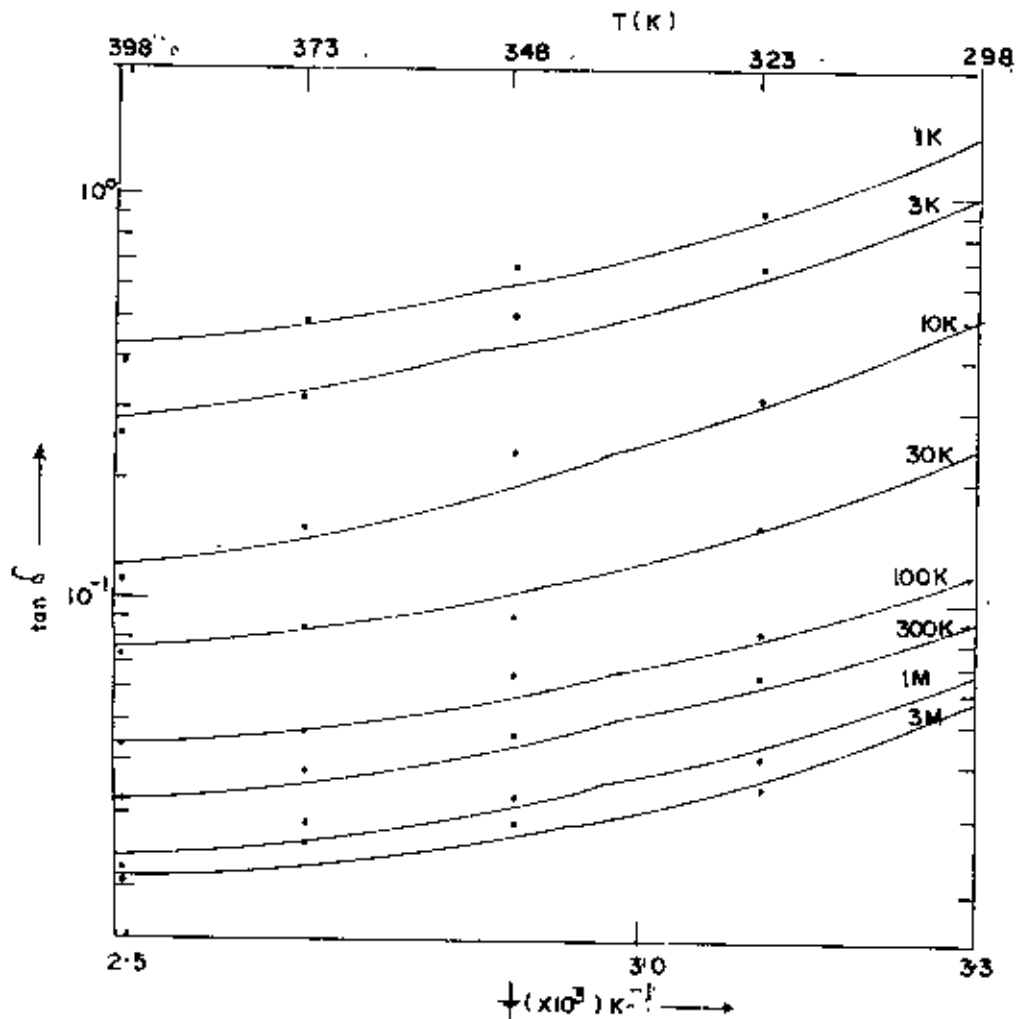


Fig 5-23(a) $\tan \delta$ Variation as a function of inverse temperature for washed and 773 K heat treated sample (Pressure 2000 psi) at different frequencies.

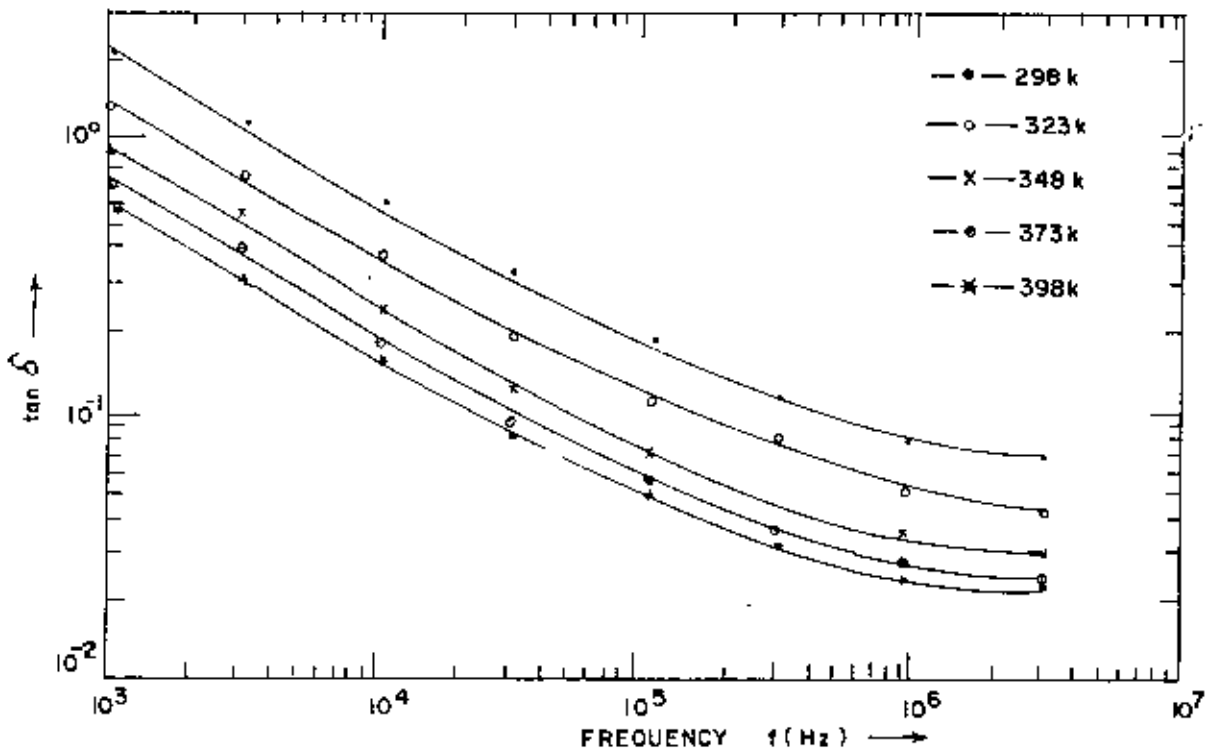


Fig 5-22(b) $\tan \delta$ Versus frequency for washed and 773K heat treated sample (Pressure 3000 psi) at different temperatures.

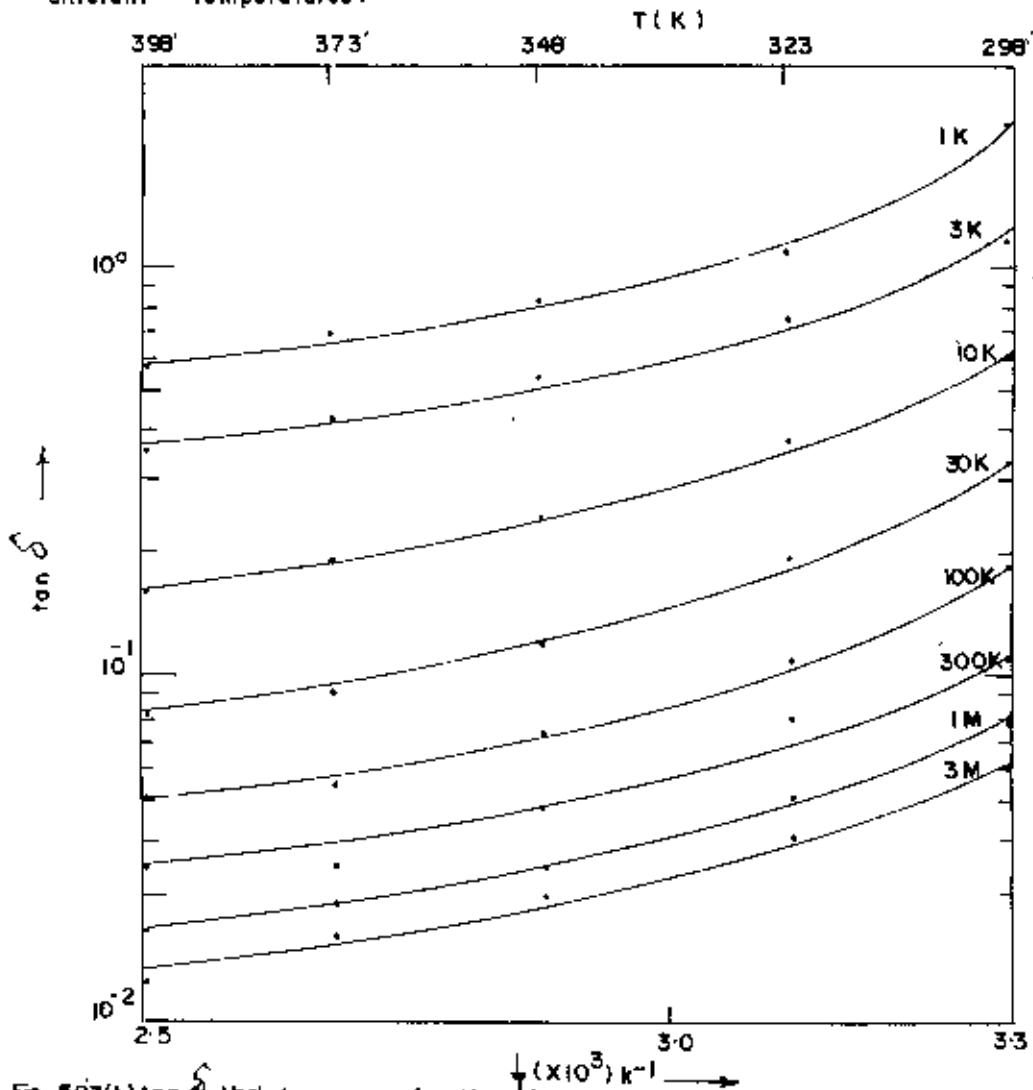


Fig. 5-23(b) $\tan \delta$ Variation as a function of inverse temperature for washed and 773 k heat treated sample (pressure 3000psi) at different frequencies.

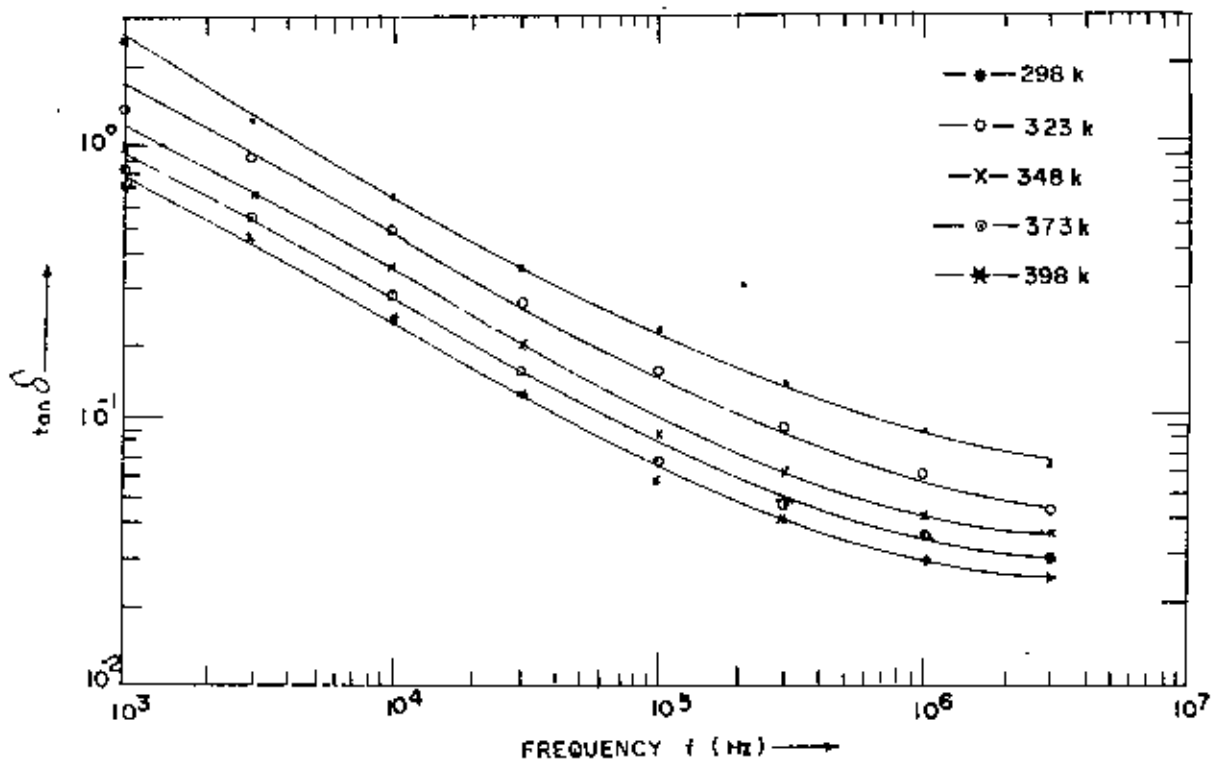
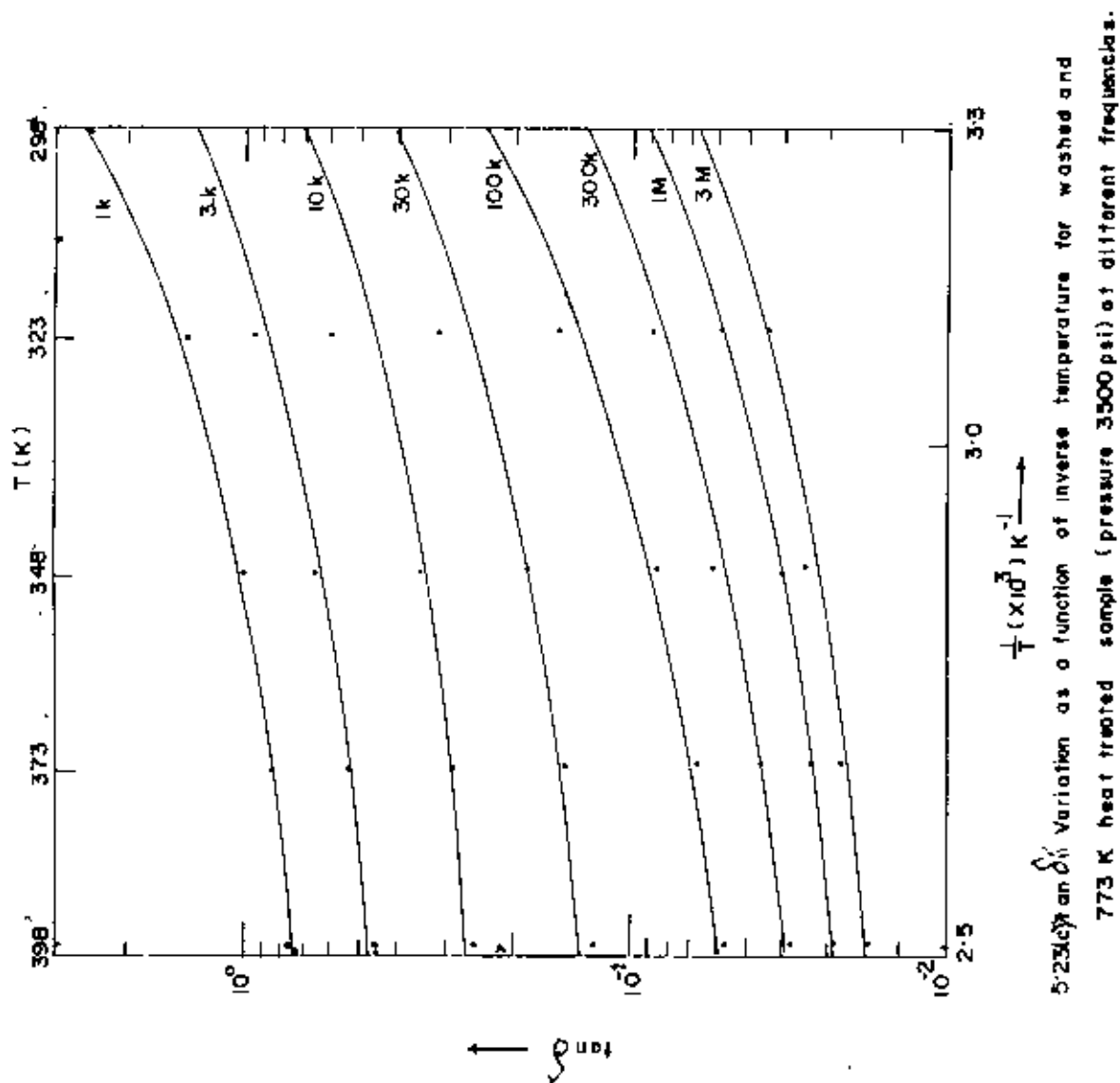


Fig 5-22(c) $\tan \delta$ Versus frequency for washed and 773 K heat treated sample (pressure 3500 psi) at different temperatures :



5-23(c) $\tan \delta$ Variation as a function of inverse temperature for washed and 773 K heat treated sample (pressure 3500 psi) at different frequencies.

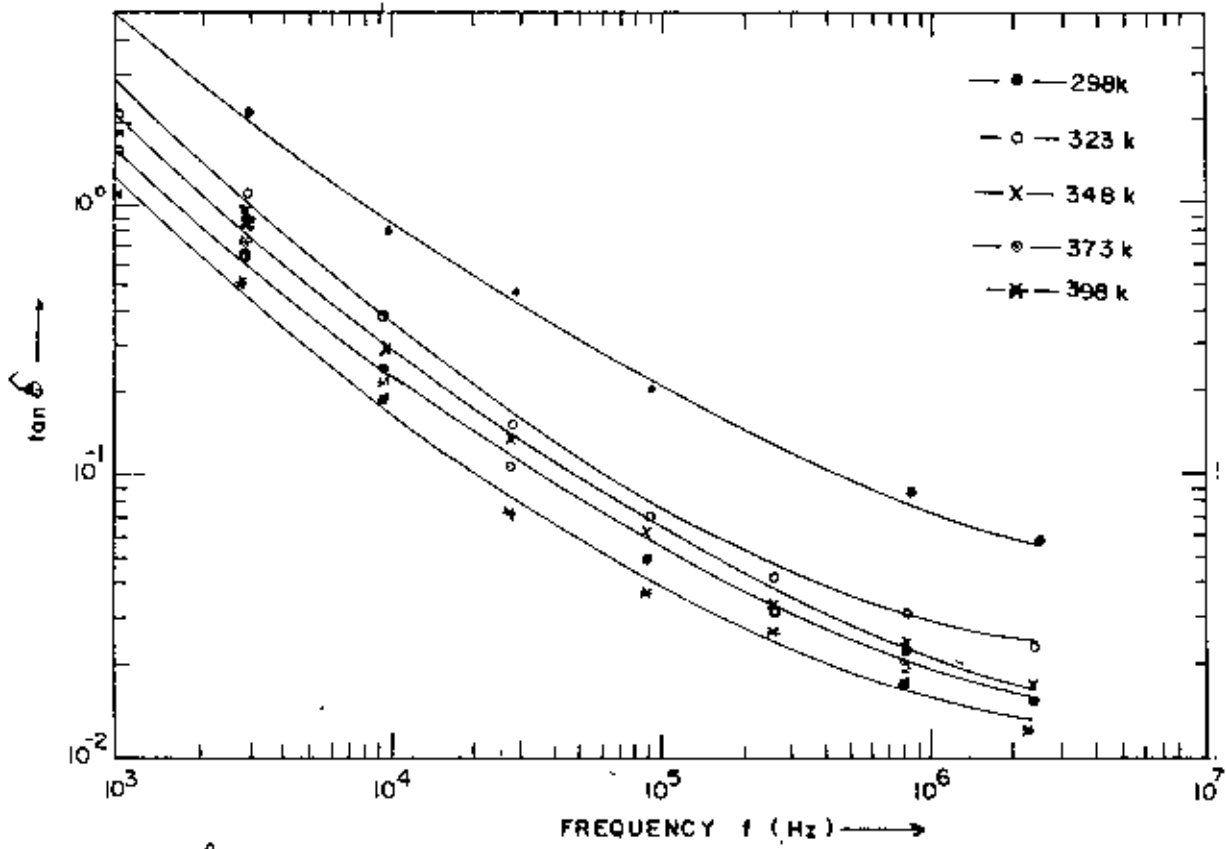


Fig.5.24 $\tan \delta$ Versus frequency for washed and 1273 K heat treated sample (pressure 2000 psi) at different temperatures.

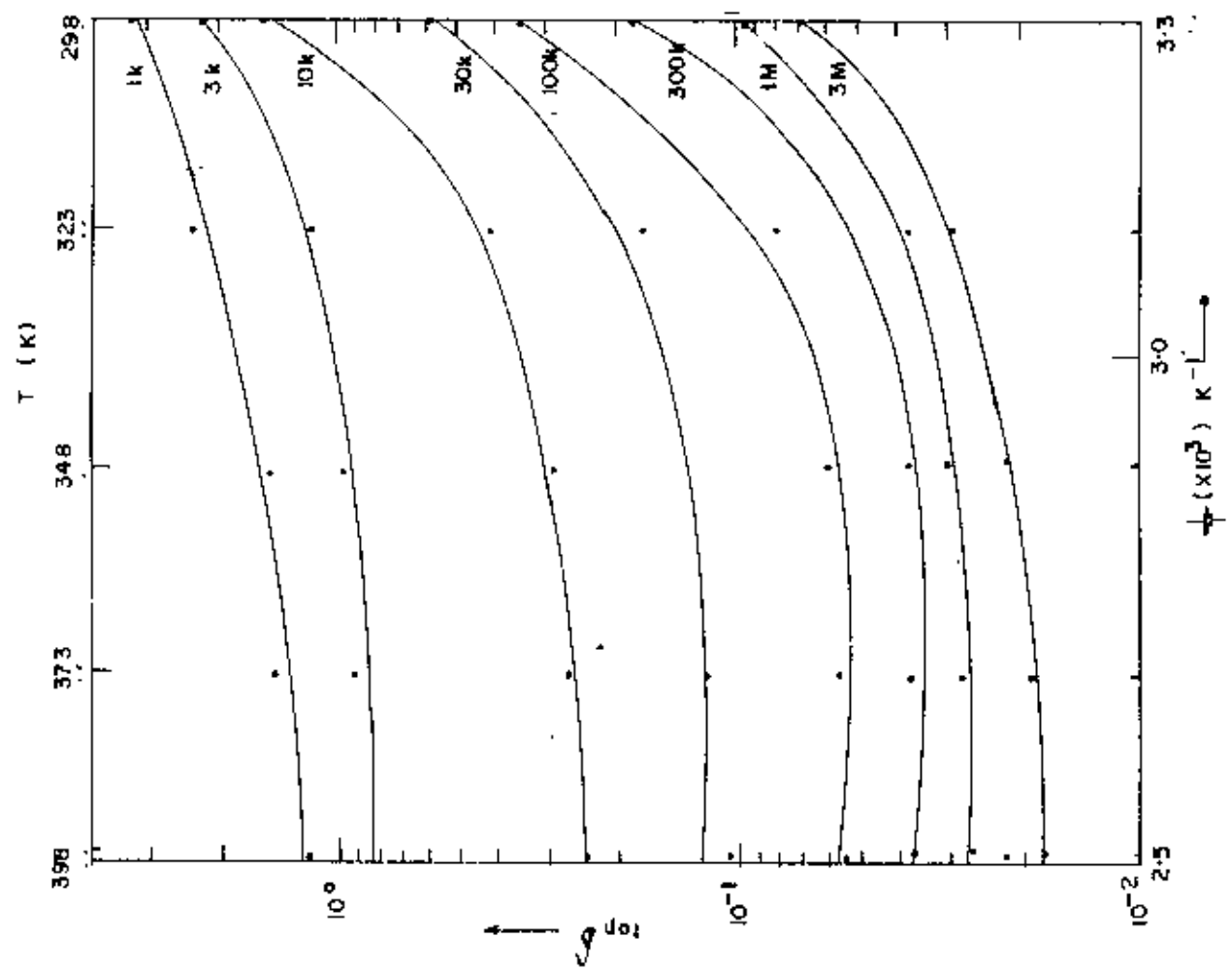


Fig.5.25 Variation of $\tan \delta$ as a function of inverse temperature for washed and 1273 K heat treated sample (pressure 2000psi) at different frequencies.

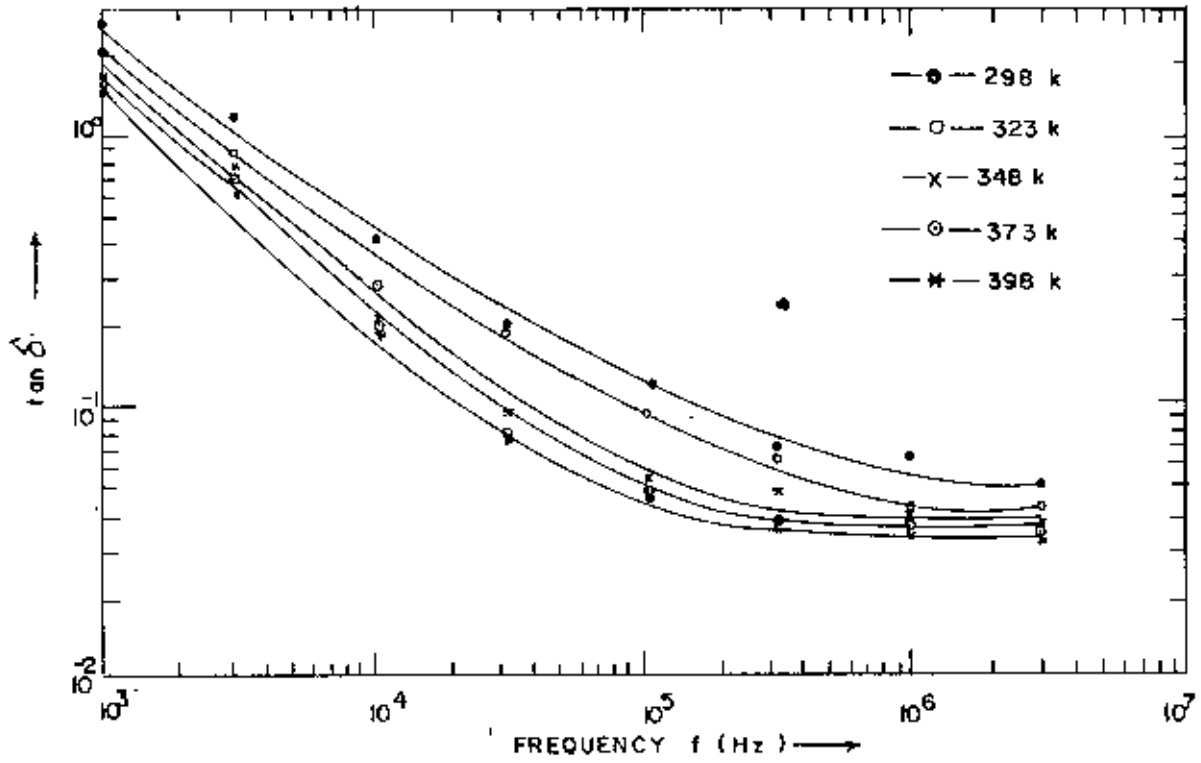
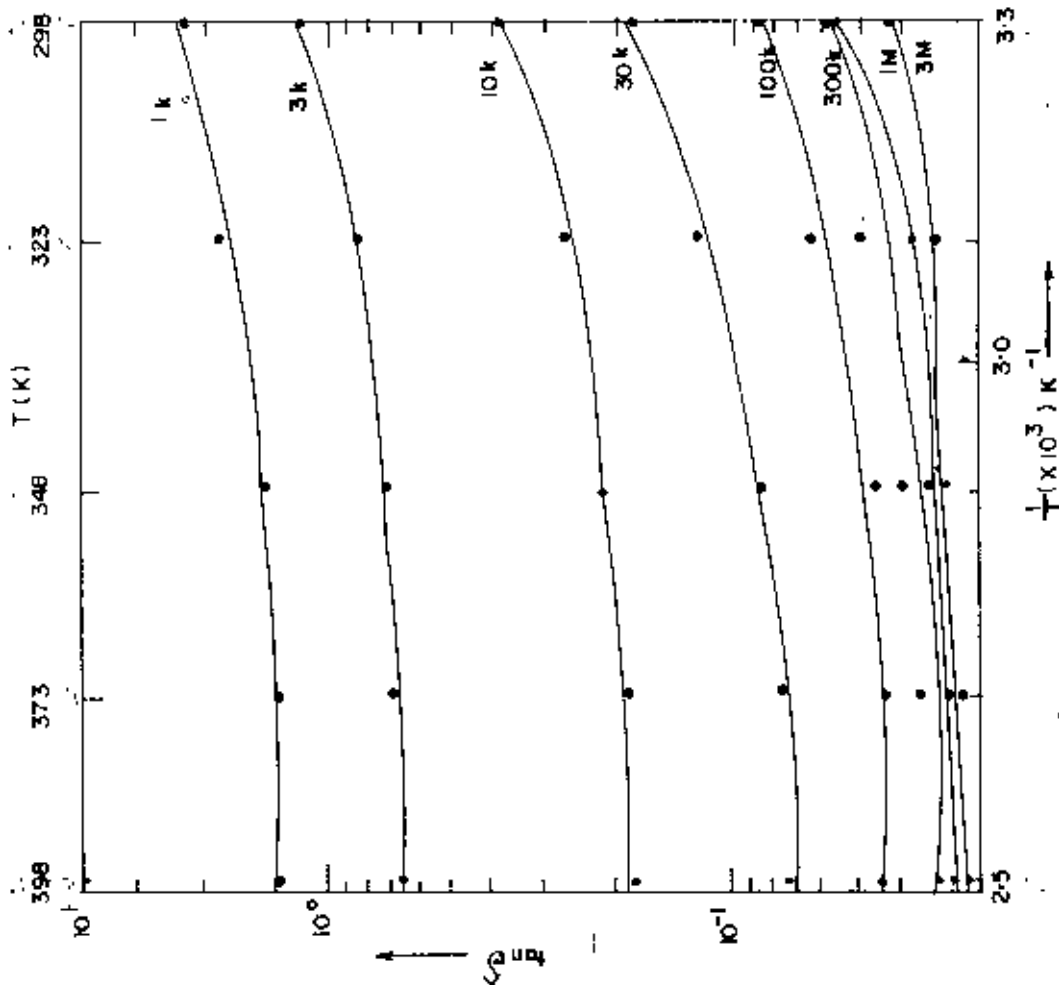


Fig. 5.24(b) $\tan \delta$ Versus frequency for washed and 1273 K heat treated sample (pressure 3000 psi) at different temperatures.



5.25(b) $\tan \delta$ Variation as a function of inverse temperature for washed and 1273 K heat treated sample (pressure 3000 psi) at different frequencies.

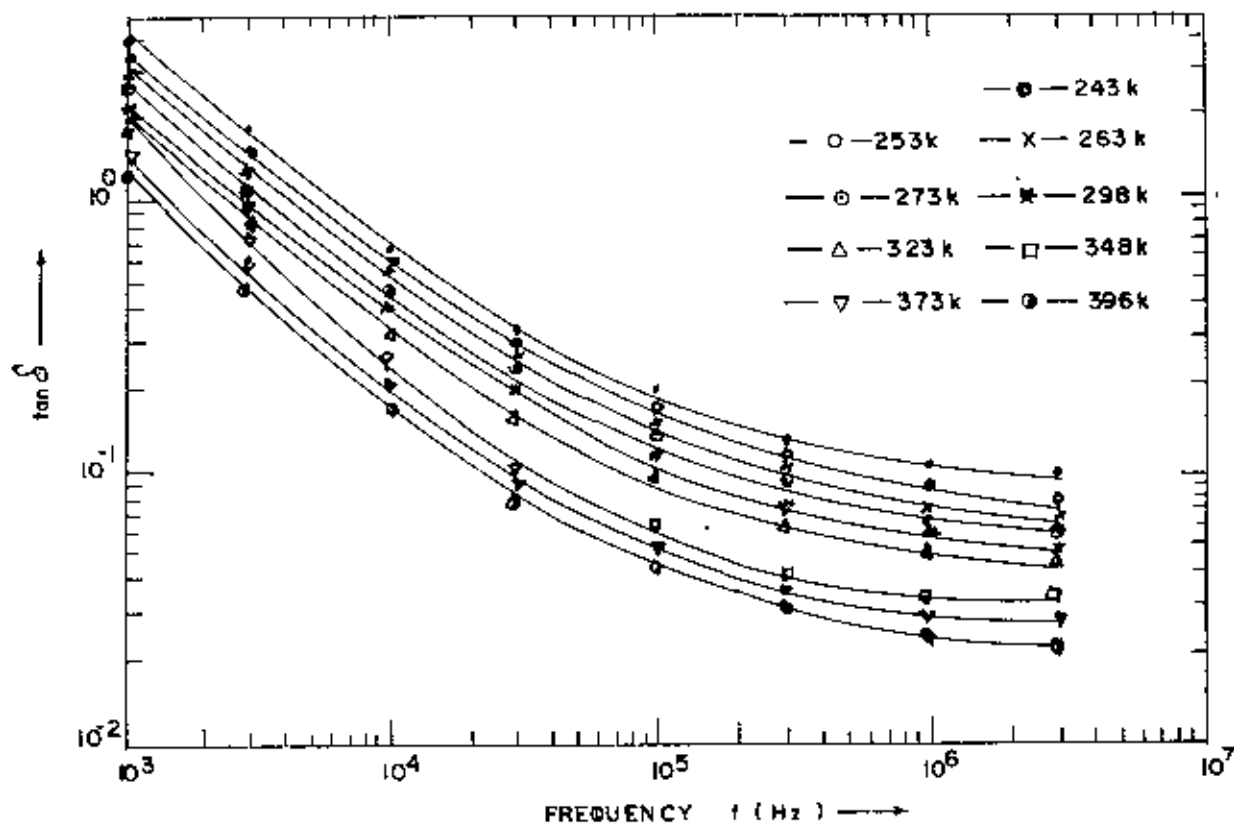


Fig 524(c) $\tan \delta$ Versus frequency for washed and 1273 K heat treated sample (pressure 3500 psi) at different temperatures.

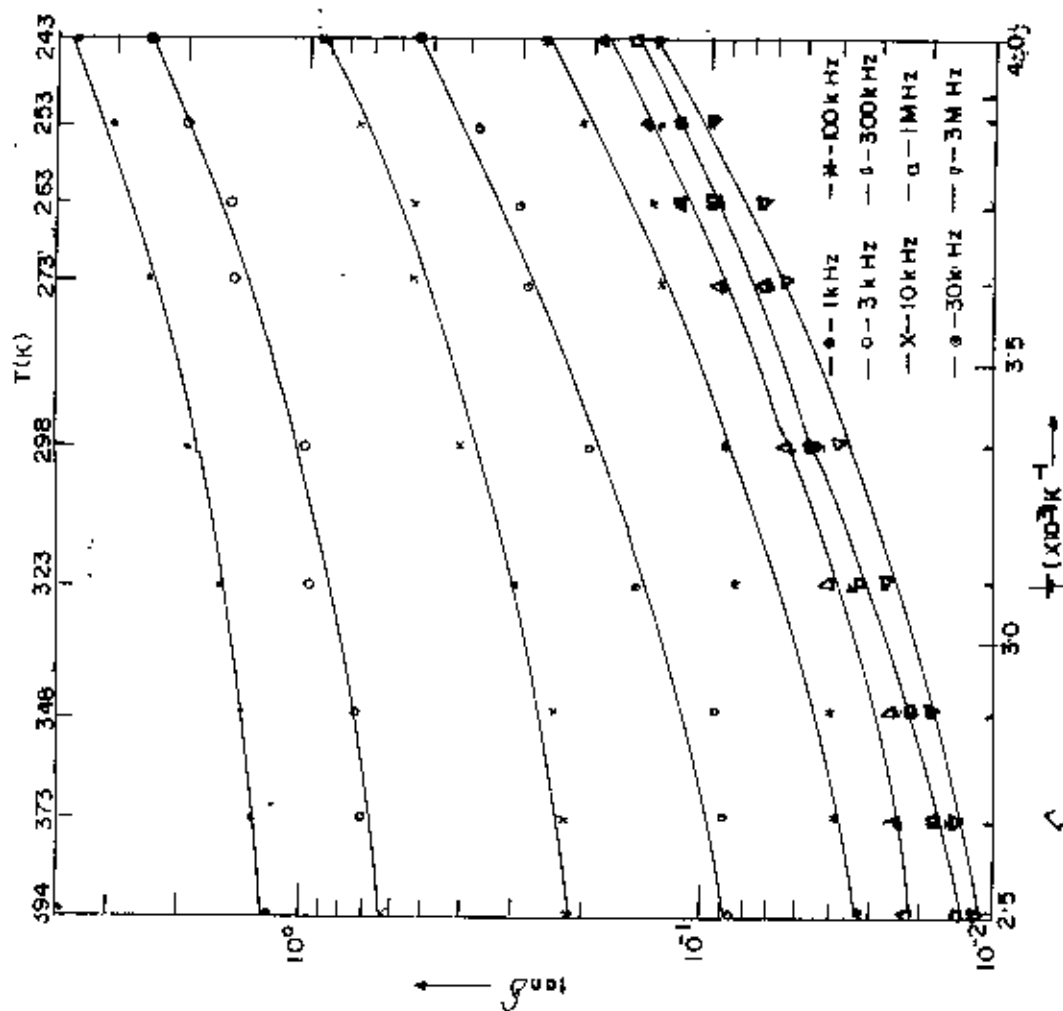


Fig 525(c) $\tan \delta$ Variation as a function of inverse temperature for washed and 1273 K heat treated sample (press 3500 psi) at different frequencies.

of dipoles in the material with the increase of temperature.

5.5.3 Dielectric loss tangent

The variation of $\tan\delta$ with frequency at different temperatures for samples B, C and D is presented in fig. 5.20, 5.22 and 5.24 respectively. The general trend for different temperature curves is to decrease with the increase of frequency. It is apparent that steepness of the temperature curves increases significantly on heat treatment at higher temperatures in the respective samples.

In sample B, it is observed that the temperature curves become steeper on going from low pressure to high pressure samples at all temperatures. In sample C, all the temperature curves are steeper than those of sample B. And there is not much change in the steepness of the temperature curves for the different pressure samples. In sample D, it is seen that curves become much steeper up to 200 KHz and above this, the temperature curves tend to become flatten.

However no relaxation peak is observed in any of the samples. Because of this the experiment has been extended to low temperature (243 K). But no loss peak is observed.

From all these curves, it is apparent that relaxation peak may occur at low frequency and high temperature or at low temperature and high frequency. As no peak is observed in the temperature curves the $\tan\delta$ is plotted against inverse

temperature for frequencies 1 K, 3 K, 10 K, 30 K, 100 K, 300 K, 1 M and 3 MHz for the sample B, C and D and is shown in fig. 5.21, 5.23, 5.25. The $\tan \delta$ decreases with increasing temperature in all the samples. The relaxation time τ is long at the lower frequency and short in the higher frequency.

References :

1. Patrick S. Nicholson and Richard M. Fulrath, "Differential Thermal Calorimetric Determination of the Thermodynamic Properties of Kaolinite," J. Am. Ceram. Soc., 53 [5] 237-240 (1970)
2. Akshoy Kumar Chakravorty and Dilip Kumar Ghosh, "Synthetic and 980°C Phase Development of Some Mullite Gel," J. Am. Ceram. Soc., 7 [4] 978-987 (1988)
3. D. X. Li and W. J. Thomson, "Mullite Formation Kinetics of a Single Phase Gel," J. Am. Ceram. Soc., 73 [4] 964-969 (1990)
4. R. C. Mackenzie, "The Differential Thermal Investigation of Clays," Min. Soc., The central press, London (1957)
5. "DTA trace of 100% pure kaolin" collected from Bangladesh Insulator and Sanitary Factory, Mirpur, Dhaka
6. M. Lampert, Rep. Prog. in Physics, 27, 329 (1964).
7. A. Rose, Phys. Rev. 97, 1538 (1955).

CHAPTER - VI

6.1 Conclusions

(i) The XRD analysis of Bijoypur white clay (BWC) reveals that it is possible to remove a major part of silica, metal oxides and other impurities by washing.

(ii) On heat treatment, as has been seen from the XRD analysis, at 1273 K the washed BWC transforms to a compound containing metakaolinite and/or γ -alumina, mullite.

(iii) The DTA experiment reveals that precursor to metakaolinite is formed after evolution of water of crystallization on heat treatment at 853 K.

(iv) The photomicrographs manifest the formation of clusters of different sizes on heat treatment. It is also seen that the porosity decreases as the pressure of pellet preparation is increased.

(v) From the I-V characteristic it is evident that space-charge-limited conduction is operative in this material.

(vi) The d.c. conduction mechanism, in this material, may be thermally activated hopping of carriers between localized states. On heat treatment ρ_{dc} increases from 10^{11} to 10^{14} Ohm-cm.

(vii) In the dielectric study it is seen that dielectric constant increases with heat treatment. The relaxation process with long τ is operative in this material.

6.2 Suggestions for future work

In the present investigation, it is seen that a sufficient amount of silica remains in the washed BWC. To use BWC as kaolinite material, it is important to remove silica as much as possible. To do this, other methods are to be devised.

Since, kaolinite materials are used in different purposes, such as insulator, at high voltages and temperatures, it needs to investigate the structural transformations due to heat treatment at higher temperatures, i.e., above 1273 K. This structural transformation changes the overall electrical properties of BWC. Alternatively, the effect of heat treatment on the electrical properties is related to the structural transformations on heat treatment of BWC.

Therefore, it is important to wash the BWC by other methods to bring the silica content to a minimum. After washing, the washed BWC should be heat treated above 1273 K. The DTA must be taken to higher temperature to observe possible changes. It is seen that absorbed water affects the electrical properties. So, it is suggested that all the measurements should be performed in vacuum.

It is observed that the relaxation process is very slow, i.e., the relaxation time is long. Therefore, the measurement

should be extended from very low frequency to very high frequencies and from low temperatures to high temperatures.

It is also important to see the effect of radiation on the electrical properties of the different heat treated BWCs.

TABLE 6.1

2 θ , d_{hkl} and the plane of reflections
of different constituents of raw sample
(diffractogram A)

2 θ in degree	d _{hkl} in A	Kaoli- nite	Sili- con oxide	Alumi- nium oxide	Iron oxide	Magne- sium oxide	Potassium Aluminium Silicate Hydroxide
9.2	9.21						001
12.6	7.03	001					
18.0	4.93				111		
20.0	4.44	110					
21.2	4.15			101			
25.0	3.56	002					
26.8	3.32		101	102			022
35.2	2.53	130		103	311		201
36.8	2.44		110		222	111	113
38.0	2.37	003	102	112			
40.3	2.24			004			
40.6	2.22	201	111				220
42.8	2.11		200	202	400	200	202
46.0	1.96	221	201				223
50.2	1.82	004	003		422		
55.0	1.67	150	202	204			006
60.0	1.54	114	211	213			312
62.4	1.49	060			440	220	
64.2	1.45	330		205			226
67.8	1.38	062	212	220			225
68.4	1.36		104				
73.6	1.28	402			533	311	401
75.8	1.24		302		622		
80.0	1.20		213	400		222	

TABLE 5.2

2 θ , d_{hkl} and the plane of reflections of different constituents of washed sample (diffractogram B)

2 θ in degree	d _{hkl}	Kaoli- nite	Sili- con oxide	Alumi- nium oxide	Iron oxide	Magne- sium oxide	Potassium Aluminium Silicate Hydroxide
9.2	9.21						001
12.6	7.03	001					
18.0	4.93				111		
20.0	4.44	110					
21.2	4.15			101			
25.0	3.56	002					
26.8	3.32		101	102			002
35.2	2.53	130		103	311		201
36.8	2.44		110		222	111	113
38.0	2.37	003	102	112			
40.3	2.24			004			
40.6	2.22	201	111				220
42.8	2.11		200	202	400	200	202
46.0	1.96	221	201				$\bar{2}23$
50.2	1.82	004	003		422		
55.0	1.67	150	202	204			006
60.0	1.54	114	211	213			312
62.4	1.49	060			440	220	
64.2	1.45	330		205			$\bar{2}26$
67.8	1.38	062	212	220			225
68.4	1.36		104				
73.6	1.28	$\bar{4}02$			533	311	401
75.8	1.24		302		622		
80.0	1.20		213	400		222	

TABLE 6.3

2 θ , d_{hkl} and the plane of reflections of different constituents of washed sample heat treated at 773 K (diffractogram C)

2 θ in degree	d _{hkl}	Kaoli- nite	Sili- con oxide	Alumi- nium oxide	Iron oxide	Magne- sium oxide	Potassium Aluminium Silicate Hydroxide	Alumi- nium Sili- cate
9.2	9.61						001	
12.6	7.03	001						
20.0	4.44	110						
21.2	4.15			101				$\bar{1}10$
26.8	3.32		101	102			002	022
35.2	2.53	130		103	311		$\bar{2}01$	$\bar{2}10$
36.8	2.44		110		222	111	113	
40.3	2.24			004				220
40.6	2.22	201	111				220	
42.8	2.11		200	202	400	200	202	$\bar{1}33$
46.0	1.96	221	201				223	
50.2	1.82	004	003		422			$\bar{1}15$
55.0	1.67	150	202	204			006	105
60.0	1.54	114	211	213			312	$\bar{1}53$
64.2	1.45	330		205			226	251
67.8	1.38	062	212	220			225	$\bar{2}52$
68.4	1.36		104					
73.6	1.28	$\bar{4}02$			533	311	401	
75.8	1.24		302		622			

TABLE 6.4

2 θ , dhkl and the plane of reflections of different constituents of washed sample heat treated at 1273 K (diffractogram D)

2 θ in degree	dhkl	Silicon oxide (Quartz, low)	Alumi- nium oxide	Mullite	γ -Alumina	Potassium Alumini- Silicate
21.2	4.15	100	101			$\bar{2}01$
26.8	3.32	101	102			022
36.8	2.44	110		130	311	$\bar{1}51$
40.3	2.24		004		222	$\bar{3}32$
40.6	2.22	111		121		$\bar{3}30$
42.8	2.11	200		320		$\bar{4}02$
46.0	1.96	201		221	400	222
50.2	1.82	003		330		$\bar{2}04$
60.0	1.54	211	213	331	511	$\bar{5}33$
67.8	1.38	212	220		440	
68.4	1.36	104				
73.6	1.28	104				
75.8	1.24	302				

Note : The hkl values of different compounds of BWC are taken from Powder Diffraction File Sets (published by the Joint Committee on Powder Diffraction Standards, Volume 1-32, USA, 1980).

